DEVELOPMENT OF FOOD ADULTERATION DETECTION METHODS UTILIZING NMR SPECTROSCOPY

A Dissertation

Presented to

the Faculty of the Graduate School

University of Missouri-Columbia

In Partial Fulfillment

of the Requirements for the Degree

Doctor of Philosophy

---

by

Colleen Ray

Dr. C. Michael Greenlief, Dissertation Supervisor

December 2022

The undersigned, appointed by the dean of the Graduate School, have examined the dissertation entitled

DEVELOPMENT OF FOOD ADULTERATION DETECTION METHODS UTILIZING NMR SPECTROSCOPY

Presented by Colleen Ray,

A candidate for the degree of doctor of philosophy,

And hereby certify that, in their opinion, it is worthy of acceptance.

Professor C. Michael Greenlief

Professor Michael Harmata

Professor Gary Baker

Professor Chung-Ho Lin

ACKNOWLEDGMENTS

I would like to thank my partner Kellie for her saintlike support and tolerance while enduring my adventure in starting graduate school at the age of 38. Many late nights staring at data in a trance-like state, missed family gatherings, even later nights preparing for exams, and no shortage of grouching about misbehaving analyses and spectrometers were endured by her without complaint. How she managed this I may never fully comprehend.

My advisor Dr. C. Michael Greenlief was also a great mentor and friend throughout the entire process. Granting me the unconventional degree of freedom I had to explore projects on my own was not at all expected when I applied to this program. It lead me to push myself harder and attempt unconventional approaches to solve problems, several of which paid off greatly and ended up becoming chapters in this dissertation.

I would like to thank the Department of Chemistry at the University of Missouri-Columbia for the opportunity to achieve this goal. Many faculty members were invaluable in helping me overcome research difficulties including but absolutely not limited to Dr. Harmata, Dr. Atwood, Dr. Brorsen, Dr. Gawenis, and Dr. Jurisson. Finally a special thanks to Dr. Jiang of the NMR Core for all of his help.

TABLE OF CONTENTS

List of Figures

Chapter 1

Chapter 2

Chapter 3

Chapter 5

List of Tables

Chapter 2

Chapter 3

Chapter 4

Chapter 5

Development of Food Adulteration Detection Methods Utilizing NMR Spectroscopy

Abstract

Food adulteration is the act of diluting foodstuffs with undeclared fillers or outright substitution with other materials. While this practice has occurred since the dawn of recorded history it has remained difficult to combat. The reason for this struggle is simple; as new methods of detecting adulteration are developed, new adulteration methods are invented with the aim of circumventing detection. This invariably leads to a constant game of cat and mouse between those who commit fraud and anyone wishing to detect it.

The motivation behind adulterating food is nearly always one of simple greed. So long as the fillers used as adulterants or substitute products are less expensive than the genuine product, the potential for greater profit is obvious. This research sought to address several of these practices by developing new or improved methods of detection with emphasis on speed, simplicity, and the use NMR spectrometers. Here we detect the presence of inexpensive robusta coffee (*coffea canephora var. robusta)* in coffees declared as being composed entirely of arabica coffee (*coffea arabica)*. The addition of seed oil to dilute olive oils using a 400 MHz NMR instrument, particularly oils from high-oleic acid cultivars of safflower and sunflower is investigated. This research effort culminated with the discovery of the dilution of bovine hard cheeses with plant based oils and development of a method to detect it.

Quantification of impurities in Δ-8 tetrahydrocannabinol and identification of the same served as a critique on existing methods of determining the purity of these products. Finally, the effects of cyclodextrins on NMR internal shift reference compounds were identified and published as a serendipitous discovery made while performing research on honey authenticity.

Chapter 1: NMR Internal Standard Signal Shifts Due to Cyclodextrin Inclusion Complexes

1.1 Abstract

Nuclear magnetic resonance (NMR)-based screening of materials is a powerful tool for quality control, authenticity testing, and purity testing of compounds. However, reliance on 3-(trimethylsilyl)-propane-1-sulfonate (DSS) and 3-(trimethylsilyl)propanoic acid (TMSP) for referencing the spectra of aqueous samples is not without hazard, particularly with automated analyses. The assumption that these reference signals always represent 0 ppm is ubiquitous in NMR spectroscopy and is routinely used for spectral alignment. However, it has been found that cyclodextrins readily generate inclusion complexes with DSS and TMSP with the effect of rendering this assumption incorrect. These inclusion complexes alter the electronic shielding of the trimethylsilane functional groups on DSS and TMSP yielding a small, but significant, shift to a higher frequency in the signal relied upon for spectral referencing. As a result, samples containing traces of these compounds may be incorrectly declared fraudulent, inconsistent with standards, or adulterated. In order to maintain the viability of this screening method, vigilance and/or improved referencing of spectra is needed.

1.2 Introduction

Cyclodextrins are a family of cyclic oligosaccharide molecules possessing many interesting and useful qualities. α-cyclodextrin (α-CD), β-cyclodextrin (β-CD) and γ-cyclodextrin (γ-CD) are macrocycles composed of 6, 7, and 8 glucose subunits,

respectively, with an overall toroid shape.[1.1] Most notable is the ability to render ordinarily insoluble organic compounds soluble in aqueous solutions. Cyclodextrins possess a hydrophobic cavity allowing them to act as supramolecular capsules for lipophilic molecules via non-covalent complexation. This property allows for convenient application, greater bioavailability, and greater efficacy of agricultural, pharmaceutical, and other products.[1.2,1.3] These features along with being well tolerated by organisms including humans makes cyclodextrins an appealing addition to a wide variety of products. As such, the use of cyclodextrins can be expected to increase in the future, and their influence on NMR based screening methods needs to be elucidated.

NMR based analysis of compounds, food products, and end products has greatly improved the accuracy and throughput of many quality control processes. An internal reference compound is typically added to samples in order to properly align NMR spectra. 3-(trimethylsilyl)-propane-1-sulfonate (DSS) or 3-(trimethylsilyl)propanoic acid (TMSP) are widely used NMR reference standards for aqueous samples. The methyl protons in the trimethylsilane functional group of DSS and TMSP ordinarily exhibit nearly no deshielding effects and thus make for a convenient zero ppm reference in aqueous solution NMR spectroscopy.

During routine authenticity testing of honey samples several samples analyzed in our lab were reported as inconsistent with honey by automated analysis. Upon further investigation it was found that the honey spectra were consistent with authentic honey. The sole aberration from normal was that the entire spectrum shifted to a lower frequency while the reference peak from TMSP remained at 0 ppm. In the interest of elucidating

potential causes of this misalignment several samples of honey were prepared with cyclodextrins in low concentrations. Honey was used in these experiments as the phenomenon had already been observed in the honey samples and honey serves as an example of a complex natural product mixture that is routinely analyzed by NMR.

Further experiments using a mixture of DSS and cyclodextrins in D_2O were performed to further explore the possibilities of internal reference compounds being affected by cyclodextrin complexation. DSS was used for these experiments to take advantage of the three methylene peaks present in non-deuterated DSS, which are absent in deuterated TMSP-d4. These methylene peaks provided greater depth to the analysis of potential inclusion complexes.

It has long been held that cyclodextrins do not interfere with aqueous NMR spectroscopy.[1,4] While Li et al. did report distortions in the spectra of cyclodextrins due to inclusion complexes similar to what is demonstrated here, the shift in the internal reference peak was not reported. However, in samples containing concentrations of cyclodextrins similar to that of TMSP or DSS it has been shown that the spectral effect from the formation of inclusion complexes composed of DSS or TMSP inside of a cyclodextrin cavity is a pronounced shift to a higher frequency of the trimethylsilane peak. Upon processing of the data, this has the effect of shifting the rest of the spectrum to a lower frequency. The signal shift is sufficient to cause spectral inconsistencies when compared to statistical models or reference spectra of the analytes. α-CD produces the most profound shift. However, while β-CD and γ-CD have a less pronounced effect, the resulting spectral deviation may still cause automated analysis to fail even at low CD

concentrations. This effect is exasperated due to advances in NMR technology allowing for the use of lower amounts of D_2O in aqueous samples, with only 10% D_2O being quite common. As such, the amount of reference compound introduced to the sample is also significantly reduced.

1.3 Materials and Methods

1.3.1 Chemicals and Materials

Deuterium oxide (D_2O, 99.9% D, 1% w/w DSS, Sigma-Aldrich), deuterium oxide (D_2O, 99.9%D, Sigma-Aldrich), 3-(trimethylsilyl)-propane-1-sulfonate, sodium salt (MSD Isotopes), 3-(trimethylsilyl)propionic-2,2,3,3-d_4 acid sodium salt (Supelco), α-cyclodextrin (≥ 98%, Sigma-Aldrich), β-cyclodextrin (≥ 98%, Fisher Scientific), γ-cyclodextrin (≥ 98%, Sigma-Aldrich), 1 M HCl, and NaOH (Fisher Scientific) used for pH adjustment were used as received.

1.3.2 Honey Sample

The honey sample used is a blossom honey sourced from the United States.

1.3.3 Sample Preparation

2.5±0.05 g honey was added to a 15 mL conical centrifuge tube. The sample was diluted to 10 mL with 18 MΩ deionized water. Sample tubes were placed on a tube rotator for 15 min to ensure thorough mixing. The sample was centrifuged at 3000×g for 30 min to settle dissolved solids. 900 µL of the supernatant was added to a vial and 100

µL of pH 2.5 phosphate buffer prepared in D_2O with 0.1%w/w DSS was added. The sample pH was adjusted to 3.1 using 1 M NaOH and 1 M HCl. 600 µL of the pH-adjusted sample was added to a 5 mm NMR tube and analyzed.

Cyclodextrin spiked honey samples were prepared identically save for the addition of 50 mg of the respective cyclodextrin added to the centrifuge tube prior to dilution, mixing, and centrifugation.

The DSS-cyclodextrin inclusion complex study samples were prepared with 1% w/w DSS containing D_2O with a 1.3:1 molar ratio of cyclodextrin to DSS.

1.3.4 Sample Analysis

NMR spectra was collected with a Bruker (Bruker BioSpin Rheinstetten, Germany) Avance IIIHD spectrometer operating at 400.13 MHz using TopSpin 3.6. The probe used was a 5 mm BBI room temperature probe. The sample temperature was 298 K. A water suppressed proton experiment was performed (32 scans, 4 dummy scans, 20 ppm sweep width, 65536 data points).

Cyclodextrin and DSS containing samples were analyzed with 2D NOESY and 1D proton experiments (32 scans, 4 dummy scans, 20 ppm sweep width, 65536 data points) with water suppression.

Spectral processing was performed with Mestrenova 14.1 (Mestrelab, Santiago de Compostela, Spain).

1.4.1 Results and Discussion

Four samples of honey were prepared for comparison. A baseline sample and three samples, each with a single cyclodextrin type added.

All collected spectra appeared normal until the spectra were overlaid, revealing significant deviation in chemical shifts (**Figure 1.1**).

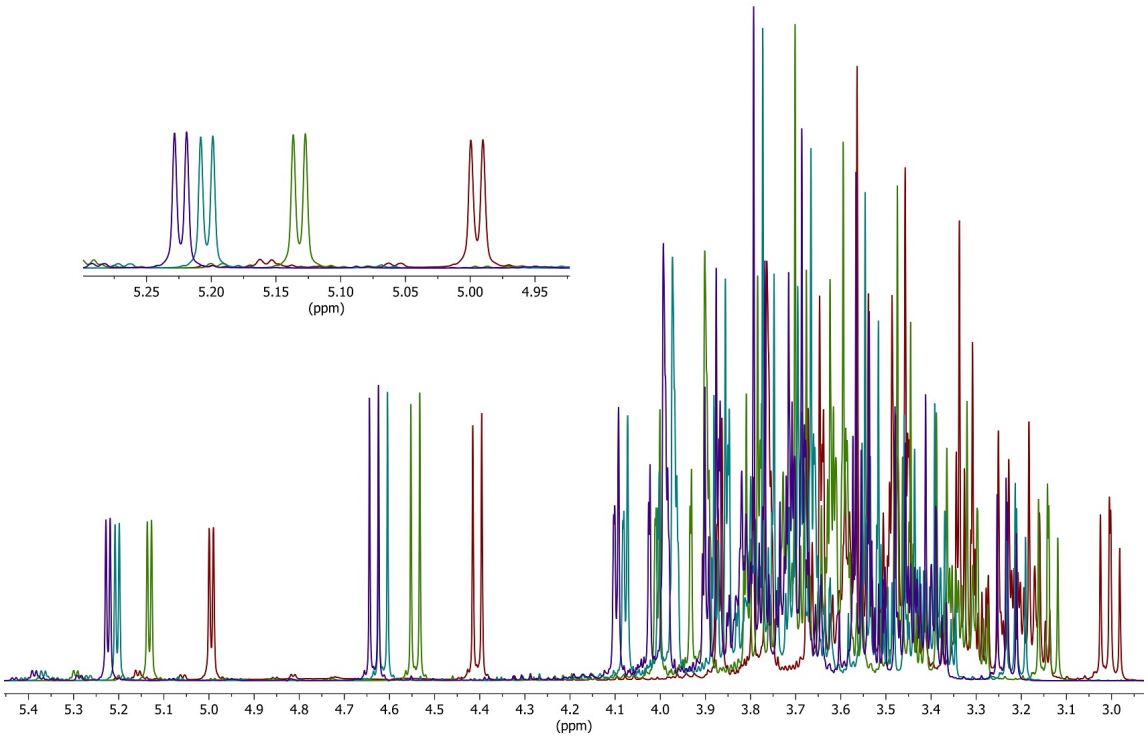

Figure 1.1. ^{1}H NMR spectra of honey (400 MHz): no added cyclodextrin (purple), α-CD (red), β-CD (green) and γ-CD (teal) added spectra referenced to DSS peak. The inset shows an expanded scale of the 5.22 ppm glucose doublet.

This discrepancy in the four honey samples of identical bulk composition is quite surprising. The spectra were automatically referenced to the trimethylsilane peak from the TMSP internal standard during spectral processing. When the spectra are manually

aligned with the doublet peak at 5.22 ppm, belonging to the glucose carbon 1 proton, all major peaks in the spectra aligned as expected (**Figure 1.2**).

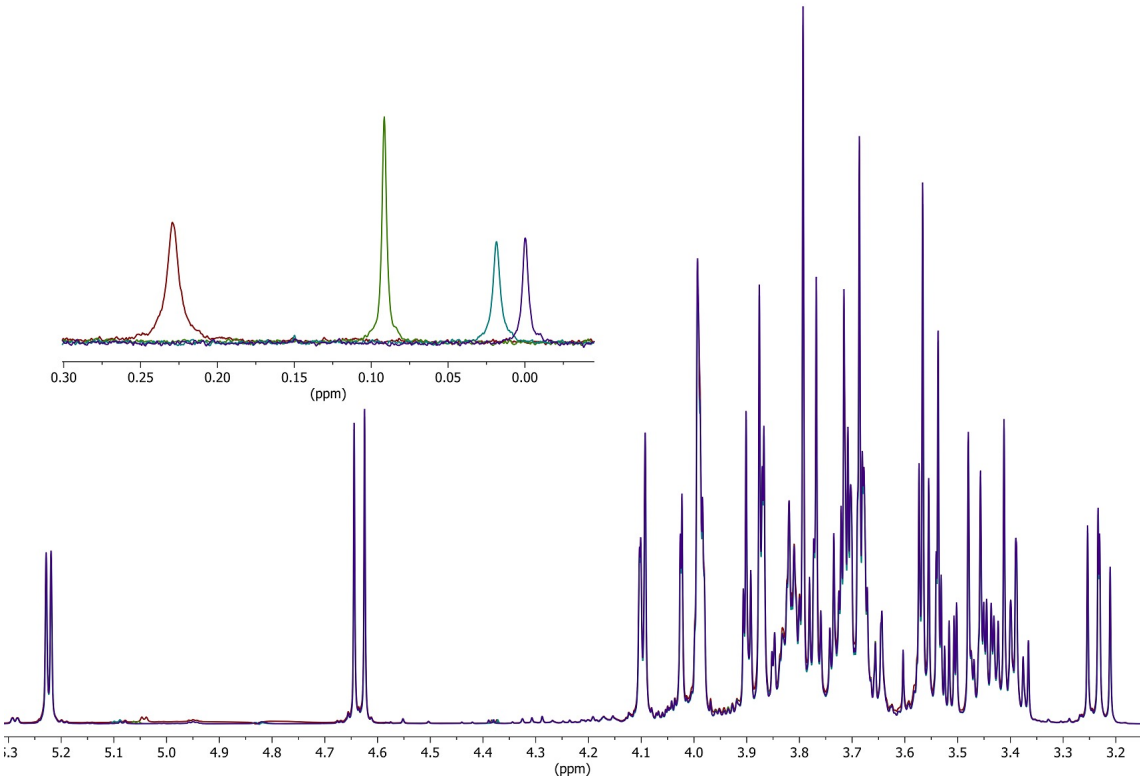

Figure 1.2. ^{1}H NMR spectra of honey (400 MHz) overlay of all spectra (no added cyclodextrin [purple], γ-CD [teal], β-CD [green], and α-CD [red]) aligned at 5.22 ppm doublet of baseline sample. Inset shows the trimethylsilane reference peak detail.

The source of the misalignment is the TMSP trimethylsilane peak to which the spectra were automatically aligned. Alignment was made with the assumption that TMSP represented 0 ppm. In the presence of cyclodextrins this is no longer the case (**Figure 1.2**). The increased frequency shift of the trimethylsilane singlet signal for the α-CD, β-

CD, and γ-CD samples were 0.229 ppm, 0.091 ppm, and 0.018 ppm, respectively, and can be seen clearly in the inset to **Figure 1.2**.

A study investigating supramolecular inclusion complexes between DSS and cyclodextrins was performed in D_2O. The spectra were collected using the previously described water suppressed 1D proton experiment and aligned to the residual suppressed water peak (**Figure 1.3**).

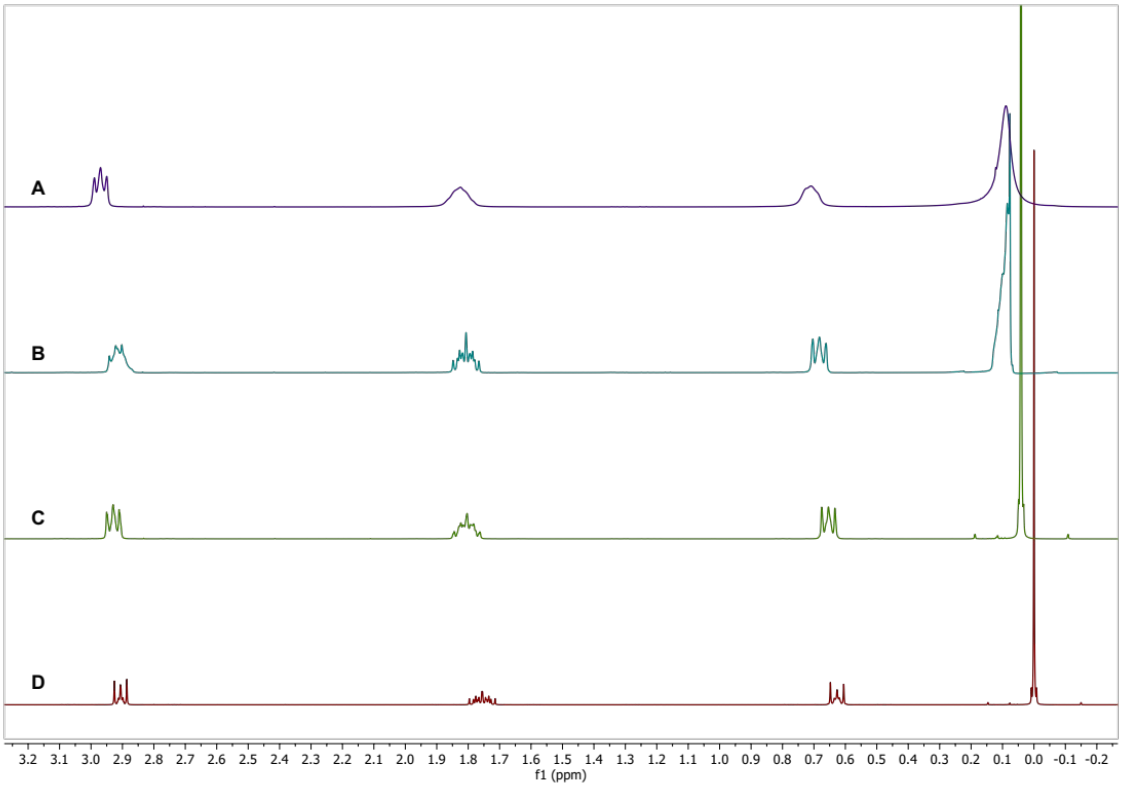

Figure 1.3. ^{1}H NMR spectra (400 MHz, aligned at residual solvent peak) overlay of proton spectra showing effects of cyclodextrins on DSS signals. Top to bottom: (A) α-CD, (B) β-CD, (C) γ-CD, and (D) DSS in D_2O and H_2O.

These spectra clearly show peak broadening in the signals from the propane chain of DSS. The distortions become more pronounced as the size of the cyclodextrin is reduced. The increased frequency and broadening of the trimethylsilane peaks followed a similar trend.

The increased frequency of the trimethylsilane peak may suggests a complex placing these methyl groups in close proximity to the hydroxyl groups on a rim of the cyclodextrin. Electron withdrawing groups in such proximity would distort the methyl group electron density enough to cause the observed frequency shift in the trimethylsilane group peak.

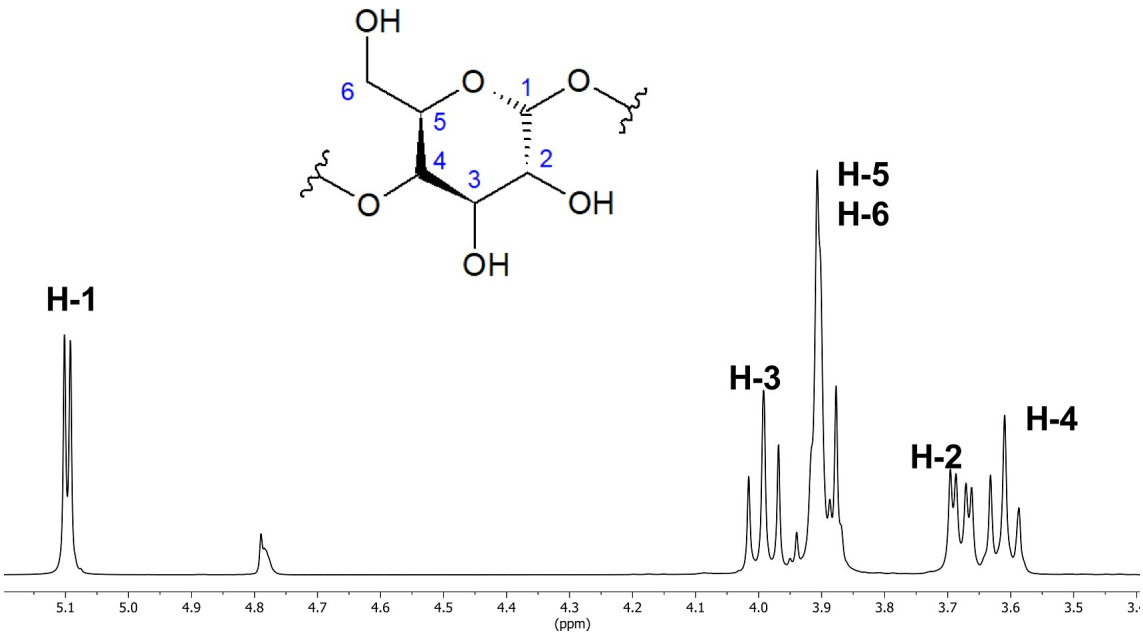

Figure 1.4. [1]H NMR (400MHz) peak assignments for β-cyclodextrin, α and γ cyclodextrin spectra are similar.[1,5] Cyclodextrin glucose subunit numbering scheme inserted for clarity.[1,5]

Figure 1.4 shows the ^{1}H NMR spectrum of β-cyclodextrin along with the conventional numbering scheme of the protons.[1.5] α-CD and γ-CD spectra are similar to that of β-CD.[1.5] Further distortion effects in the signals arising from the cyclodextrins are also seen (**Figure 1.5**).

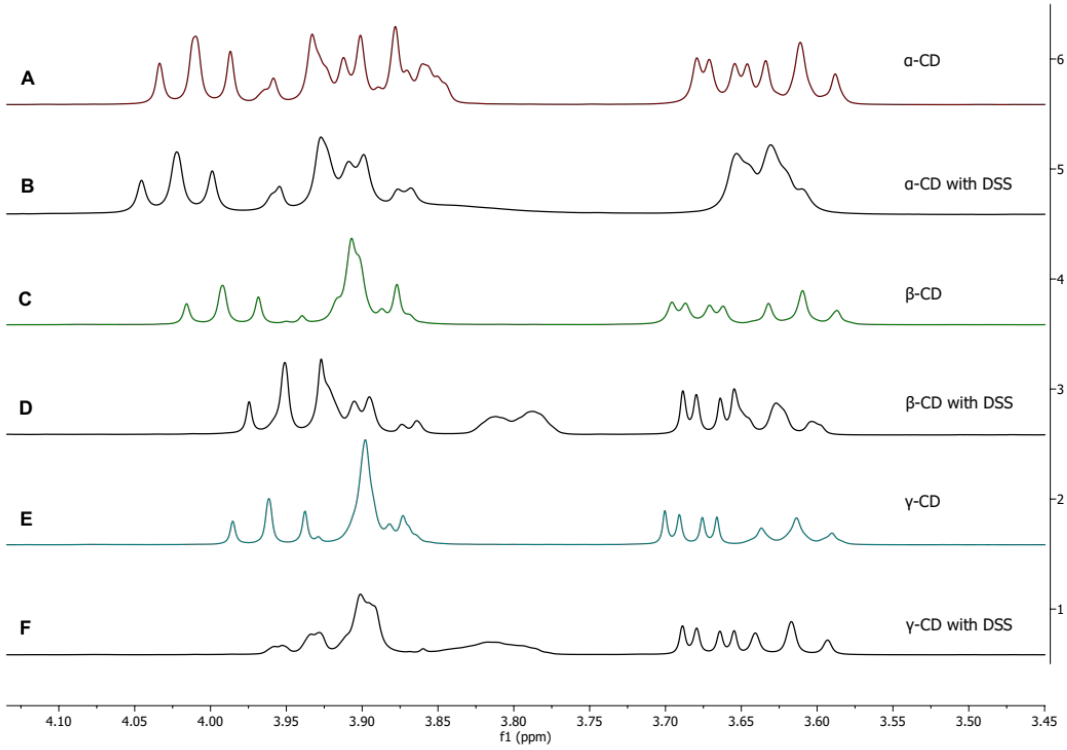

Figure 1.5. ^{1}H NMR spectra (400 MHz) comparison of inclusion complex effects of DSS in cyclodextrins. (A) α-CD, (B) α-CD with DSS, (C) β-CD, (D) β-CD with DSS, (E) γ-CD, and (F) γ-CD with DSS.

These distortions can be readily observed by comparison with the spectrum in Figure 1.4. Of note is the progression in signal distortions of differing protons in each

cyclodextrin as the size of the macrocycle shrinks. α-Cyclodextrin exhibits substantial distortions in the H-2 and H4 signals. β-cyclodextrin shows a more shielded spectral shift in H-3, and a clear separation of the ordinarily overlapping signals from H-5 and H-6 due to a shielded shift of the H-6 signal. γ-cyclodextrin exhibits distortion and signal shifts in H-3, H-5, and H-6 signals.

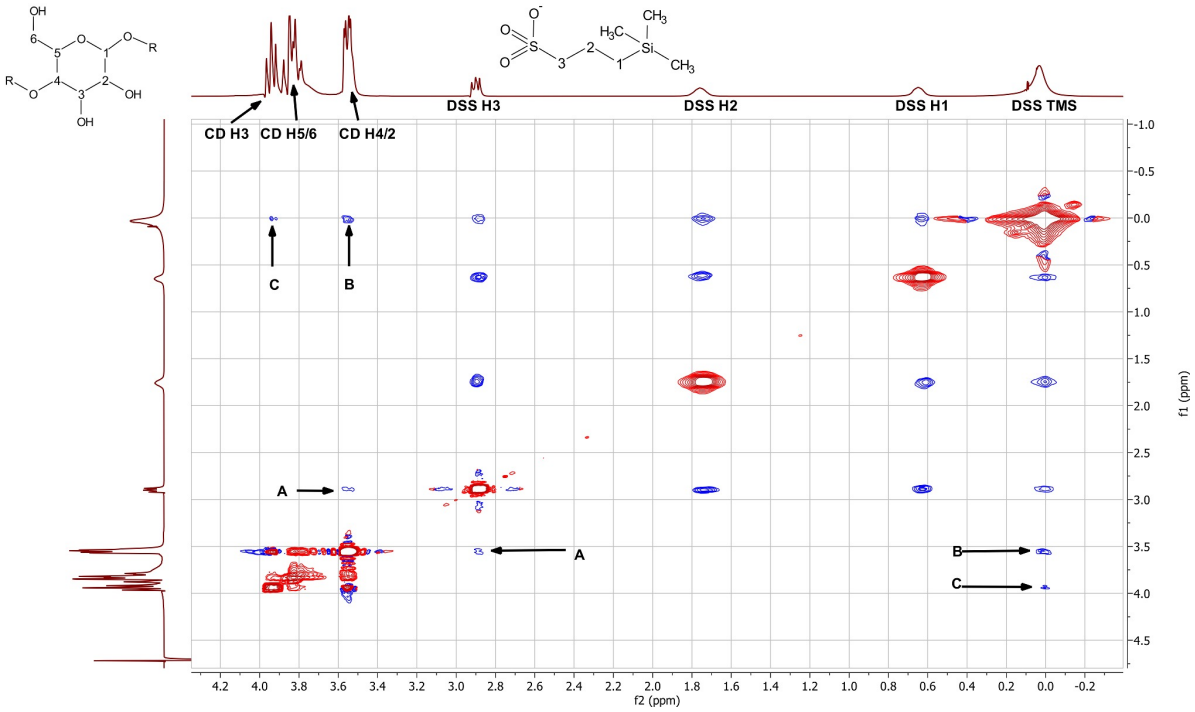

Figure 1.6. NOESY NMR (400 MHz, 1s mixing time) spectrum of α-cyclodextrin with DSS showing a weak cross peak between the DSS H3 peak and the α-CD H4 and H2 signals at 3.52 ppm by 2.9 ppm as indicated by (**A**), the DSS trimethylsilane singlet and the α-CD H4 and H2 signal at 0 ppm by 4.0 ppm as indicated by (**B**), and the DSS trimethylsilane signal and the α-CD H3 signal at 0 ppm by 3.9 ppm as indicated by (**C**). Proton numbering schemes for DSS and cyclodextrin subunit inset for reference.

NOESY spectra of α-CD and DSS in D_2O show several cross peaks between DSS and α-cyclodextrin (**Figure 1.6**). These cross peaks are indicative of protons from DSS and α-cyclodextrin being within 5 Å of each other and suggests an inclusion complex. Cross peaks B and C show a strong correlation between the DSS methyl groups and the protons on carbons 2 and 3 of the cyclodextrin. This would suggest that the TMS group of DSS is inserting itself into the cyclodextrin from the more open end of the toroid. Cross peak A shows a fairly weak signal arising from the carbon 3 protons (H3) on DSS being in fairly close proximity of the protons on carbons 2 or 4 in the cyclodextrin ring. The absence of cross peaks from the other DSS methylene signals seems to show that DSS is not entirely enclosed inside of the cavity of the cyclodextrin and that cross peak A is caused by some other, as of yet unexplored, interaction between the molecules.

1.5 Conclusions

The occurrence of cyclodextrins in agricultural, pharmaceutical, and food products is likely to increase in coming years as new applications are developed. As such, it is important to be aware of these effects on analyses that currently rely on DSS or TMSP for spectral reference. In particular in the case of honey screening, effects similar to the phenomena demonstrated in this publication have already been observed in routine sample analysis.

To maintain accuracy and avoid industry backlash from mistakenly labeling genuine products as inconsistent with standards, vigilance must be maintained. As most aqueous samples are analyzed using solvent suppression, the residual water peak may not be a

viable candidate. Alternatively, alignment of spectra to a prominent peak from the product of interest could avoid the issue altogether. For example, a potential alternative reference signal for honey or other glucose containing sweeteners could be the glucose H-1 doublet signal arising at 5.22 ppm. This is due to the high concentration of glucose in these samples and the convenient location of the signal. Additionally, the glucose H-1 is a non-labile proton its signal is unlikely to be affected greatly by minor pH deviations or other effects. However, as samples vary the choice ultimately lies with the analyst.

1.6 References

1.1 Del Valle, E., Cyclodextrins and their uses: a review. *Process Biochemistry* **2004**, 39, 1033-1046.

1.2 Yáñez, C.; Cañete-Rosales, P.; Castillo, J.; Catalán, N.; Undabeytia, T.; Morillo, E. Cyclodextrin Inclusion Complex To Improve Physicochemical Properties Of Herbicide Bentazon: Exploring Better Formulations. *PLoS ONE* **2012**, *7*, e41072.

1.3 Loftsson, T.; Brewster, M. E. Pharmaceutical Applications of Cyclodextrins: Basic Science and Product Development. *Journal of Pharmacy and Pharmacology* **2010**, 62, 1607–1621.

1.4 Li, Z.-Z.; Guo, Q.-X.; Ren, T.; Zhu, X.-Q.; Liu, Y.-C. Can TMS and DSS Be Used as NMR References for Cyclodextrin Species in Aqueous Solution? *Journal of Inclusion Phenomena and Molecular Recognition in Chemistry* **1993**, 15, 37–42.

1.5 Schneider, H.-J.; Hacket, F.; Rüdiger, V.; Ikeda, H. NMR Studies of Cyclodextrins and Cyclodextrin Complexes. *Chemical Reviews* **1998**, 98, 1755–1786.

Chapter 2: NMR Analysis of Robusta Coffee Adulteration in Arabica Coffees

2.1 Introduction

Arabica coffee (*coffea arabica*) and robusta coffee (*coffea canephora var. robusta)* are the two most commonly consumed coffee varieties with nearly 60% of the worldwide crop being composed of arabica beans.[2.1] In the western world arabica is the most commonly consumed coffee and as such it commands a higher price. Robusta trees are generally hardier than arabica trees, produce more fruit, and grow well in more accessible low elevation areas. These factors along with clever marketing suggesting that arabica is superior contributes to robusta beans fetching a lower price. The lower cost and similar flavor makes robusta coffee an appealing adulterant for arabica coffee products.

NMR was the instrument of choice for this study for several reasons: speed, simplicity, and structural information. Particularly when compared to methods involving chromatography, NMR has a distinct speed advantage. The experiments used in this research took no longer than fifteen minutes; chromatography-based analyses generally take far longer regardless of the detector used. This is quite important when faced with the prospect of running many samples in an environment such as a contract laboratory that relies on high throughput to both remain profitable and keep up with demand.

The chemical makeup of robusta and arabica beans is largely similar with the exception of 16-O-methylcafestol (16-OMC), a diterpenoid molecule found in robusta coffee but absent in arabica.[2.2] 16-OMC is already an established marker used for the detection of robusta coffee using the DIN 10779 HPLC method.[2.3] The DIN method is

extremely slow involving a five-hour Soxhlet extraction in methyl tert-butyl ether before analysis of the extract via an HPLC system.

NMR analysis of organic extracts from robusta coffee in deuterochloroform ($CDCl_3$) shows a singlet peak from the 16-O methoxy group in 16-OMC at 3.16 ppm. As this is an uncluttered region of the spectrum it makes an ideal target for screening. (See Figure 2.1)

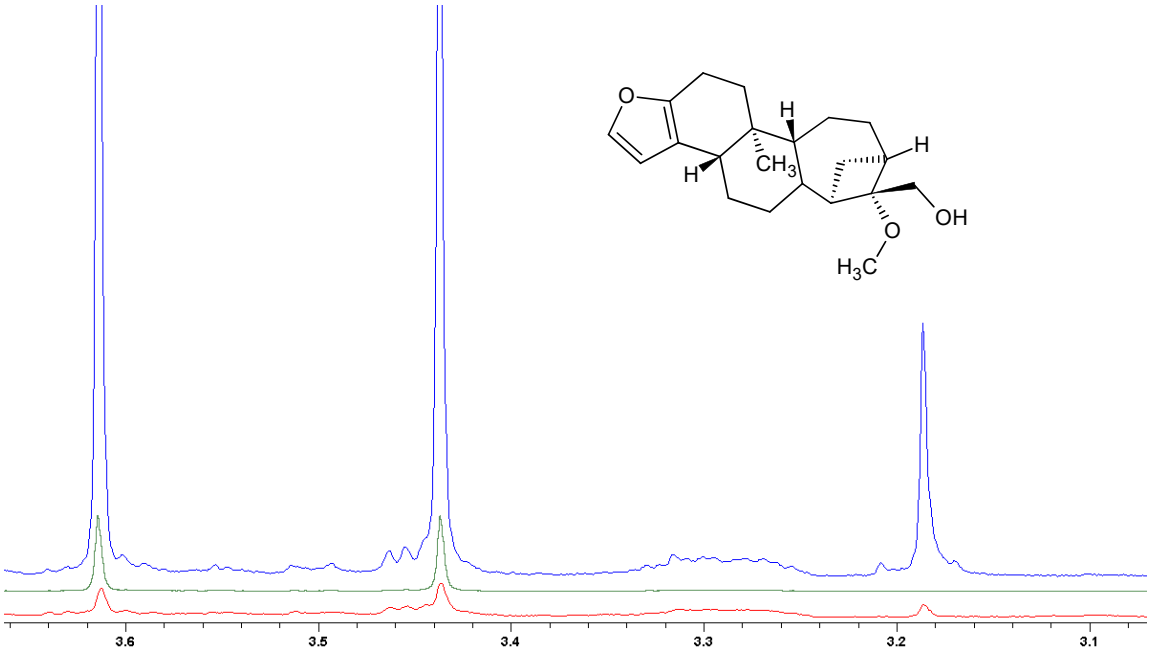

Figure 2.1. ^{1}H NMR spectrum of coffee extracts. From top to bottom: Vietnamese robusta (blue), Columbian arabica (green), adulterated decaffeinated coffee labeled as "100% arabica" (red). Note 3.16 ppm peak due to 16-OMC content. Peaks at 3.44 and 3.61ppm are from caffeine. 16-OMC structure inset for detail.

Previously published NMR based methods made use of grinding coffee in liquid nitrogen, and qualitative analyses.[2.4,2.5] While both methods are significantly faster than

the HPLC-based DIN 10779 method the preparations are cumbersome, prone to cross contamination, and do not make full use of available technology.

2.2 Materials and Method

2.2.1 Materials

Coffee samples of assured origin were obtained from several retailers. All samples used for baseline purposes were purchased green, or unroasted, except for the Vietnamese robusta coffee used in this study. Baseline studies of known origin green coffee beans were performed after roasting the beans in the laboratory. All green coffees were roasted for 7 minutes in a consumer grade hot air roaster, yielding a medium roast. Grinding for all whole bean samples was performed in a consumer grade blade grinder which was thoroughly cleaned between samples to prevent cross contamination.

Coffee bean samples were obtained from a number of locations to account for regional differences. Robusta beans were of Vietnamese, Indian, and Tanzanian origin. Arabica beans of Burundian, Colombian, Ethiopian, Kenyan, and Sumatran origin were obtained for comparison. The coffee products screened as part of the retail product survey were largely of unspecified origin.

$CDCl_3$ was purchased from Cambridge Isotope Laboratories and Acros, p-dioxane was obtained from Sigma-Aldrich, D_2O was obtained from Cambridge Isotope Laboratories.

2.2.2 Method

50 ±5 mg ground coffee was placed into a 1.5 mL centrifuge tube. 1 mL of $CDCl_3$ was pipetted into the tube and the mixture was shaken for 30 minutes. The extract was then filtered through glass wool directly into an NMR tube. A standard 90° pulse proton experiment with 16 scans, two dummy scans, and a 15 second relaxation time was utilized. The long relaxation time was chosen to ensure maximum signal recovery allowing for greater precision. The spectrometer used was a Bruker Avance IIIHD 600 MHz system equipped with a TCI cryoprobe.

Liquid-liquid extractions of brewed coffee were performed by adding 1.5 mL of $CDCl_3$ directly to a 15 mL centrifuge tube filled with 10 mL of coffee. The tube was shaken for 15 minutes and centrifuged at 1790 × g for 10 minutes. The organic layer was collected and dried over sodium sulfate. The dry $CDCl_3$ extract was filtered through glass wool directly into an NMR tube.

Brewing coffee using D_2O was performed by adding 2 mL of boiling D_2O to 100 mg of ground coffee in a centrifuge tube. The mixture was allowed to steep for 10 minutes, then centrifuged at 4000 RPM for 5 minutes. The extract was filtered through glass wool directly into an NMR tube.

Quantification was performed using Electronic REference To access In vivo Concentrations (ERETIC.) ERETIC is a method of electronically adding a signal of known concentration to an NMR spectrum allowing accurate concentrations determination of peaks in a sample spectrum. The experiment must be run under largely identical experimental conditions as the calibration experiment. Calibration isperformed

using a 10 mmol p-dioxane in $CDCl_3$ standard. ERETIC behaves as a virtual external standard and eliminates the need for preparing spiked samples.

2.3 Results and Discussion

Initial efforts to analyze brewed coffee via liquid-liquid extraction using $CDCl_3$ did not extract detectable levels of 16-OMC from these products. Analysis of coffee brewed with D_2O yielded similar results. While unsurprising considering the structure and relatively non-polar character of the compound, it does limit this screening method to analyzing coffee bean products.

Combining the use of ERETIC with an extraction procedure similar to that used by Monakhova[2.4] but with smaller samples allowed for a more rapid extraction, identification, and quantification of 16-OMC in coffee beans. The trend of fraudulent coffees detected seemed to be more common in lower cost store branded products. This finding is not entirely unexpected as the pressure to offer store brand products at lower prices encourages the use of adulterants. Combining this with store brand products often being produced by third parties, a target customer who is less likely to be discerning, and it is a relatively low risk market for adulterated products.

2.3.2 Baseline studies

Determination of the expected levels of 16-OMC in coffee beans was necessary to explore the validity of ERETIC in this application. Previous literature also suggested the possibility of 16-OMC content in arabica beans.[2.5] However no 3.16 ppm peak belonging

to 16-OMC were detected in arabica coffee extracts in this study. All robusta bean samples yielded a clear singlet at 3.16 ppm consistent with 16-OMC content. Of note is how the concentration of 16-OMC varied by up to 44% depending on origin suggesting the need for a weighted average calculation for adulteration percentage. For later adulteration percentage calculations, a weighted average value of 1012 mg/kg was used.

Table 2.1. 16-OMC content in robusta coffee extracts

Coffee	Mass (mg)	extraction 1 (mmol)	Extraction 2 (mmol)	Extraction 3 (mmol)	Total 16-OMC content (mg/kg)
Vietnamese	51.6	0.2352	0.0201	Below LOQ	1635
Tanzanian	50.6	0.1696	0.0104	Below LOQ	1175
Indian	51.7	0.1368	0.082	Below LOQ	926

Calculation of Adulteration Content

In order to estimate the percentage of robusta coffee content in adulterated samples the Equation 2.1 was used:

$$\frac{(Sample\,16-OMC concentration\,(mMol))*(330.469\,g/Mol)}{1000\,g/Kg}\cdot 1000 = mg\,16\,OMC/Kg\,coffee \tag{2.1}$$

1233.37 mg/kg is the weighted average of all baseline robusta samples determined by extracting each sample three times. Each extraction used one mL of solvent simplifying the calculation. For all samples calculations were run using the concentration for Indian (926.847 mg/kg), Vietnamese (1635.05mg/kg), and the weighted average. This yields a high, low, and average range for potential adulteration accounting for variation based upon origin.

2.3.3 Limit study

To determine the lower limit of adulteration that could be reliably detected and quantified via NMR a series of serial adulterations were made using Indian robusta beans mixed with Ethiopian arabica beans. Ethiopian arabica beans were found to contain no detectable 16-OMC and the Indian robusta beans had the lowest content of 16-OMC of the available robusta samples.

Table 2.2 Limit of detection and quantification study results excerpt

Sample	Robusta adulteration percentage	3.16 ppm peak SINO value
1	0	0 (peak absent)
2	6.7	18.6
3	11	55.9

As shown by a significantly higher than LOQ signal to noise, detection of samples of at least 6.7% adulteration of a low 16-OMC containing robusta coffee is possible.

2.3.4 Optimization of method

Initial efforts made use of 100 mg quantities of coffee but proved to be difficult to handle using 1.5 mL centrifuge tubes. 50 mg was found to be a more practical, and economical mass.

In order to further streamline the screening process of coffee, a more efficient method using available equipment was necessary. In order to utilize 1.5 mL flip-top

centrifuge tubes a sample mass of 50 mg extracted with 1 mL of $CDCl_3$ was used. In order to determine the necessary number of extractions needed per sample, a series of extractions were performed on two known adulterated commercially available coffees and three samples of robusta coffees. The lower limit of quantification was set to a signal to noise ratio of 10. All samples were shaken for 30 minutes for each extraction.

Table 2.3. 16-OMC content of coffee samples extracted three times with $CDCl_3$

Coffee	Mass of sample (mg)	16-OMC (mmol) Extraction 1	16-OMC (mmol) Extraction 2	16-OMC (mmol) Extraction 3
Commercial 1	50.6	0.0150	Below LOQ	Below LOQ
Commercial 2	50.7	0.0130	Below LOQ	Below LOQ
Vietnamese	51.6	0.2352	0.0201	Below LOQ
Tanzanian	50.6	0.1696	0.0104	Below LOQ
Indian	51.7	0.01368	0.0082	Below LOQ

As adulterated coffees are unlikely to contain more than 50% robusta content due to the flavor difference being easily detected by the casual drinker, a single extraction should reliably quantify adulteration. Exceptionally high 16-OMC content samples should be doubly extracted and tested for 3.16 ppm peaks above the LOQ. However, for rapid simple qualitative testing a second extraction is unnecessary.

2.3.5 Blind Testing

A package containing seven ground coffee samples was submitted for analysis. All samples were contained in zip-top plastic baggies with no identifying features other than a piece of tape with a number marked on it to differentiate each sample. All were

analyzed using the streamlined method and all were negative for 16-OMC except for the sample labeled “5.” The supplier of the blinded samples later confirmed this to be the sole adulterated sample supplied in the batch, confirming the ability of this method to discriminate between genuine and adulterated arabica coffee samples.

2.3.6 Survey of Retail Coffee Samples

A total of 87 retail sourced pre-ground coffees were submitted for screening. Whole bean coffees were excluded as it is possible to visually discriminate between robusta and arabica coffee beans in most cases. Samples were analyzed using the previously described method. Nine samples total were positive for robusta coffee contamination at a level above the limit of quantification. A further three samples had the signature 3.16 ppm peak of 16-OMC but were below the 10:1 signal to noise limit. This translates to an 18.4% rate of adulteration rate of tested pre-ground retail coffees with 14.9% being quantifiable. Of the coffees screened all detected adulterated samples were store brands. See appendix A1 for a complete list of samples and results.

2.4 Conclusions

While NMR based coffee analysis for the purposes of detecting robusta adulteration is not an entirely new development, this study achieved its goal of developing a more efficient sample preparation method. Eliminating the need to perform lengthy soxhlet extractions or similar time and labor intensive sample preparation greatly reduces the workload involved in these analyses. As shown by the results of this study

robusta adulterated coffee sold as 100% arabica coffee remains a problem in the coffee market.

Reducing the workload of the analyst with this method will improve throughput of any lab performing NMR based coffee analyses. The benefits of this are twofold: increased sample throughput, and significantly reduced cost per analysis. Both of these benefits are of great importance to contract laboratories with greater revenue generation and also reduced overhead costs in the form of labor and materials. Additionally the significant reduction in waste solvents compared to methods such as a soxhlet extraction reduces the environmental impact of these analyses as well.

With greater than 18% of these samples being adulterated it is clear that the coffee market is rife with fraud. The fact that some of the extremely low level adulteration rates may be from incidental contamination cannot be ignored. However the majority of these samples are adulterated at rates far beyond what may be passed on via grinder contamination or incomplete emptying of product handling containers and is thus more likely to be economically motivated. Due to the lower cost of robusta beans and the similar flavor, robusta adulteration will likely remain a problem in this market for the foreseeable future.

2.5 References

2.1 Coffee: World Markets and Trade. <https://www.fas.usda.gov/data/coffee-world-markets-and-trade> (accessed Aug 18, 2019).

2.2 Gunning, Y.; Defernez, M.; Watson, A. D.; Beadman, N.; Colquhoun, I. J.; Le Gall, G.; Philo, M.; Garwood, H.; Williamson, D.; Davis, A. P.; et al. 16-O-Methylcafestol Is Present in Ground Roast Arabica Coffees: Implications for Authenticity Testing. *Food Chemistry* **2018**, *248*, 52–60. https://doi.org/10.1016/j.foodchem.2017.12.034.

2.3 Agilent Application Note, Publication number 5991-2853EN **2016**.

2.4 Schievano, E.; Finotello, C.; De Angelis, E.; Mammi, S.; Navarini, L. Rapid Authentication of Coffee Blends and Quantification of 16- *O* -Methylcafestol in Roasted Coffee Beans by Nuclear Magnetic Resonance. *J. Agric. Food Chem.* **2014**, *62* (51).

2.5 Monakhova, Y. B.; Ruge, W.; Kuballa, T.; Ilse, M.; Winkelmann, O.; Diehl, B.; Thomas, F.; Lachenmeier, D. W. Rapid Approach to Identify the Presence of Arabica and Robusta Species in Coffee Using 1H NMR Spectroscopy. *Food Chemistry* **2015**, *182*, 178–184. https://doi.org/10.1016/j.foodchem.2015.02.132

Chapter 3: A New Method for Olive Oil Screening Using Multivariate Analysis of Proton NMR Spectra

3.1 Abstract

A new NMR-based method for the discrimination of olive oils of any grade from seed oils and mixtures thereof was developed with the aim of allowing the verification of olive oil authenticity. Ten seed oils and seven monovarietal and blended extra virgin olive oils were utilized to develop a principal component analysis (PCA) based analysis of ^{1}H NMR spectra to rapidly and accurately determine the authenticity of olive oils. Another twenty-eight olive oils were utilized to test the principal component analysis (PCA) based analysis. Detection of seed oil adulteration levels as low as 5% v/v has been shown using simple one-dimensional proton spectra obtained using a 400 MHz NMR spectrometer equipped with a room temperature inverse probe. The combination of simple sample preparation, rapid sample analysis, novel processing parameters, and easily interpreted results, makes this method an easily accessible tool for olive oil fraud detection by substitution or dilution compared to other methods already published.

3.2. Introduction

Olive oil is the oil collected from the fruit of the olive tree (*Olea Europaea L.*) typically through simple mechanical pressing. Olive oil is somewhat unusual as the oil is extracted from the flesh of the fruit instead of the seed as is common in most other food oils. This oil has been consumed by humans since antiquity and remains a highly valued

food oil today. Due to the high market price of olive oil compared to other oils, it is a popular target for adulteration through dilution with other oils or label fraud by selling non-olive sourced oils as genuine olive oil [3.1]. The aim of this work is to develop a rapid analysis for the detection of seed oil adulteration in any grade of olive oil.

The motivation for adulteration is one of simple greed. If olive oil is diluted with a less costly oil or is completely replaced by said oil, the profits from selling it as genuine olive oil can be quite large. Adulteration of olive oils can affect consumers beyond the obvious economic impact of paying a premium for fraudulent goods. Olive oil is often consumed for its reputed health benefits due to its unique composition, which would be reduced if diluted or absent if the product contains no olive oil whatsoever. Inadvertent consumption of oils ordinarily avoided by people with allergies could have significantly more serious and immediate effects on the consumer if the so-labeled olive oil contains products to which the consumer is sensitive.

NMR spectroscopy has long been the gold standard method for the elucidation of unknown molecular structures and is often used in synthetic chemistry for verification of products. In recent years the ability for NMR spectroscopy to screen products and materials for quality control or authenticity has gained significant attention. The data analysis methods employed in this study are broadly similar to those used for untargeted metabolomic fingerprinting commonly performed with mass spectrometry. While mass spectrometry has greater sensitivity, NMR is capable of more rapidly screening complex mixtures such as foodstuffs in a non-destructive manner. Coupling NMR results with principal component analysis (PCA) allows even subtle differences in overall

composition to be useful for discriminating between oil sources and detecting adulterated samples. Utilizing a 400 MHz NMR to detect lower levels of adulteration of olive oil with oils such as high-oleic acid cultivars of sunflower and safflower oil is challenging due to these adulterants having lipid profiles very similar to those found in olive oils.[3.2]

Olive oil is composed of fatty acid triglycerides with lower concentrations of a variety of phenolic and polyphenolic compounds.[3.3] Oleic acid is the most abundant fatty acid found in olive oils with varying levels of linoleic acid, linolenic acid, and palmitic acid. The ratios of the various fatty acids in olive oil differs from those found in many seed oils, particularly due to the high levels of oleic acid and low levels of ω-3 α-linolenic acid. The spectral signature of the lower concentration fatty acids contribute significantly to differentiating olive oils from high oleic acid varietals of seed oils.

These differing levels manifest themselves spectrally and allow these oils to be differentiated via analysis. A spectral comparison of hempseed oil and a sample of monovarietal picual olive oil demonstrates many of these differences (**Figure 3.1**).[3.4]

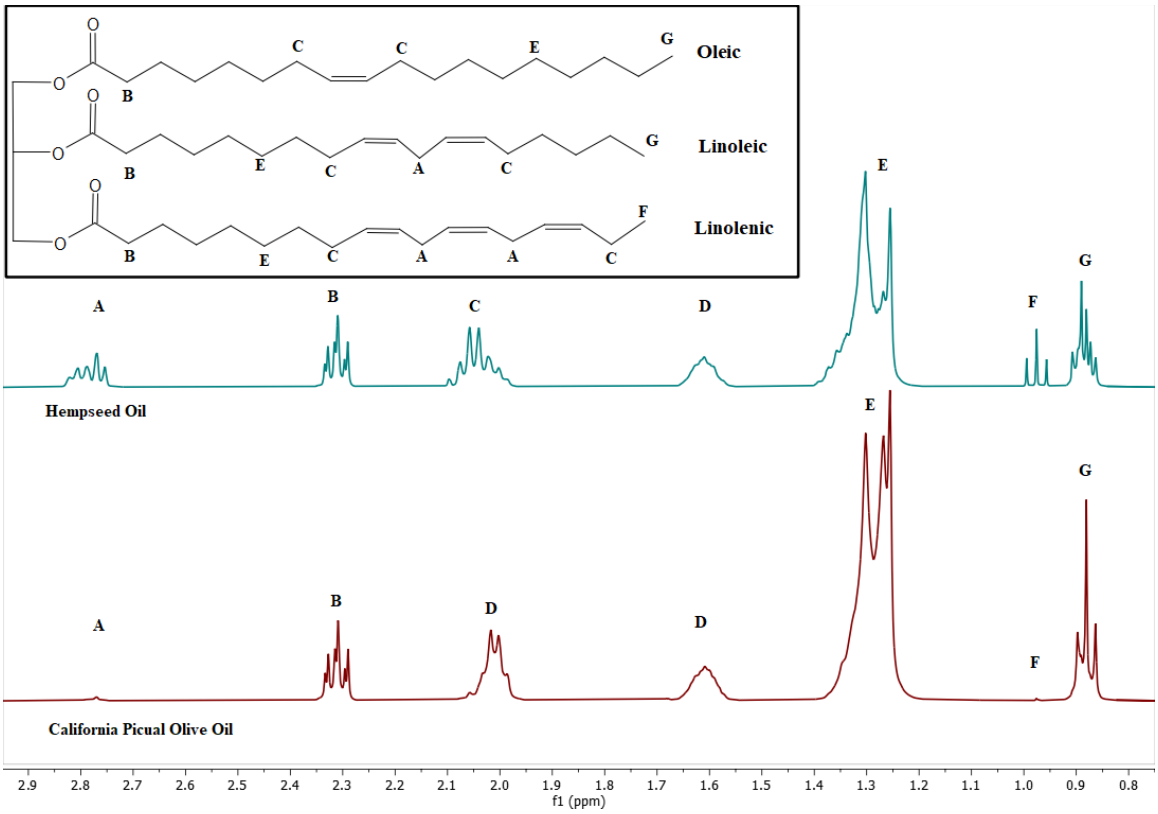

Figure 3.1. Comparison of 400 MHz ^{1}H NMR spectra of hempseed and olive oil with model triglyceride structure detailing origins of specific labeled peaks from various fatty acid subgroups.

The triplet "F" at 0.977 ppm arises from the terminal methyl group of ω-3 fatty acids, most often α-linolenic acid, which is found in significantly higher concentrations in hempseed oil than olive oil. The proximity of the π-bond between carbons 2 and 3 in ω-3 fatty acids deshields the terminal methyl group resulting in a shift away from peak "G" at 0.881 ppm belonging to the same functional groups in other fatty acids.

Multiplet "A" at 2.78 ppm (**Figure 3.1**) is due to the methylene protons positioned between two π-bonds in polyunsaturated fatty acids, such as linoleic and linolenic. Polyunsaturated fatty acids are plentiful in hempseed oil and are in relatively low

abundance in olive oils as seen by the intensity difference of this feature in the two spectra.[3.4]

Analyzing these spectra manually via peak area ratiometrics is possible but is time intensive and tedious due to the number of peaks and variables involved. Utilizing PCA to group similar spectra together accomplishes a similar overall goal while being far easier to automate and produces easily interpreted results.[3.5] PCA is often used in many complex analyses and has been shown here to work well to discriminate between spectra of various food oils. Not only is the method described herein able to differentiate pure oils by source, but the method can also detect olive oil that has been diluted by other oils.

Olive oil authenticity testing via gas chromatography (GC) and liquid chromatography (LC) are well established methods. These GC and LC methods are comparatively slow, often involving several sample preparation steps, and sample analysis runs on the order of 30 minutes with longer run times being commonplace.[3.6, 3.7] NMR analysis of oil samples requires no sample preparation aside from mixing the sample with a deuterated solvent and experiment run times are on the order of 15 minutes for a simple one-dimensional proton NMR. PCA of food oil NMR spectra is not entirely a novel development in and of itself.[3.8, 3.9] However, previous studies did not demonstrate the ability to detect adulteration via dilution, and generally dealt with differentiating olive oils by geographical location. These studies also used NMR spectrometers with higher field magnets that are more expensive and less widely available than the comparatively inexpensive 400 MHz system used in this study.

3.3. Materials and Methods

3.3.1 Chemicals and Materials

Deuterated chloroform ($CDCl_3$ 99.9% D, 1% w/w TMS) was obtained from Acros Organics (Switzerland).

3.3.2 Oil Samples

Olive oil and seed oil samples were purchased from local and online retailers. Olive oil samples consisted of monovarietal and blended oils of European, Mediterranean, and North American origin. A single premixed blend of 70% canola, 20% olive oil, and 10% (all v/v) grapeseed oil was used as a blended sample for comparison. Table 3.1 lists the olive oil samples used in this study.

Table 3.1. List of olive oil samples used

Sample	**Varietal**	**Grade**
1	Arbequina	Extra Virgin
2	Picual	Extra Virgin
3	Nocellara	Extra Virgin
4	Manzanillo	Extra Virgin
5	Hojiblanca	Extra Virgin
6	Coratina	Extra Virgin
7	Koroneiki	Extra Virgin
8	Blend	Extra Virgin
9	Manzanillo	Extra Virgin
10	Hojiblanca	Extra Virgin
11	Blend	Extra Virgin
12	Kilkai	Extra Virgin

13	Manzanillo	Extra Virgin
14	Ascolano	Extra Virgin
15	Arbequina	Extra Virgin
16	None Specified	Extra Virgin
17	None Specified	Extra Virgin
18	None Specified	Extra Virgin
19	Pendolino	Extra Virgin
20	Coratina	Extra Virgin
21	Picual	Extra Virgin
22	Coratina	Extra Virgin
23	None Specified	Olive Oil
24	None Specified	Olive oil
25	None Specified	Refined
26	None Specified	Extra Virgin
27	None Specified	Extra Virgin
28	Blend	Extra Virgin

The seed oils used for comparison and adulteration studies were: almond, argan, high-oleic canola, cottonseed, grapeseed, hazelnut, hempseed, peanut, high-oleic safflower, soybean, and high-oleic sunflower oils. All seed oils were purchased from online and local retailers.

3.3.3 Sample Preparation

50 µL of oil was added directly to a clean 5 mm NMR tube (Deutero Boroeco 8, Deutero GmbH, Kastellaun, Germany) with a pipette. 550 µL of $CDCl_3$ was then added to the NMR tube. The tube was then capped, inverted to ensure complete mixing, and then analyzed.

3.3.3.1 Adulterated Samples

Sample 20, a coratina monovarietal olive oil from California, was mixed with varying levels of canola, hazelnut, peanut, safflower, and sunflower oils to test the ability of this method to detect adulteration via dilution. Canola and hazelnut oil adulteration samples were prepared with 10%, 15%, and 20% (v/v) of adulterant. The same olive oil was also adulterated with 10%, 20%, 30%, and 40% peanut, safflower, and sunflower oils. A premixed commercially available blend of 70% canola, 20% olive oil, and 10% grapeseed oil (all v/v) was also analyzed to further test the model.

All adulterated samples were prepared to a final volume of 5 mL. Olive oil and adulterants were measured into a 15 mL conical tube, vortexed for 20 seconds to ensure complete mixing, and prepared for analysis as described in Section 2.3.

3.3.4 NMR Analysis

NMR spectra was collected using a Bruker Avance IIIHD spectrometer operating at 400.13 MHz. The probe used was a 5 mm BBI room temperature probe. The sample temperature was 298 K. A simple proton experiment was performed (30° pulse, 64 scans, 2 dummy scans, 20 ppm sweep width, 65536 data points). A 10 second relaxation delay was used in order to ensure complete relaxation between scans based upon a 1 second T_1 measurement.

3.3.5 Spectral Processing Parameters

Spectral processing was performed with Mestrenova 14.1 (Mestrelab, Santiago de Compostela, Spain). Automatic phase adjustment and polynomial baseline correction with an order of 5 was applied. All spectra were then normalized for intensity to the central peak of the ω-3 terminal methyl triplet at 0.975 ppm.

3.3.6 Principal Component Analysis

PCA analysis was performed using Mestrenova 14.2 (Mestrelab, Santiago de Compostela, Spain). The PCA analysis was blinded to six regions to eliminate portions of the spectrum irrelevant to oil analysis using the parameters outlined in Table 3.2. The PCA settings were as follows: binning mode regular with summed intensity, bin width: 0.05 ppm. Pareto scaling was applied.

Table 3.2. List of blinded regions used in the PCA analysis

High frequency limit (ppm)	**Low frequency limit (ppm)**	**Item eliminated**
-3.9	-1.0	Low frequency noise region
-0.2266	0.1892	TMS peak and satellites
6.995	7.006	$CDCl_3$ satellite peak
7.195	7.325	$CDCl_3$ main peak
7.502	7.548	$CDCl_3$ satellite peak
13.02	16.17	High frequency noise region

3.4. Results

*3.4.1 Normalization of spectra***.**

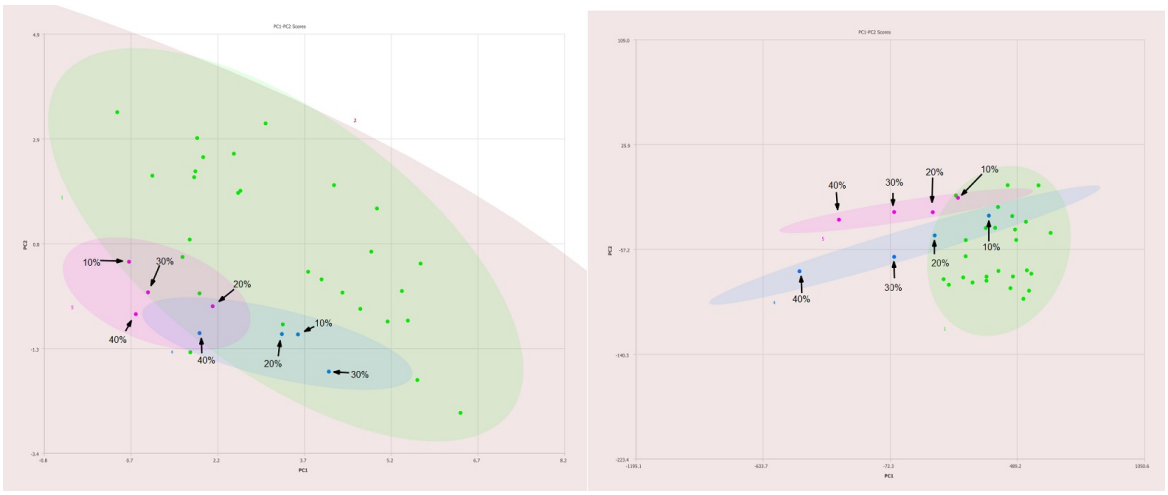

Figure 3.2. Comparison of PC1-PC2 plots of 400 MHz ^{1}H NMR spectra of pure olive oils (green), safflower oil adulterated olive oil (magenta) and sunflower oil adulterated olive oil (blue) showing the differences between traditional normalization (left) and normalization to ω-3 fatty acids (right).

As shown in Figure 3.2, reasonable grouping of olive oils (green) was observed with principal components 1 and 2 accounting for 97.7% and 1.8% of total variance respectively. The blue- and magenta-colored ellipses contain information about the adulterated olive oil samples. The percentages shown on the figure indicate the amount of adulterant oil added to olive oil. In the PC1-PC2 plot on the left-hand side, the intensities are normalized to the tallest peak in the spectrum. It is not possible to differentiate these samples easily even at adulteration levels of 40% v/v. However, when the spectra are normalized to the ω-3 methyl signal, as shown in right hand side of Figure 3.2, this technique becomes significantly more sensitive to adulteration with these oils and also

shows far tighter grouping of olive oil samples. Based on these results, all spectra were normalized to the ω-3 methyl signal in the remainder of the study.

3.4.2 Differentiation of olive and seed oils

A total of 28 single varietal and blended olive oils and 10 seed oils were analyzed via NMR with PCA performed on the collected spectra. Figure 3.3 summarizes the results.

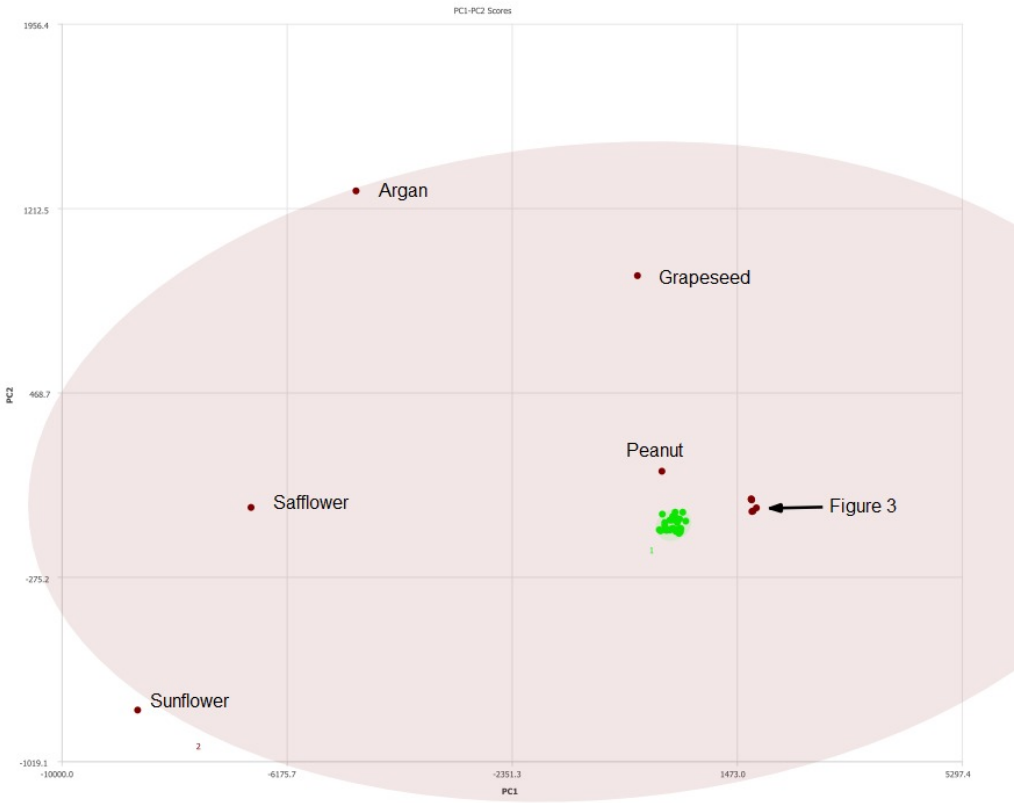

Figure 3.3. PC1-PC2 plot of 400 MHz ^{1}H NMR spectra of seed oils (labeled) versus olive oils (green). Ellipses represent the 95% confidence interval. The congested region is expanded in Figure 3.4.

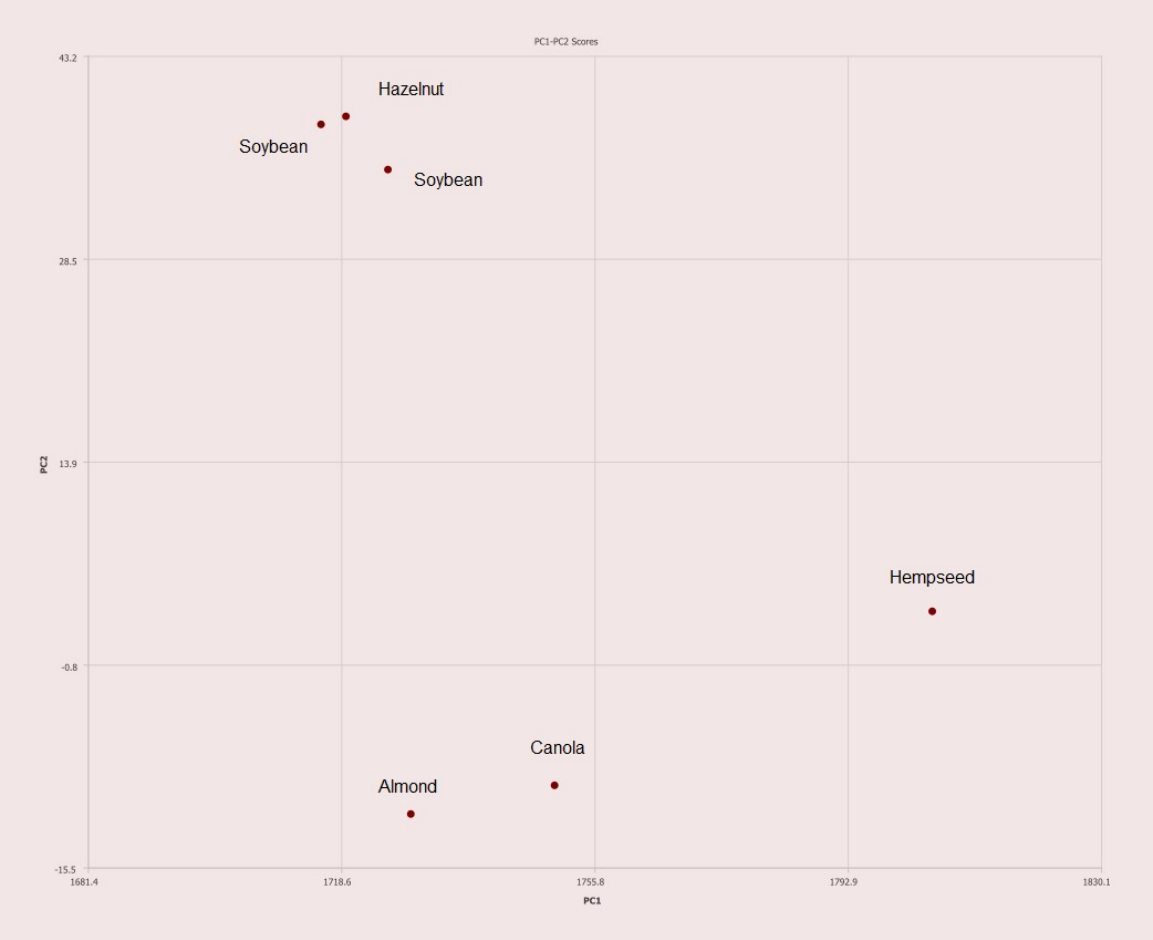

Figure 3.4. PC1-PC2 plot expansion of congested region in Figure 3.3.

The cluster of green dots are the different olive oils samples and are observed in a tight cluster. The seed oils are shown as maroon dots and are clearly separated from the olive oils. There is a cluster of seed oils (maroon) in Figure 3.3 to the right of the olive oils. This region is expanded in Figure 3.4. The expanded region clearly shows the differences between hazelnut oil and hempseed oil, for example.

3.4.2 Testing against mixtures of olive oil and seed oils.

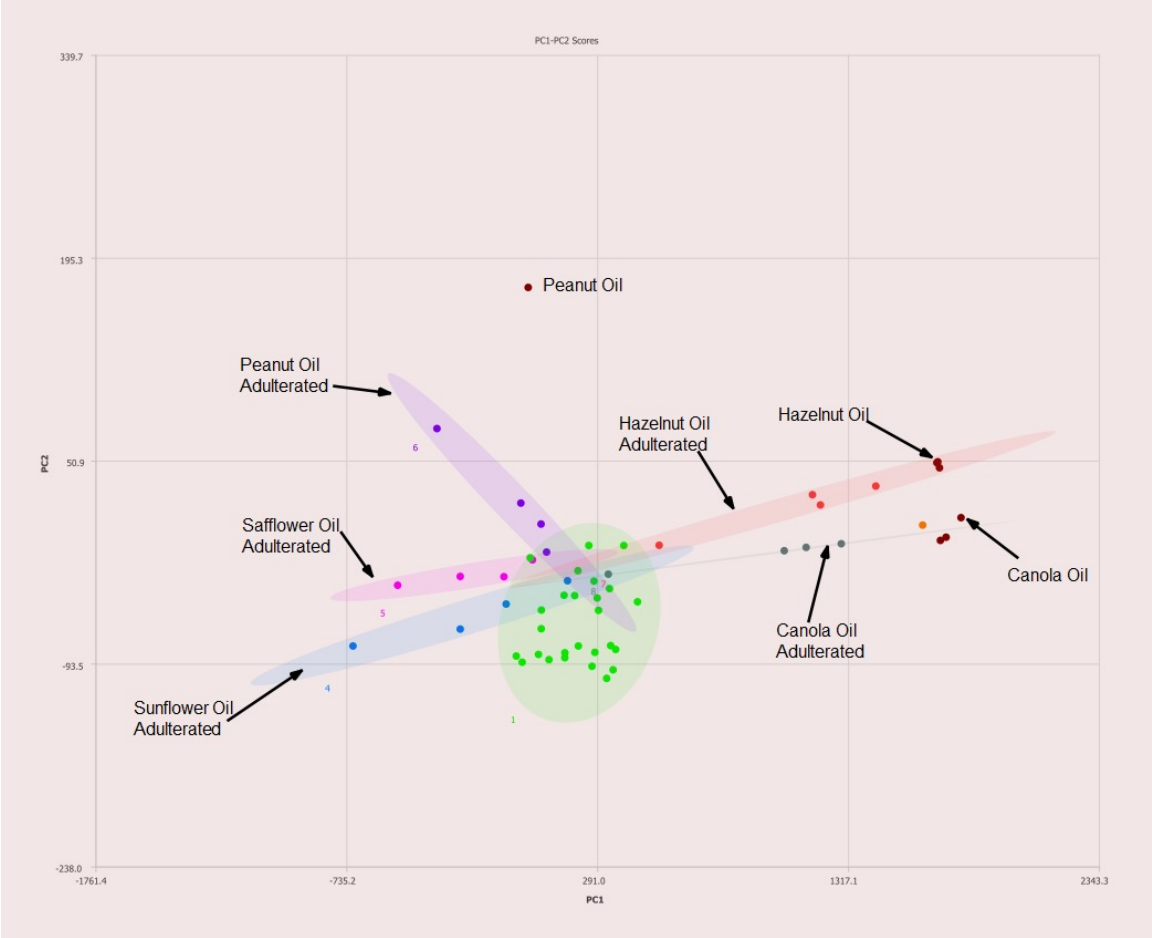

Figure 3.5. PC1-PC2 plot of 400 MHz ^{1}H NMR spectra of seed oils (labeled) versus olive oils (green). Ellipses represent the 95% confidence interval.

In Figure 3.5, the green dots represent the same olive oils shown in Figure 3.2. The extended ellipses represent olive oils samples that have been adulterated as described in the previous section. To the far right of the figure, the labeled maroon dots indicate the location of pure hazelnut oil (also indicated by an arrow in the figure). As the concentration of olive oil is increased the red dots show how the samples moved towards

the pure olive oil region (green). Four other oils were used to dilute olive oil. In each case, the undiluted sample (pure olive oil) resides in the green region. As the concentration of the adulterant oil increases, the ellipses move towards the respective oil used to dilute the olive oil (peanut, safflower, sunflower, or canola oil). Due to the greater degree of separation, particularly in the case of high-oleic canola, safflower, and sunflower oils, this allows for identification of the adulterant oil.

Figure 3.6 shows the results for different concentrations of canola oil compared to different olive oils. Pure canola oil shows excellent separation from pure olive oils as shown in Figure 3.6 with an ability to discriminate pure olive oils from those adulterated with canola at levels under 10% v/v.

Figure 3.6. PC1-PC2 plot of 400 MHz ^{1}H NMR spectra of olive oil adulterated with canola oil with percentages of adulteration noted. Ellipses represent the 95% confidence interval.

The results from the same type of experiment, but using hazelnut oil adulterated olive oil is easily detected even at levels as low as 5% v/v are shown in Figure 3.7. The pure hazelnut oil is easily distinguished from pure olive oil. The adulterated samples following a grouping between the two pure oils as the concentration of adulterated hazelnut oil is varied.

Figure 3.7. PC1-PC2 plot of 400 MHz ^{1}H NMR spectra of olive oil adulterated with hazelnut oil with percentages of adulteration noted. Ellipses represent the 95% confidence interval.

Peanut oil adulterated olive oil is detectable at concentrations below 20% v/v as shown in Figure 3.8. Again, pure peanut oil is easily separated from pure olive oil samples using the PCA analysis.

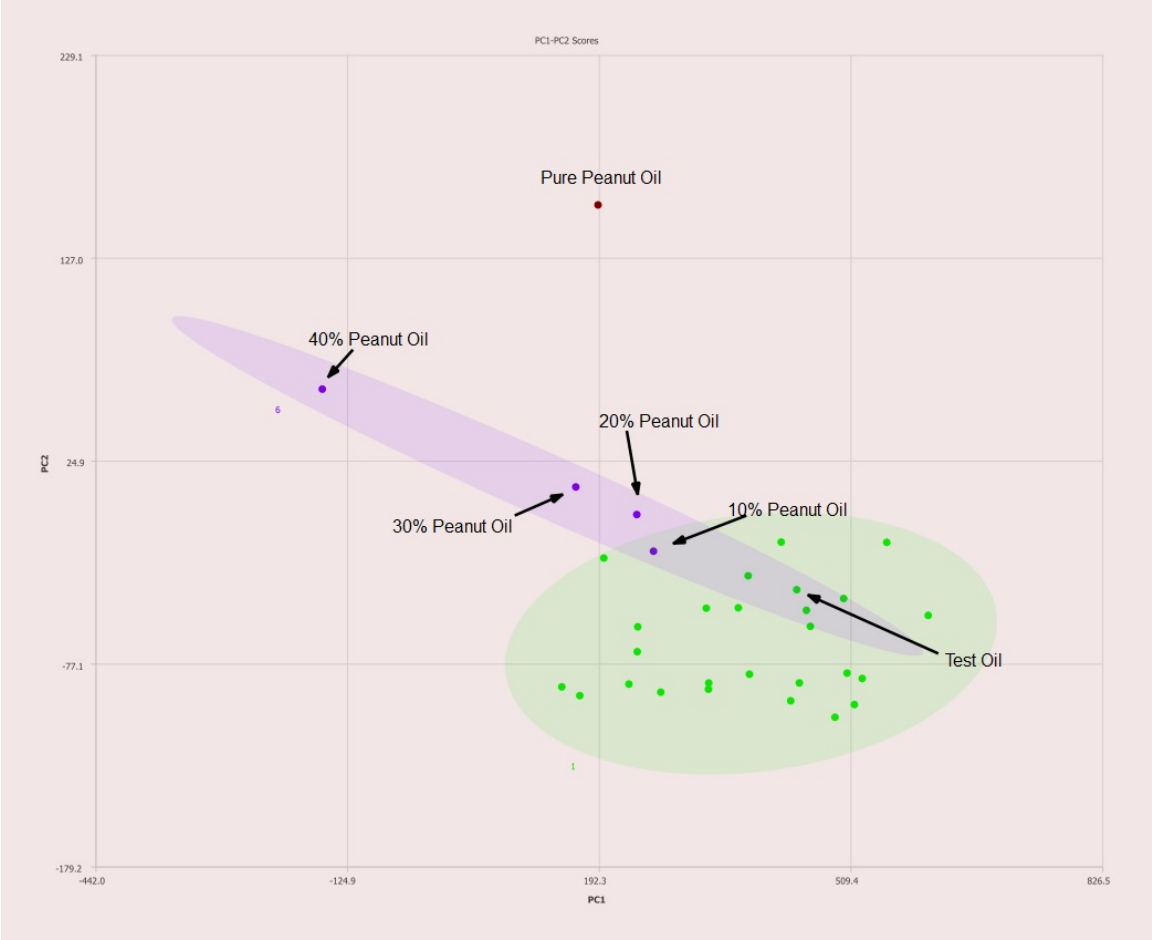

Figure 3.8. PC1-PC2 plot of 400 MHz ^{1}H NMR spectra of olive oil adulterated with peanut oil with percentages of adulteration noted. Ellipses represent the 95% confidence interval.

High oleic acid safflower oil is ordinarily rather difficult to distinguish from olive oils due to having similar lipid profiles. However, using this method it is detectable in levels slightly under 20% v/v as observed in Figure 3.9. Samples above this level are readily detected as not being olive oil.

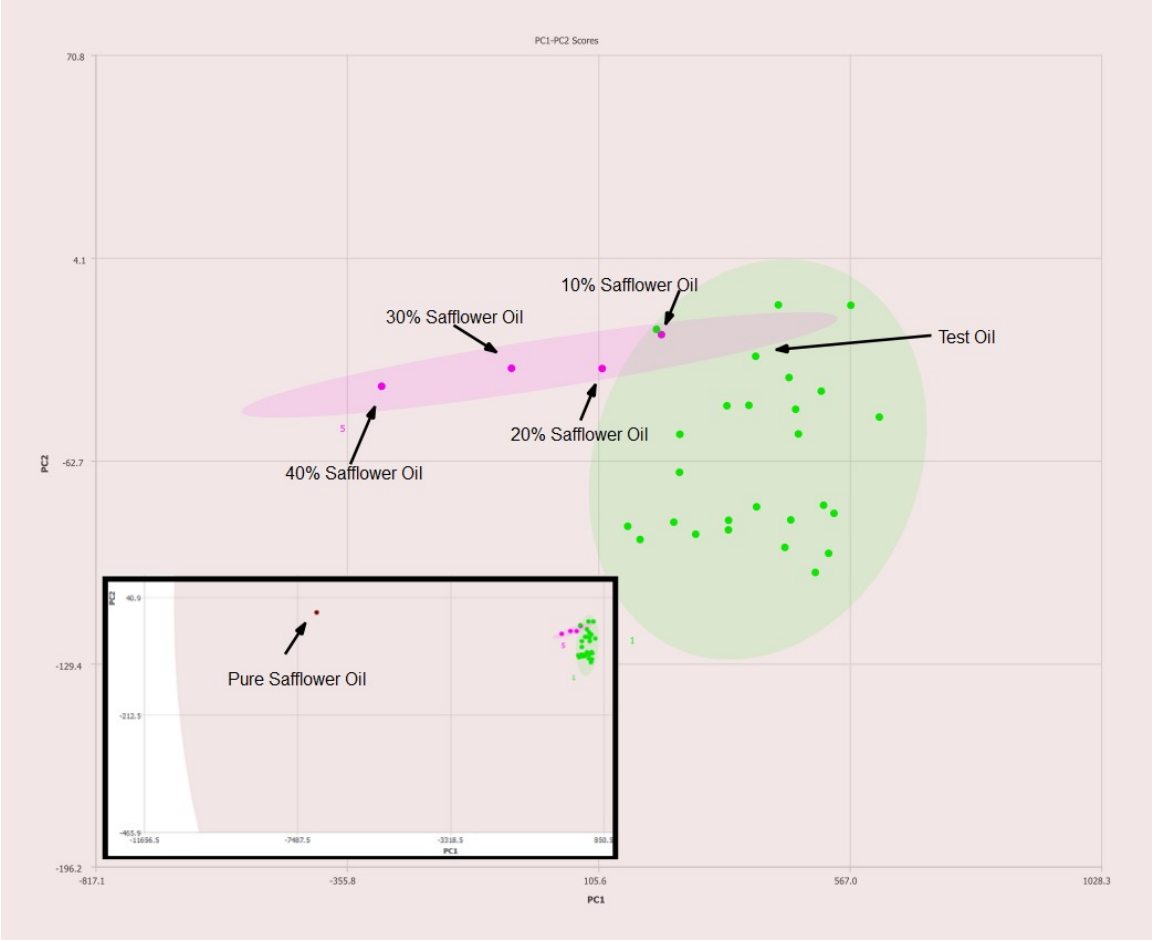

Figure 3.9. PC1-PC2 plot of 400 MHz ^{1}H NMR spectra of olive oil adulterated with safflower oil with percentages of adulteration noted. Ellipses represent the 95% confidence interval. The inset shows the expanded PCA plot to show the position of pure safflower oil with respect to the pure olive oil samples.

High oleic acid sunflower oil is another ordinarily difficult to detect adulterant of olive oils, yet it is detectable at levels just over 20% v/v using this method as seen in Figure 3.10. As the concentration of sunflower oil increases, the sample points on the PCA plot trend toward the pure sunflower oil sample. Differences in the adulterated oil

will affect the end result as not all olive oil samples fall exactly together on the PCA plot, but this tool will still identify high-oleic sunflower oil adulterated olive oils at economically viable levels.

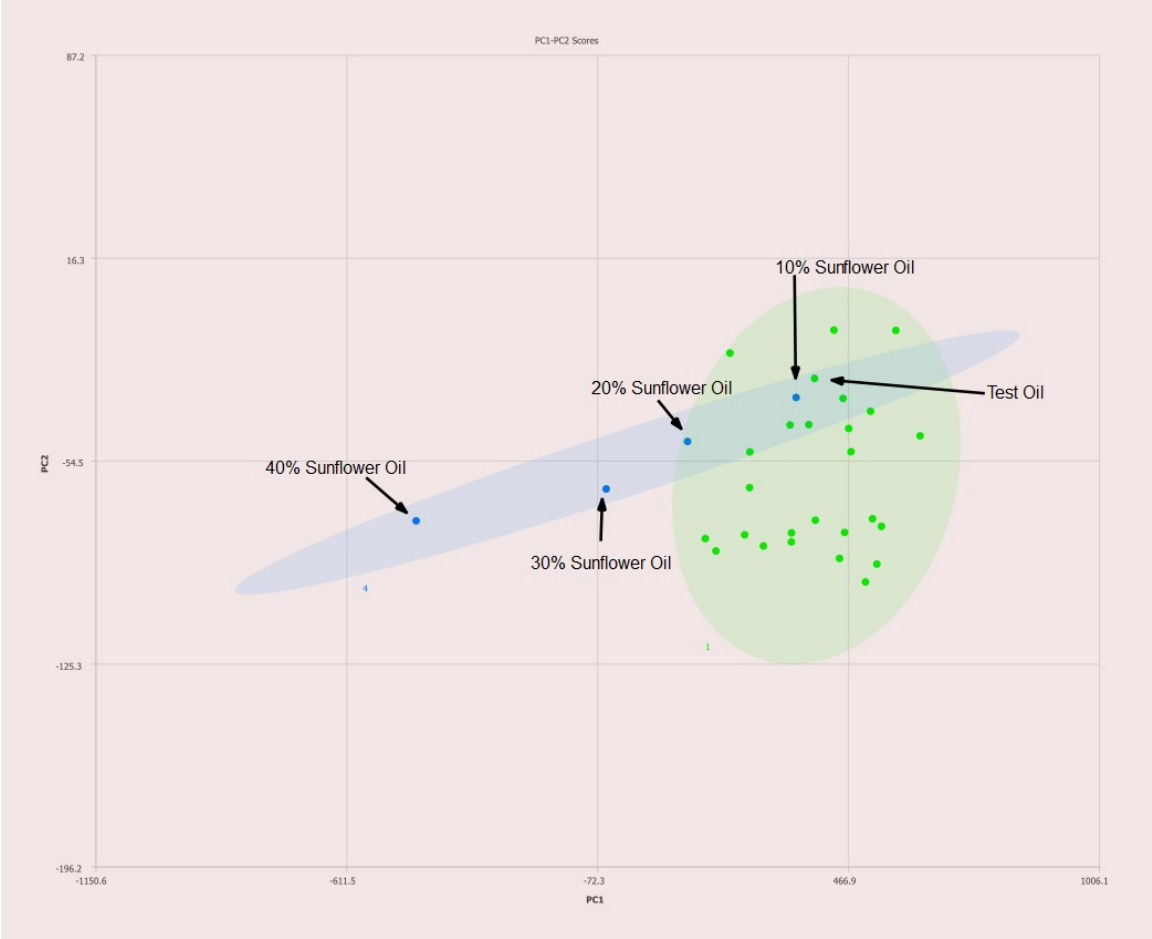

Figure 3.10. PC1-PC2 plot of 400 MHz ^{1}H NMR spectra of olive oil adulterated with sunflower oil with percentages of adulteration noted. Ellipses represent the 95% confidence interval.

A commercially available blend of 70% canola, 20% grapeseed, and 10% olive oils was tested for the sake of comparison. As expected, the placement on the PC1-PC2

plot is nearest to canola oil with slight deviation toward both olive and grapeseed oils as seen in Figure 3.11.

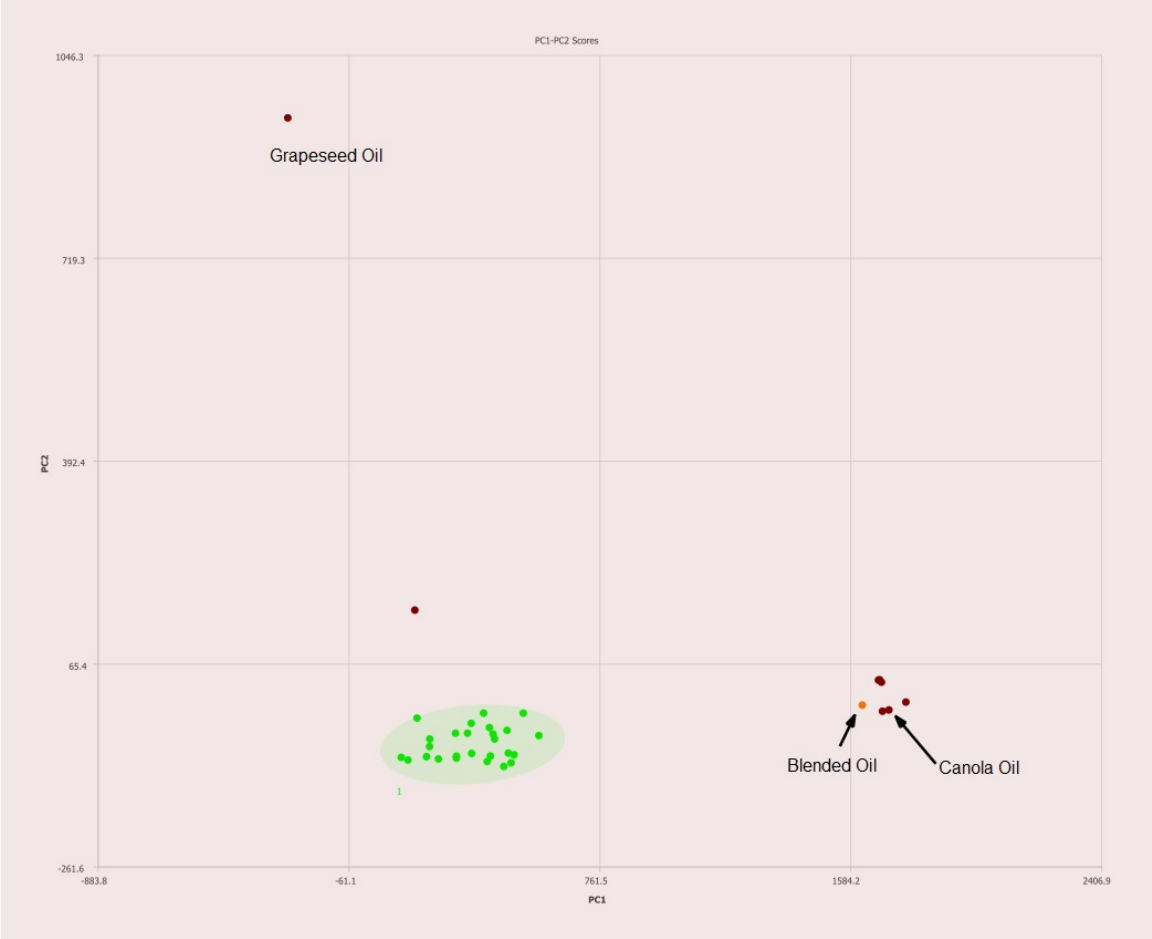

Figure 3.11. PC1-PC2 plot of 400 MHz ^{1}H NMR spectra of a commercially available blended oil composed of 70% canola, 20% grapeseed, and 10% olive oils (v/v). Ellipses represent the 95% confidence interval.

3.4.3 Detection of Adulterated Olive Oils

Upon successfully configuring this method it became clear that two of the olive oils, samples 1 and 27, originally purchased to determine a baseline for genuine olive oils appear to be adulterated themselves (Figure 3.11) as they lay outside the 95% confidence interval. Sample 1 was sold as a monovarietal arbequina extra virgin olive oil purchased from a from a boutique olive oil shop, and sample 27 was purchased from a grocer specializing in Middle Eastern products and was simply labeled "Moroccan Extra Virgin Olive Oil." Sample 1 was claimed to have been screened for authenticity via HPLC as part of grading. No testing was claimed for sample 27. Due to placement on the PC1-PC2 plot outside of the 95% confidence ellipse for olive oils, it is likely that both oils are adulterated at relatively low levels. Sample 1 is trending toward peanut or grapeseed oil. Sample 27 is trending toward a cluster of many other oils known to be used as adulterants and as such it is unclear as to which adulterant is included.

3.5. Discussion

Olive oils are known for having low levels of ω-3 fatty acids. By using the expected composition of olive oil during processing of oil spectra it is possible to greatly enhance the adulteration detection capability of a 400 MHz NMR. Typically, NMR spectra is normalized to the tallest peak in each spectrum. However, when one normalizes the intensity of oil spectra to the terminal methyl triplet of ω-3 fatty acids at 0.975 ppm as demonstrated here the spectral differences in non-olive oils are enhanced. As such adulterants such as high-oleic safflower and high-oleic sunflower oils that are ordinarily difficult to detect become readily detectable at economically viable levels of adulteration

with a 400 MHz instrument. The data summarized in Figures 3.9 and 3.10 demonstrate the enhanced ability to discern olive oils adulterated with high oleic sunflower oil and safflower oil compared to traditional normalization techniques.

Adulteration of olive oils with low ω-3 fatty acid containing oils such as peanut, high-oleic safflower, high-oleic sunflower and high oleic canola oils are still quite easy to detect when using this method. This method does not specifically rely on the presence of sterols, terpines, phenolic compounds, or other low abundance marker compounds that are often destroyed or removed during refining, allowing this method to be used on refined olive oils, as well as virgin, or extra virgin oils.

While effective detection of olive oil adulteration remains a challenge, this method of leveraging processing techniques in order to determine the authenticity of olive oils quickly using more accessible NMR instrumentation should allow for wider availability of NMR-based authenticity testing. Even with only 26 genuine olive oils in this series of experiments, it was possible to detect two probable adulterated olive oils already with real world samples. The accuracy of the model will improve with greater numbers of genuine olive oil samples. The greatest benefit is the ability to screen these oils effectively with a 400 MHz NMR system without the need for a cryogenically cooled probe or specialized diffusion probe.[3.10] The significantly reduced cost of the equipment needed to perform these analyses and the higher throughput of NMR compared to chromatography-based analyses should make NMR a very competitive instrumentation choice for authenticity analysis purposes.

3.6 References

3.1 Yan, J.; Erasmus, S.; Aguilera Toro, M.; Huang, H.; van Ruth, S. Food Fraud: Assessing Fraud Vulnerability In The Extra Virgin Olive Oil Supply Chain. *Food Control* 2020, *111*, 107081.

3.2 Boskou, D. Olive Oil, 2nd ed.; American Oil Chemists' Society: Urbana, 2006; pp 41-72.

3.3 Castejón, D.; Fricke, P.; Cambero, M.; Herrera, A. Automatic 1H-NMR Screening Of Fatty Acid Composition In Edible Oils. *Nutrients* 2016, *8* (2), 93.

Callaway, J. Hempseed As A Nutritional Resource: An Overview. *Euphytica* 2004, 140 (1-2), 65-72.

3.4 Stoyanova, R.; Brown, T. NMR Spectral Quantitation By Principal Component Analysis. *NMR in Biomedicine* 2001, *14* (4), 271-277.

Jabeur, H.; Zribi, A.; Makni, J.; Rebai, A.; Abdelhedi, R.; Bouaziz, M. Detection Of Chemlali Extra-Virgin Olive Oil Adulteration Mixed With Soybean Oil, Corn Oil, And Sunflower Oil By Using GC And HPLC. *Journal of Agricultural and Food Chemistry* 2014, *62* (21), 4893-4904.

3.5 Fang, G.; Goh, J.; Tay, M.; Lau, H.; Li, S. Characterization Of Oils And Fats By 1H NMR And GC/MS Fingerprinting: Classification, Prediction And Detection Of Adulteration. *Food Chemistry* 2013, *138* (2-3), 1461-1469.

3.6 Mannina, L.; Sobolev, A. High Resolution NMR Characterization Of Olive Oils In Terms Of Quality, Authenticity And Geographical Origin. *Magnetic Resonance in Chemistry* 2011, *49*, S3-S11.

3.7 Alonso-Salces, R.; Moreno-Rojas, J.; Holland, M.; Reniero, F.; Guillou, C.; Héberger, K. Virgin Olive Oil Authentication By Multivariate Analyses Of ^{1}H NMR Fingerprints And $\delta^{13}C$ and $\delta^{2}H$ Data. *Journal of Agricultural and Food Chemistry* 2010, *58* (9), 5586-5596.

3.8 Šmejkalová, D.; Piccolo, A. High-Power Gradient Diffusion NMR Spectroscopy For The Rapid Assessment Of Extra-Virgin Olive Oil Adulteration. *Food Chemistry* 2010, *118* (1), 153-158.

Chapter 4. Detection of Vegetable Oil Adulteration in Pre-Grated Bovine Hard Cheeses Via ^{1}H NMR

4.1 Abstract

Adulteration of food products is a widespread problem of great concern to society and dairy products are no exception to this. Due to new methods of adulteration being devised in order to circumvent existing detection methods, new detection methods must be developed to counter fraud. Bovine hard cheeses such as Asiago, Parmesan, and Romano are widely sold and consumed in pre-grated form as a convenience item. Due to being a processed product there is ample opportunity for the introduction of inexpensive adulterants and as such there is concern regarding the authenticity of these products. An analytical method was developed using a simple organic extraction to verify the authenticity of bovine hard cheese products by examining the lipid profile of these cheeses via proton NMR.

In this study, 52 samples of pre-grated hard cheese were analyzed as a market survey and a significant number of these samples were found to be adulterated with vegetable oils. This method is well suited to high throughput analysis of these products and relies on ratiometrics of the lipids in the samples themselves. Genuine cheeses were found to have a very consistent lipid profile from sample to sample, improving the power of this approach to detect vegetable oil adulteration. The method is purely ratiometric with no need for internal or external references, reducing sample preparation time and reducing the potential for the introduction of error.

4.2 Introduction

Bovine hard cheeses are a widely consumed dairy product throughout much of the world and pre-grated products made from these cheeses are popular as a condiment for many foods. The majority of these products are composed of grated cheese with small amounts of antimycotic preservatives, potassium sorbate was used in many samples in this study, and anti-caking agents such as cellulose powder. Some grated cheeses with no additives are also encountered. Adulteration of these products has previously been discovered involving addition of cellulose powder as a filler at levels far beyond those sufficient to prevent caking.[4.1] Due to the nature of this product's manufacture and its typical use as a garnish on other foods, it would seem a prime candidate for adulteration with a low chance of discovery by the consumer. This study was conducted in order to develop a method to test if cheese could and was being adulterated with vegetable sourced oils as a filler.

NMR analysis of food products is a powerful tool for the detection of adulteration. It is ideal for analyses of this type due to high sample throughput, the ability to discriminate based on structural differences of metabolites with similar masses, and the ability to examine samples in either their native state or with little sample preparation. Despite these abilities, NMR does not appear to have previously been applied to detecting adulteration of cheese with vegetable oils.

NMR simplifies analysis of structural features in analytes, and this becomes a very powerful tool to detect food fraud. While structural information can be inferred from chromatography retention times or from tandem mass spectrometry, it is inherent to NMR

experiments. It is particularly valuable when identifying lipids in edible oils or cheese. For example both α-linolenic acid and γ-linolenic acid are 18 carbon, triply unsaturated fatty acids found in edible oils with identical molecular weights of 278.436 daltons. Via LC-MS these fatty acids would only vary by retention time assuming adequate separation in the chromatography step. Tandem mass spectrometry can also be used to differentiate these, but this involves a separate experiment. However as α-linolenic acid is an ω-3 fatty acid with an unsaturated bond located 3 carbons from the terminal methyl group, its methyl group displays a distinct triplet proton resonance at approximately 0.97 ppm, where the ω-6 γ-linolenic's methyl signal is closer to 0.85 ppm.[4.2] This allows for much easier quantification of ω-3 fatty acids with NMR, and speeds the determination of a sample's lipid profile. Additionally this structural information is invaluable when comparing levels of polyunsaturated fatty acids, total numbers of unsaturated bonds, and ω-3 fatty acid levels present in a sample. While not an exhaustive analysis of the sample's composition, it is often sufficient to determine the authenticity of said sample.

The simplicity of NMR sample preparation is a natural compliment to its inherent speed of analysis. Simple dilution or liquid extractions are much less labor intensive than some sample preparation regimens required for other methods. Avoiding the need for steps such as derivatization for gas chromatography of non-volatile compounds, hydrolysis of triacylglycerols for analysis of lipids in mass spectrometry, and others greatly improves laboratory throughput and reduces the opportunity for sample contamination or errors. This also has the benefit of analyzing samples in their native or near-native state without chemical modification.

Analysis of cheese via NMR has been performed for quite some time. However, previous works were typically focused on aqueous extracts in order to determine point of origin[4.3, 4.4], or a combination of origination and the process of cheese ripening.[4.5] ^{1}H NMR based lipid profiling of cheese has been performed before, however this approach involved a lengthy soxhlet extraction step making it less appealing for routine screening of samples, and the study did not address adulteration.[4.5] The spectral differences between the lipid profiles of genuine cheese and imitation cheese prepared from vegetable oil was demonstrated previously but this method was also not applied to the detection of adulterated products in a market survey.[4.6] Mass spectrometry has also been used to profile the lipids in cheese but was similarly not used as an approach for detecting adulteration.[4.7]

The aim of this study was to create and test a method for the analysis of hard cheese products with the aim of detecting vegetable oil adulterants. The method was designed to be rapid in order to facilitate the use of it in high-throughput situations. The difference in lipid profiles between cheese and vegetable oils makes detection of adulterated cheeses relatively straightforward with a simple ratiometric analysis.

4.3 Experimental

4.3.1 Samples

Nine ungrated samples and one grated sample of various cheeses were analyzed in order to ascertain a lipid profile of unadulterated cheese samples. Of these baseline samples three were Parmesan, two were Romano, and one was Asiago. To gain a broader

understanding of cheese lipid profiles a sample of Mimolette, one sample of Piave cheese, and one sample each of ungrated and pre-grated mozzarella were also analyzed.

All market survey grated hard cheese samples were obtained from retailers, restaurants, and public school cafeteria kitchens. All samples were composed of Parmesan, Romano, Asiago, and combinations thereof. All samples are detailed in Table 4.1.

Table 4.1. List of all samples analyzed in this study

Sample	**Variety**	**Form**	**Type of Sample**
B1	Parmesan	Ungrated	Baseline
B2	Parmesan	Ungrated	Baseline
B3	Parmesan	Ungrated	Baseline
B4	Piave	Ungrated	Baseline
B5	Asiago	Ungrated	Baseline
B6	Romano	Ungrated	Baseline
B7	Romano	Ungrated	Baseline
B8	Mimolette	Ungrated	Baseline
B9	Mozzarella	Ungrated	Baseline
B10	Mozzarella	Grated	Baseline
1	Parmesan and Romano	Grated	Market Survey
2	Romano	Grated	Market Survey
3	Parmesan	Grated	Market Survey
4	Parmesan and Romano	Grated	Market Survey
5	Parmesan	Grated	Market Survey
6	Parmesan and Romano	Grated	Market Survey
7	Romano	Grated	Market Survey
8	Parmesan	Grated	Market Survey
9	Parmesan	Grated	Market Survey
10	Parmesan Romano and Asiago	Grated	Market Survey
11	Parmesan	Grated	Market Survey
12	Parmesan and Romano	Grated	Market Survey

13	Parmesan	Grated	Market Survey
14	Romano	Grated	Market Survey
15	Romano	Grated	Market Survey
16	Parmesan	Grated	Market Survey
17	Parmesan	Grated	Market Survey
18	Parmesan	Grated	Market Survey
19	Parmesan	Grated	Market Survey
20	Parmesan and Romano	Grated	Market Survey
21	Parmesan	Grated	Market Survey
22	Parmesan and Romano	Grated	Market Survey
23	Parmesan	Grated	Market Survey
24	Parmesan	Grated	Market Survey
25	Parmesan	Grated	Market Survey
26	Parmesan	Grated	Market Survey
27	Parmesan	Grated	Market Survey
28	Parmesan	Grated	Market Survey
29	Parmesan Romano and Asiago	Grated	Market Survey
30	Parmesan	Grated	Market Survey
31	Parmesan	Grated	Market Survey
32	Romano	Grated	Market Survey
33	Parmesan and Romano	Grated	Market Survey
34	Parmesan	Grated	Market Survey
35	Parmesan	Grated	Market Survey
36	Romano	Grated	Market Survey
37	Parmesan	Grated	Market Survey
38	Parmesan	Grated	Market Survey
39	Parmesan	Grated	Market Survey
40	Parmesan	Grated	Market Survey
41	Parmesan and Romano	Grated	Market Survey
42	Parmesan	Grated	Market Survey
43	Parmesan	Grated	Market Survey
44	Parmesan	Grated	Market Survey
45	Parmesan	Grated	Market Survey
46	Parmesan	Grated	Market Survey
47	Parmesan and Romano	Grated	Market Survey
48	Parmesan Romano and Asiago	Grated	Market Survey

49	Parmesan	Grated	Market Survey
50	Parmesan	Grated	Market Survey
51	Parmesan	Grated	Market Survey
52	Parmesan	Grated	Market Survey

4.3.2 Adulterant Oils

Canola, grapeseed, peanut, olive, high oleic sunflower, high oleic safflower, high linolenic safflower, soybean, and palm oils were purchased from local and online retailers and used as received.

4.3.3 Sample Preparation

50 ± 2.5 mg of each cheese was placed in a 1.5 mL flip top microcentrifuge tube. 1 mL of deuterated chloroform ($CDCl_3$ 99.8% D, 0.03% v/v TMS, Acros Organics, Switzerland) was added to and the tube was agitated for 30 minutes. The resulting extract was removed via pipette and filtered through glass wool directly into a 5 mm NMR tube for analysis.

4.4.4 ^{1}H NMR

The spectrometer used was a Bruker (Rheinstetten, Germany) Avance III HD spectrometer equipped with a TCI cryoprobe operating at 500.13 MHz. A proton experiment was performed with 16 scans (30° pulse, 20ppm sweep width, 10 second relaxation time based upon 1.0 second T_1, 65536 data points, 300 K sample temperature). Spectra was processed and analyzed using Mestrenova 14.2 (Mestrelab, Santiago de

Compostela, Spain). Processing parameters included referencing to TMS, 0.3 Hz apodization, exponential baseline correction, and automatic phase correction.

4.4.5 Ratiometric Analysis

The samples studied were found to have a spectrum consistent with lipids in the form of triacylglycerols. Five regions of interest were analyzed using the raw integral values from the associated peaks. (See Table 4.2 and Figure 4.1). All calculations were performed using LibreOffice Calc 7.1.8.1. (Berlin, Germany)

Table 4.2. Integrated regions used in this study

Peak	Range	Chemical Shift (ppm)	Description	Integration Range (ppm)
A	**Unsaturated Bonds**	5.342	Unsaturated bond protons	5.44-5.30
B	**Glycerol C2 Proton**	5.263	C2 glycerol proton	5.29-5.23
C	**Polyunsaturated bonds**	2.800	Methylene protons α to unsaturated bonds in polyunsaturated fatty acids	2.87-2.73
D	**ω-3 Methyl**	0.948	ω-3 fatty acid terminal methyl group	0.97-0.93
E	**Non ω-3 Methyl**	0.880	Terminal methyl group of all fatty acids aside from ω-3	0.91-0.85

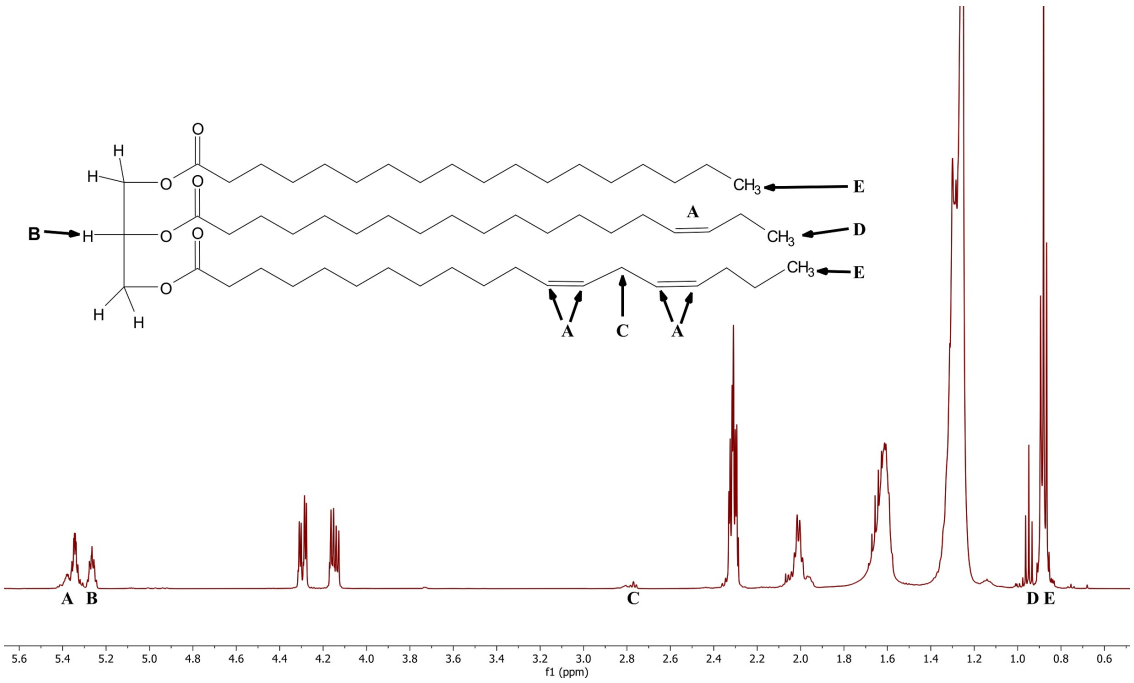

Figure 4.1. 500 MHz ^{1}H NMR spectrum of sample B1 with model triacylglycerol diagram of peaks used for analysis.

From these integral values four ratios were calculated: unsaturated bonds vs. glycerol, polyunsaturated bonds vs. glycerol, ω-3 methyl vs. remaining methyl groups, ω-3 vs. glycerol C2 proton, and unsaturated bonds vs. glycerol. Relying on these five regions eliminates spectral interference from residual water content and preservatives.

4.5 Results and Discussion

4.5.1 Results

Baseline cheese sample analysis showed acceptable consistency in all four ratios for all samples despite the variety of cheeses used (Table 4.3).

Table 4.3. Ratiometric values of all baseline cheeses

Ratio	**Mean**	**Standard Deviation**	**Relative Standard Deviation**
Unsaturated bonds/glycerol C2	1.78	0.15	8.18%
Polyunsaturated bonds/glycerol C2	0.23	0.04	15.29%
ω-3 methyl/remaining methyl	0.11	0.02	18.17%
ω-3 methyl/glycerol C2	0.89	0.11	12.31%

Analysis of the market survey cheese samples revealed many samples exhibiting significant deviations from both the values found in the baseline samples and the majority of the other survey samples tested. (**Figures 4.1-4.4, Appendix A3**)

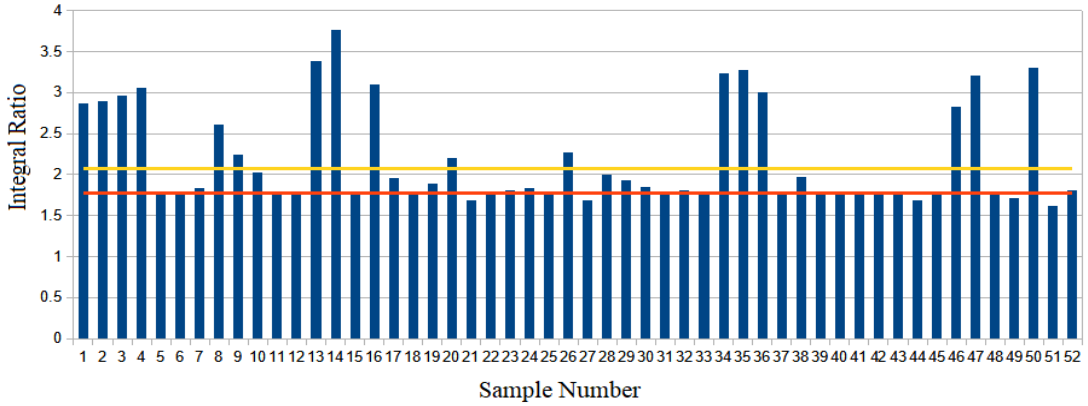

Figure 4.2. Unsaturated bond vs. glycerol C2 proton ratio of market survey samples. Baseline mean depicted with yellow line, orange line is mean plus two standard deviations.

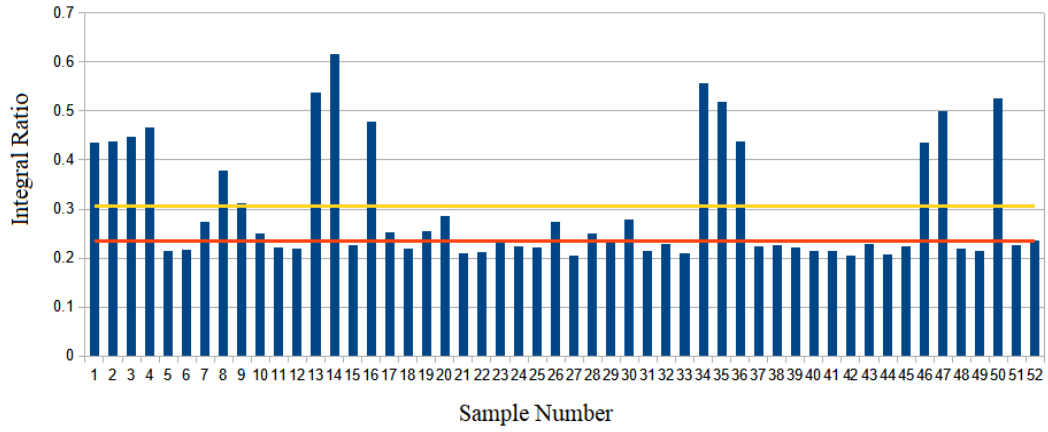

Figure 4.3. Polyunsaturated protons vs. glycerol C2 proton ratio of market survey samples. Baseline mean depicted with orange line, yellow line is mean plus two standard deviations.

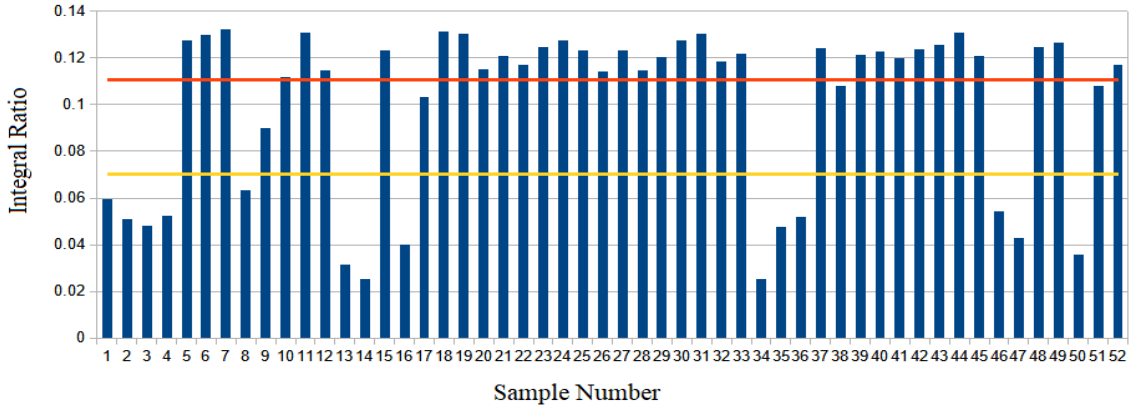

Figure 4.4. ω-3 methyl vs remaining methyl proton ratio of market survey samples. Baseline mean depicted with yellow line, orange line is mean minus two standard deviations.

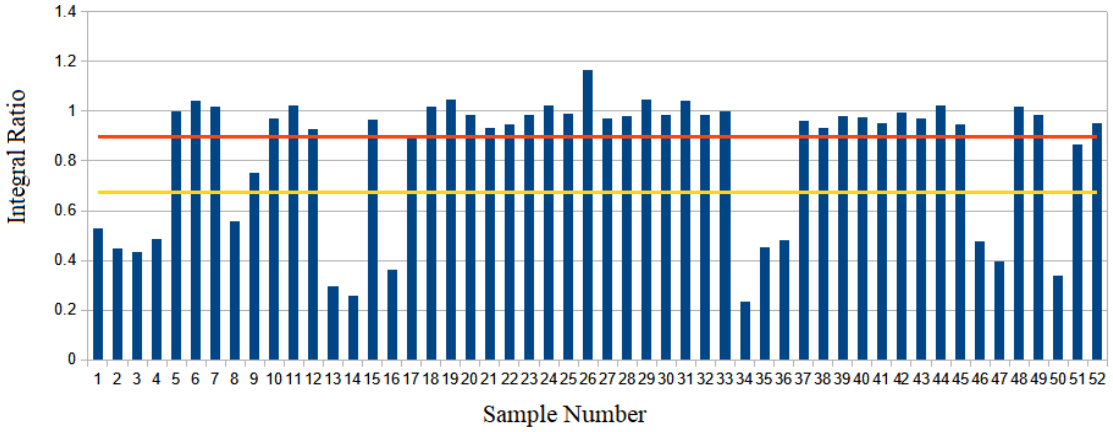

Figure 4.5. ω-3 methyl vs. glycerol C2 proton ratio of market survey samples. Baseline mean depicted with orange line, yellow line is mean minus two standard deviations.

Samples 1-4, 8, 9, 13, 14, 16, 34-36, 46, 47, and 50 all appear to be outliers with ratiometric values falling far outside of the majority and consistently do so with every ratiometric analysis. Aside from sample 9, they also consistently fall more than two standard deviations outside of the baseline mean. As such these samples were presumed to be adulterated and further investigation was pursued via comparing spectra of one outlying sample to two presumably unadulterated samples. Due to failing two ratiometric checks, sample 9 is also considered to be adulterated.

Superimposed spectra of sample 3, sample 42, and baseline sample B1 shows a radically different lipid profile in sample 3 versus the others when normalized for intensity to the 5.265 ppm glycerol C2 proton peak. The glycerol peak was used for normalization due to the majority of lipids in cheese being in the form of

triacylglycerol.[4.8] The remaining adulterated samples showed overall similar deviation from the baseline spectra with varying degrees of deviation. **Figure 4.6**

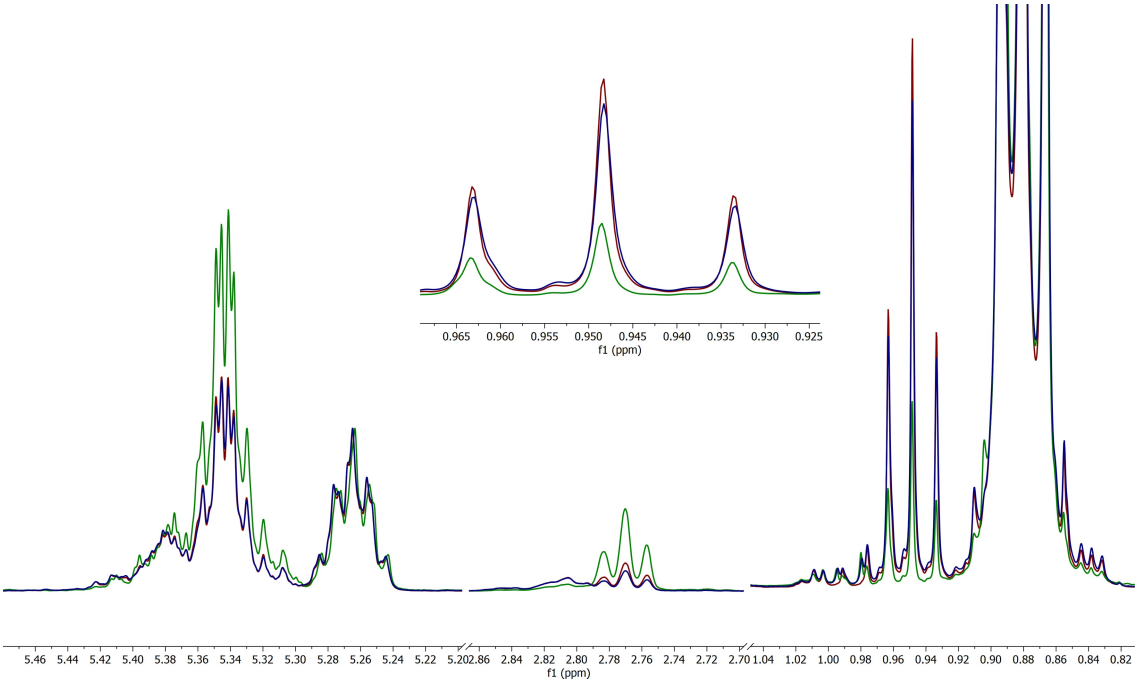

Figure 4.6. ^{1}H 500 MHz NMR spectral excerpt of samples 3 (green), 42 (blue), and B1 (maroon). Normalized for intensity to the glycerol peak at 5.265 ppm. Expansion of ω-3 terminal methyl region included for clarity.

The spectra of samples 42 and B1 are extremely similar. However sample 3 deviates in the difference in intensity between the C2 glycerol proton peak at 5.265 ppm and the unsaturated bonds peak at 5.342 ppm. This due to sample 3, relative to glycerol, containing a far greater abundance of unsaturated and polyunsaturated bonds than found

in the other cheese samples. The ω-3 fatty acid levels are far lower than what would be expected of a genuine cheese sample. An overabundance of unsaturated bonds, polyunsaturated bonds, and low levels of ω-3 fatty acids in sample 3 would suggest adulteration of this sample with a vegetable sourced oil. Despite being adulterated, sample 3 exhibited no remarkable olfactory or visual differences from any of the other grated cheese samples tested.

4.5.2 Adulterant Identification

In order to identify the adulterant used, a series of intentionally adulterated samples were prepared using sample 19 as a model cheese. Samples were prepared with vegetable oil adulteration in ranges from 5-60% by weight and analyzed as previously described. The adulterants used were Canola, grapeseed, peanut, olive, high oleic sunflower, high oleic safflower, high linolenic safflower, soybean, and palm oils. Most oils yielded lipid profiles inconsistent with the adulterated cheese samples, but palm oil yielded a lipid profile nearly identical to sample 3. The results are detailed in Table 4.4

Table 4.4. Adulterant identification trial results

Adulterant Oil	Match?	Comments
Canola	NO	ω-3 fatty acids too abundant
Grapeseed	NO	ω-3 and polyunsaturated fatty acids too abundant
Peanut	NO	ω-3, polyunsaturated and total unsaturated bonds too abundant
Olive	NO	ω-3, polyunsaturated and total unsaturated bonds too abundant
Sunflower	NO	ω-3, polyunsaturated and total unsaturated bonds

		too abundant
High Oleic Safflower	NO	ω-3 fatty acids too abundant
High Linoleic Safflower	NO	ω-3, polyunsaturated and total unsaturated bonds too abundant
Soybean	NO	ω-3 fatty acids too abundant, insufficient levels of polyunsaturated fatty acids
Palm	YES	Near perfect match at 40% adulteration (w/w)

Comparing the other samples suspected of adulteration to intentionally adulterated cheese spectra shows that all of the suspicious samples appear to be adulterated with palm oil to varying degrees. A further study was conducted in order to more conveniently estimate the rate of palm oil adulteration in suspected samples using a calibration curve using integral ratios.

4.5.3 Adulterant Quantification

Quantification of the level of palm oil adulteration in these samples was accomplished by generating calibration curves of two peak ratios. This allows for convenient and more precise estimation of the amount of palm oil in the sample versus the amount of actual cheese. It does not take into account the insoluble anti-caking agents present in all adulterated samples studied and therefore is not a measurement of the total w/w adulteration rate. Despite this limitation the calculation does yield important information as to the degree of palm oil adulteration in these samples. Baseline sample B1 was used to make samples adulterated with palm oil in the range of 10 to 90 percent by weight. All samples were extracted and analyzed as described previously. The ratios of the intentionally adulterated cheese were calculated and plotted to generate a calibration

curve allowing an estimation of the degree of palm oil adulteration versus cheese in each sample. The functions for each curve followed an exponential regression. The equation for ω-3 vs. remaining methyl peak was found to be $F_{(x)}=108.9584 \times e^{-29.7812x}$. For the ω-3 vs glycerol ratio the equation was $F_{(x)}=-112.0973 \times e^{-3.3871x}$. The correlation coefficients for these curves are values of 0.989 and 0.983 respectively. (Figure 4.7.)

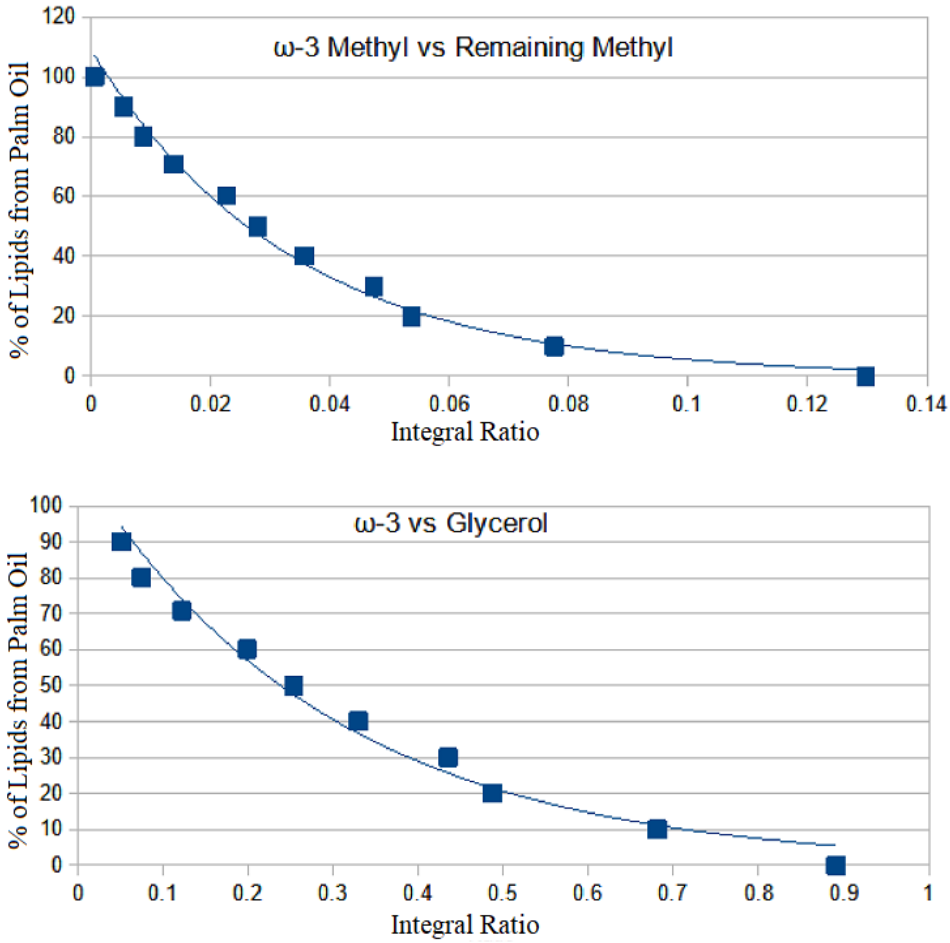

Figure 4.7. Adulteration calibration curves obtained from ^{1}H NMR spectra of serially adulterated cheese

These calibration curves were used to calculate the approximate amounts of palm oil added to each sample relative to cheese with no accounting for any additional binders. The calculated values were found to be similar to values determined by overlaying spectra of market survey samples with spectra of serially adulterated samples (Table 4.5). While this does not yield an exact determination of the level of adulteration it does serve to calculate a general estimate of palm oil adulteration levels in these products.

Table 4.5. Calculated levels of palm oil adulteration in adulterated samples.

Sample Number	Adulteration Level By Spectral Comparison	Calculated Adulteration Level
1	30%	31%
2	35%	46%
3	50%	49%
4	60%	54%
8	20%	21%
9	15%	11%
13	60%	59%
14	70%	73%
16	40%	35%
34	70%	65%
35	60%	51%
36	60%	55%
46	30%	26%
47	60%	54%
50	60%	56%

4.5.4 Conclusions

This study revealed a previously undiscovered method of adulterating pre-grated bovine hard cheeses for economic purposes. Palm oil itself is a clever adulterant owing to

its semi-solid state at room temperature, similar color to cheese, and low price compared to cheese. Presumably these adulterated products contain higher than normal levels of cellulose or other binders in order to maintain the appearance of the product. However as this study is strictly limited to the lipid profile of these products and no attempts were made to quantify any fillers aside from palm oil.

In this study 28.8% of all samples tested were certainly adulterated with palm oil. That combined with nearly half of the adulterated samples possessing lipid fractions composed of greater than 50% palm oil shows a rather brazen attitude in this industry regarding the commission of fraud through adulteration of these products. The 52 samples tested are by no means an exhaustive survey of all pre-grated hard cheeses sold, however it does reveal a new frontier in food adulteration. The method described herein will make detection of this new type of food adulteration straightforward and aid in combating the problem.

4.6 References

4.1 U.S. Food and Drug Administration. 2022. *Economically Motivated Adulteration (Food Fraud)*. [online] Available at: <https://www.fda.gov/food/compliance-enforcement-food/economically-motivated-adulteration-food-fraud> [Accessed 17 April 2022].

4.2 4.5 Tociu, M., Todasca, M., Bratu, A., Mihalache, M. and Manolache, F., 2018. Fast approach for fatty acid profiling of dairy products fats using 1 H-NMR spectroscopy. *International Dairy Journal*, 83, 52-57.

4.3 Tenori, L., Santucci, C., Meoni, G., Morrocchi, V., Matteucci, G. and Luchinat, C., 2018. NMR metabolomic fingerprinting distinguishes milk from different farms. *Food Research International*, 113, 131-139.

4.4 Segato, S., Caligiani, A., Contiero, B., Galaverna, G., Bisutti, V. and Cozzi, G., 2019. 1H NMR Metabolic Profile to Discriminate Pasture Based Alpine Asiago PDO Cheeses. *Animals*, 9(10), 722.

4.5 Consonni, R. and Cagliani, L., 2008. Ripening and geographical characterization of Parmigiano Reggiano cheese by 1H NMR spectroscopy. *Talanta*, 76(1), 200-205.

4.6 Monakhova, Y., Godelmann, R., Andlauer, C., Kuballa, T. and Lachenmeier, D., 2013. Identification of Imitation Cheese and Imitation Ice Cream Based on Vegetable Fat Using NMR Spectroscopy and Chemometrics. *International Journal of Food Science*, 2013, 1-9.

4.7 Damário, N., de Oliveira, D., Ferreira, M., Delafiori, J. and Catharino, R., 2015. Cheese lipid profile using direct imprinting in glass surface mass spectrometry. *Analytical Methods*, 7(6), 2877-2880.

4.8 Jensen, R., 2002. The Composition of Bovine Milk Lipids: January 1995 to December 2000. *Journal of Dairy Science*, 85(2), 295-350.

Chapter 5. Delta-8 Tetrahydrocannabinol Product Impurities

5.1 Abstract

Due to increased concerns regarding unidentified impurities in delta-8 tetrahydrocannabinol (Δ-8 THC) consumer products, a study using Nuclear Magnetic Resonance (NMR), HPLC, and mass spectrometry was conducted to further investigate these products. Ten Δ-8 THC products, including distillates and ready to use vaporizer cartridges, were analyzed. The results yield findings that the tested products contain several impurities in concentrations far beyond what is declared on certificates of analysis for these products. As Δ-8 THC is a synthetic product synthesized from cannabidiol (CBD), there are valid concerns regarding the presence of impurities in these products with unknown effects on the human body. Compounding this problem is apparent inadequate testing of these products by producers and independent laboratories.

5.2. Introduction

Delta-8 tetrahydrocannabinol (Δ-8 THC) is a structural isomer of the well-known active ingredient in cannabis products, Δ-9 THC, differing only by the location of an unsaturated bond. Due to a technicality in the legal definition, hemp-derived Δ-8 THC became effectively unregulated by federal law in the United States as part of section 10113 in The Agricultural Improvement Act of 2018.[5.1] This has resulted in a number of hemp product producers marketing these products in regions where local laws do not address them by using CBD derived from industrial hemp as feedstock for this synthesis.

Δ-8 THC is synthesized from CBD by a ring closure reaction often involving harsh reaction conditions (**Figure 5.1**).[5.2]

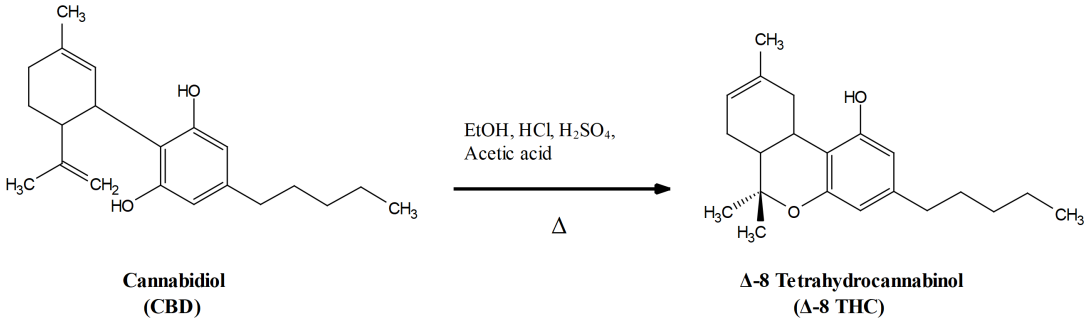

Figure 5.1. Example reaction scheme for one published synthesis of Δ-8 THC from CBD.[5.3] Inter-ring bond length on cannabidiol exaggerated for clarity.

As with many organic syntheses, it is prone to side reactions. A recent mass spectrometry-based analysis of (Δ-8 THC) products reported finding a number of unknown impurities in these products.[5.3] In order to further investigate potential unknowns in these products, a study was performed by analysis of ten Δ-8 THC products, of which half were sold as high purity distillates and the remainder were ready to use cartridges for use in vaporizer devices.

5.3. Experimental

5.3.1 Samples

All samples were purchased online or at local retailers. All vaporizer cartridges contained added non-THC hemp extracts in order to convey an organoleptic experience

similar to particular strains of cannabis. Most samples contained a certificate of analysis (COA), with some denoting analysis via high performance liquid chromatography (HPLC) equipped with an ultraviolet (UV) or diode array detector (DAD) (Table 5.1).

Table 5.1. List of samples studied

Sample	Type of Sample	Color of Sample	Terpenes added?	Certificate of Analysis (COA)
1	Distillate	Clear	N/A	≥99% Δ-8 THC
2	Distillate	Clear	N/A	94.7% Δ-8 THC
3	Distillate	Pink-brown	N/A	93.43% Δ-8 THC
4	Distillate	Brown	N/A	87.1% Δ-8 THC
5	Distillate	Light Yellow	N/A	93.4% Δ-8 THC
6	Vaporizer Cartridge	Yellow-Brown	Yes	92.96% Δ-8 THC
7	Vaporizer Cartridge	Yellow Brown	Yes	No COA Supplied
8	Vaporizer Cartridge	Yellow	Yes	93.44% Δ-8 THC
9	Vaporizer Cartridge	Yellow	Yes	93.44% Δ-8 THC
10	Vaporizer Cartridge	Yellow	Yes	93.44% Δ-8 THC

5.3.2 ^{1}H NMR

Approximately 50 mg of each product was dissolved in 600 µL of deuterochloroform ($CDCl_3$ 99.8% D, 0.03% v/v TMS, Acros Organics, Switzerland), and loaded into a 5 mm NMR tube for analysis. The spectrometer used was a Bruker (Rheinstetten, Germany) Avance III spectrometer equipped with a TCI cryoprobe operating at 800.15 MHz. All samples were allowed to thermally equilibrate for 5

minutes after loading into the magnet. A 16 scan proton experiment (30° pulse, 14 ppm sweep width, 15 second relaxation time based upon 1.4 second T_1, 128000 data points, 300 K sample temperature) was carried out. Spectra was processed using Mestrenova 14.2 (Mestrelab, Santiago de Compostela, Spain).

For comparison, a proton experiment was performed on sample 3 using a Bruker Avance IIIHD spectrometer operating at 400.13 MHz equipped with an inverse probe. All experimental and processing parameters were identical to the 800 MHz experiment.

5.3.3 HPLC Analysis

Approximately 40 mg of sample 4 was dissolved in 1 mL of HPLC grade acetonitrile (Fisher Scientific, Fair Lawn, NJ). HPLC analysis was performed using a Waters (Waters, Milford, Massachusetts, USA) 1525 HPLC equipped with a Waters 2487 UV detector operating at 210 nM. An isocratic separation was performed with a 1.4:1 acetonitrile to water mobile phase with a 15 min total run time and flow rate of 1.8 ml per minute. The stationary phase used was a Waters 5µm C18 4.6×150mm column.

2.4 HPLC-Mass Spectrometry

15 mg of sample 4 was dissolved in 1 mL of HPLC grade acetonitrile. Mass spectrometry analysis was performed using a Thermo Finnegan LCQ Deca Plus mass spectrometer equipped with an ESI source and using positive ion mode. Chromatography was performed with a 5 µm C18 column with dimensions of 2.1×150 mm (GL Sciences, Tokyo, Japan). The mobile phase used was 2.125:1 H_2O and acetonitrile each with 0.1% v/v formic acid under isocratic conditions with a flow rate of 0.5 mL per minute. The injection volume was 10 µL. Mass spectra were processed using Xcalibur 2.0.7 (Thermo

Scientific, San Jose, CA). MS-MS experiments were performed under identical conditions with a collision energy of 30%.

5.3. Results and Discussion

Initial NMR analysis of the major peaks in the collected spectra show that the major product is consistent with published chemical shifts of Δ-8 THC (**Figure 5.2**).[5.4]

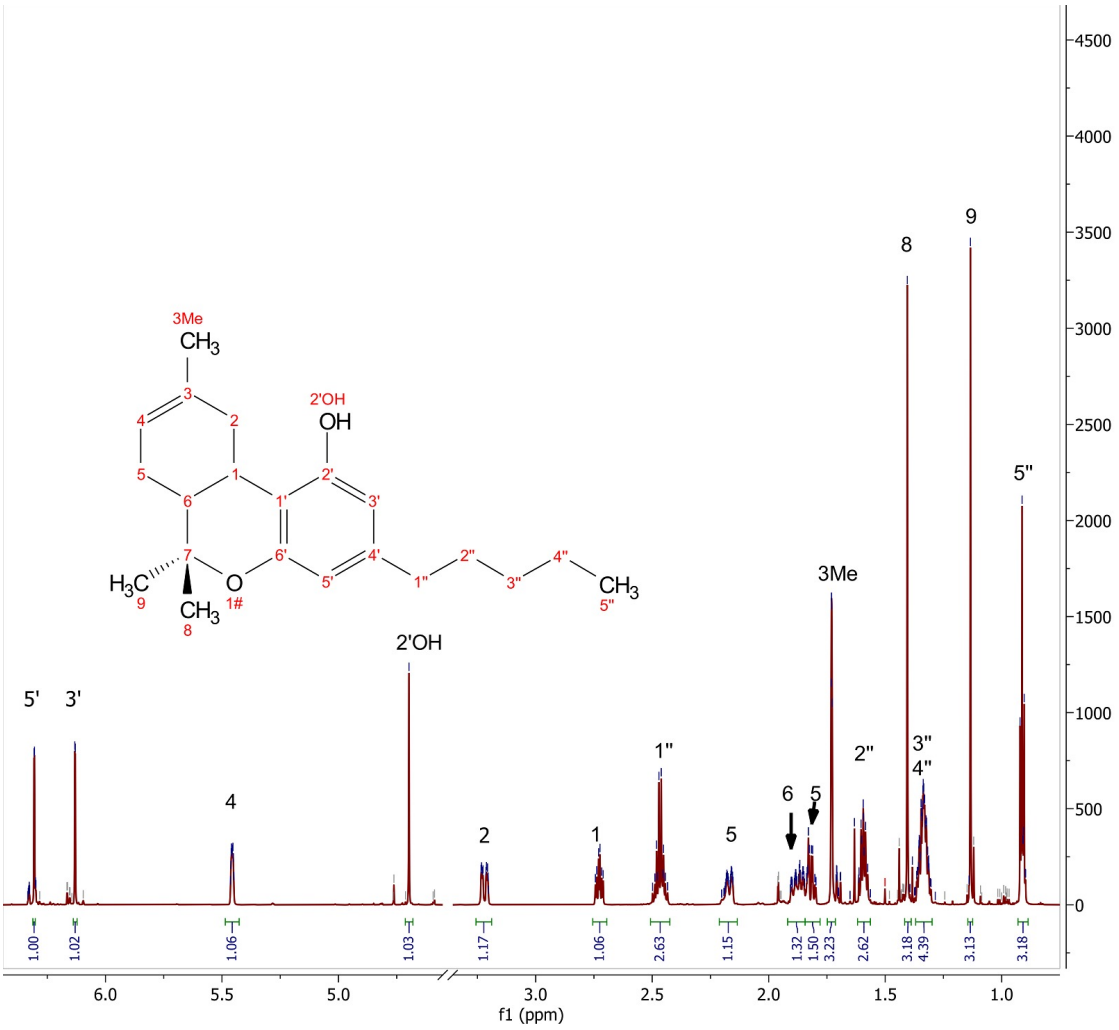

Figure 5.2. 800MHz ^{1}H NMR spectrum of selected sample 3 (empty region from 3.35 ppm to 4.55 ppm omitted) (800 MHz, $CDCl_3$) δ 6.27 (d, *J* = 1.6 Hz, 1H), 6.10 (d, *J* = 1.6 Hz, 1H), 5.49 – 5.37 (m, 1H), 4.67 (s, 1H), 3.19 (ddd, *J* = 17.6, 5.0, 1.9 Hz, 1H), 2.70 (td, *J* = 10.9, 4.8 Hz, 1H), 2.53 – 2.37 (m, 3H), 2.14 (ddt, *J* = 15.7, 4.3, 1.7 Hz, 1H), 1.89 – 1.81 (m, 1H), 1.80 – 1.75 (m, 1H), 1.70 (d, *J* = 1.2 Hz, 2H), 1.58 – 1.53 (m, 3H), 1.37 (s, 3H), 1.34 – 1.26 (m, 4H), 1.10 (s, 3H), 0.88 (t, *J* = 7.0 Hz, 3H).

With the integral for the proton signal on carbon 5' calibrated to 1.0 proton, few of the other integrals match up to the expected values. As a result, the overall proton count by

integration is 31 for Figure 5.2. A proton integration of 27 is expected for Δ-8 THC. While the deviations are slight, typically less than 10% deviation is expected, examination of the minor peaks show the presence of many impurities.

Upon closer inspection of the region surrounding the peak from the proton on carbon 5' in sample 3 it becomes very apparent that there are multiple products in this sample (**Figure 5.3**). This sample was certified as 93.43% pure Δ-8 THC with no other cannabinoids detected.

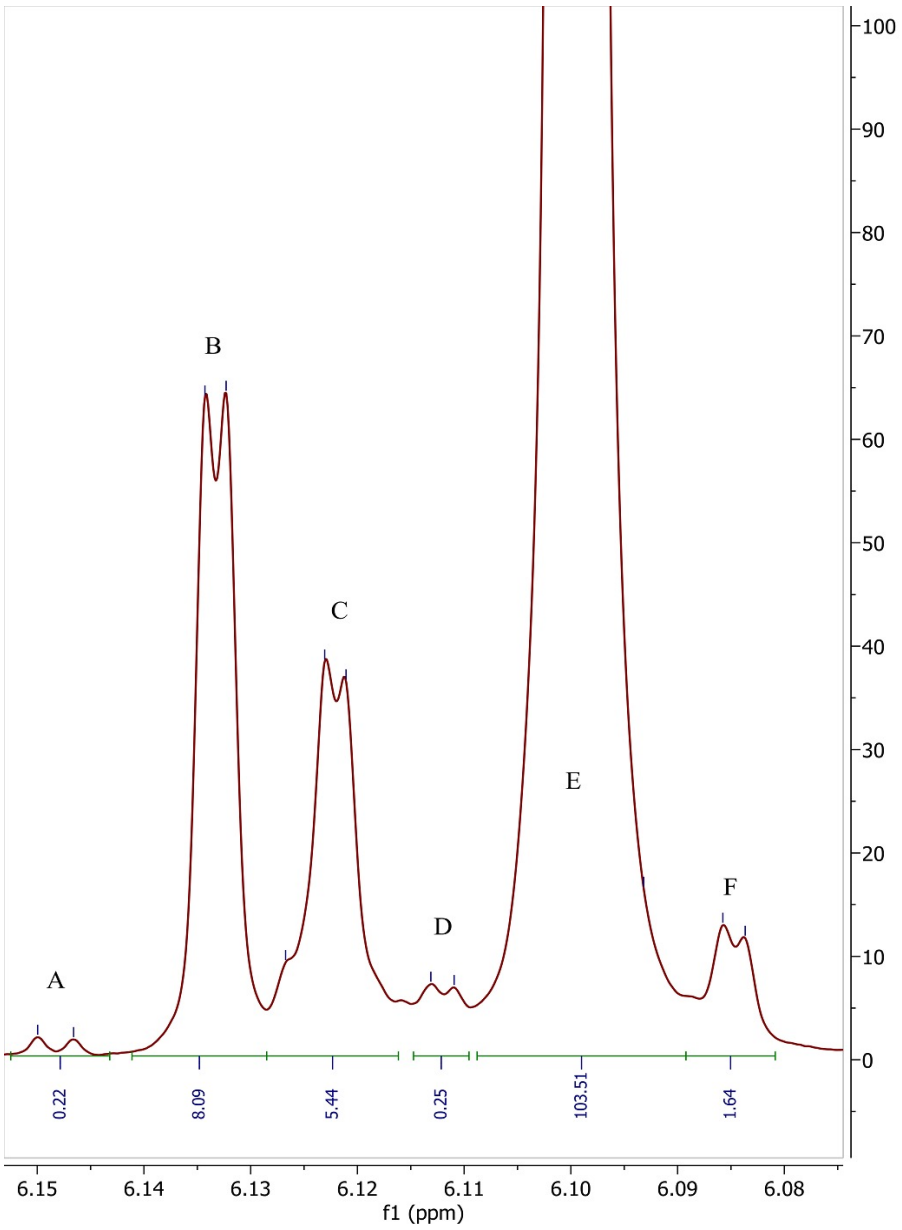

Figure 5.3. 6.075 to 6.155 ppm region detailing 3' proton resonance of sample 3. ^{1}H NMR (800 MHz, $CDCl_3$) δ 6.15 (d, J = 2.7 Hz), 6.13 (d, J = 1.6 Hz), 6.12 (d, J = 1.6 Hz), 6.11 (d, J = 1.7 Hz), 6.10 (d, J = 1.6 Hz), 6.08 (d, J = 1.7 Hz).

The presence of four extraneous doublet peaks, all with *J* values of 1.6-1.7 Hz suggests that these peaks may well be equivalent protons on isomers of Δ-8 THC or some other form of cannabinoid. All other samples show similar impurities with the expanded spectral excerpts available in the Supplemental Information (Sample S3). Peaks "A" and "D" in Figure 5.3 may potentially belong to compounds 1 and 2 described by Radwan.[5.5] Though the relatively congested peak area for carbon 3' shows no clear peak of similar integral value at 6.27 ppm and 6.24 ppm respectively (**Figure 5.4**).

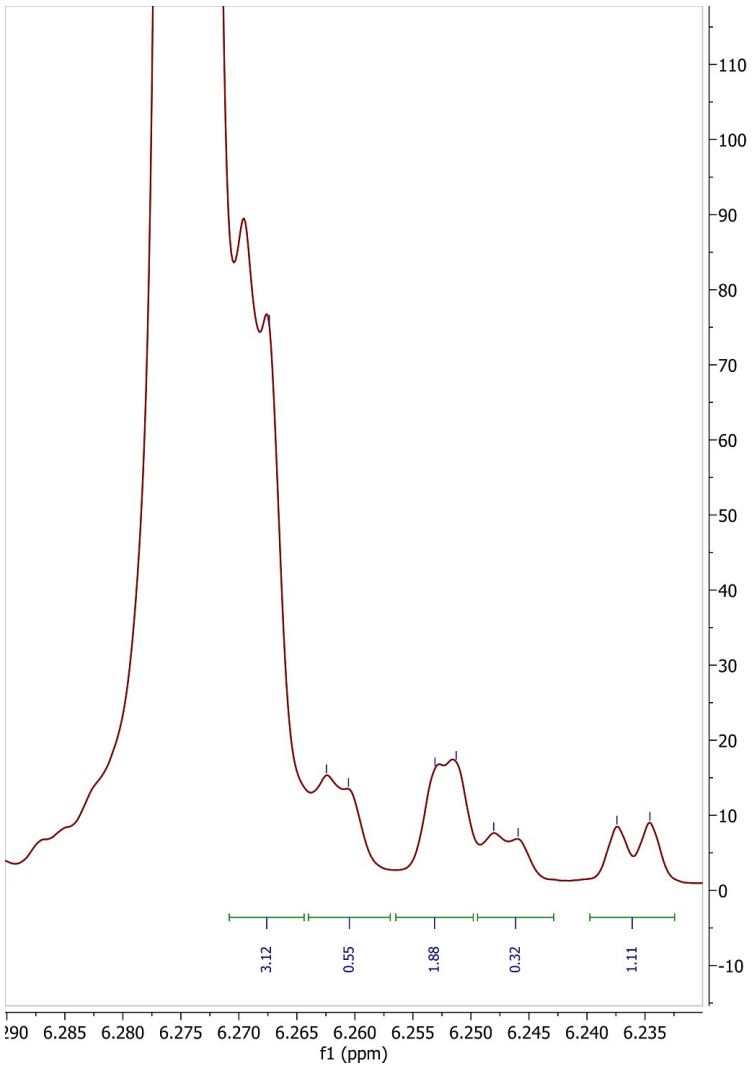

Figure 5.4. 6.23 to 6.29 ppm region detailing 5' proton resonance of sample 3. (800 MHz, $CDCl_3$) δ 6.15 (d, J = 2.4 Hz), 6.26 (d, J = 1.6 Hz), 6.25 (d, J = 1.4 Hz), 6.24 (d, J = 2.2 Hz).

When the integral of the major product peak "E" (Figure 5.3) is calibrated to 100 protons it becomes quite clear that over 15% of this product is not consistent with Δ-8 THC, even when ignoring the extraneous peaks in the lower frequency portions of the spectrum. Table 5.2 details the relative impurity totals for all samples examined.

With the Δ-8 THC 5’ peak (peak E) integral value adjusted to 100, a simple percentage value of structurally similar peaks in the same region of the spectrum can be calculated simply. Due to having similar, but slightly different, resonant frequencies peaks A, B, C, D, and F can be presumed to be compounds with a substituted arene moiety similar to that of THC. However as these peaks have differing chemical shifts than the majority Δ-8 THC product they are clearly not the same compound, and when the peak areas are added it is clear that the COA purity values supplied with these products is not consistent with the reality of each sample.

Table 5.2. Table of impurity integrals relative to the 5’ proton “E” (Figures 5.2 and 5.3). 5’ proton integral calibrated to 100

Sample	Peak A	Peak B	Peak C	Peak D	Peak E (5’)	Peak F	Total Impurities (% of 5’ peak)	COA Purity Value
1	0.05	4.33	4.86	0.56	100	1.31	11.72	≥99% Δ-8 THC
2	0.16	7.52	6.63	0.24	100	1.47	16.30	94.7% Δ-8 THC
3	0.27	7.5	5.71	0.12	100	1.76	14.76	93.43% Δ-8 THC
4	0.31	2.9	12.74	0.47	100	0.4	17.29	87.1% Δ-8 THC
5	0	2.92	12.87	0.31	100	0.48	14.50	93.4% Δ-8 THC
6	0.09	4.44	6.05	4.49	100	0.83	14.54	92.96% Δ-8 THC
7	0.44	3.29	5.1	0	100	0.22	8.28	No COA supplied
8	0.26	2.64	5.35	0.12	100	2.48	10.04	93.44% Δ-8 THC
9	0.08	3.63	6.28	0.05	100	2.11	11.30	93.44% Δ-8 THC
10	0.09	4.33	6.65	0	100	0.47	11.11	93.44% Δ-8 THC

Due to the general unavailability of 800 MHz class NMR instruments, sample 3 was also analyzed on a 400MHz NMR for comparison. While integration of the discrete peaks

in a 1d proton spectrum is more challenging due to the lower resolution it appears to be a viable option for analysis of these products. **(Figure 5.5)**

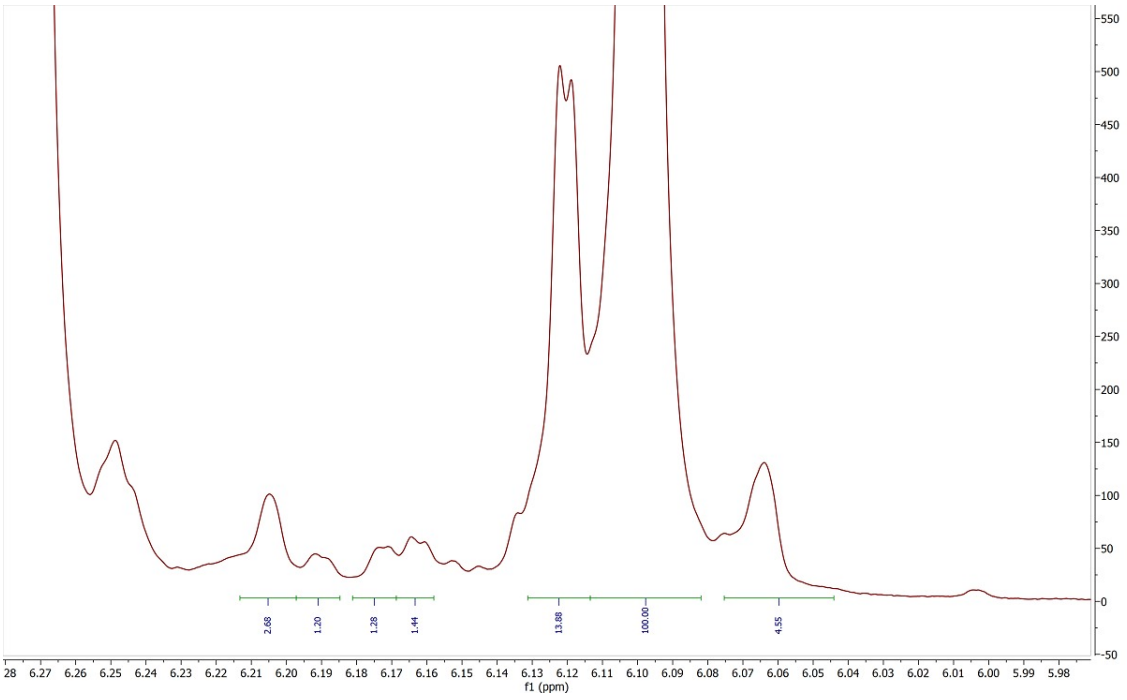

Figure 5.5. 5.97 to 6.28 ppm region detailing 5' proton resonance of sample 3. (400 MHz, $CDCl_3$)

Samples 6 through 10 (Table 5.1) contain added terpenes with resonances in the region of interest thus care must be taken when integrating impurities in this region to avoid including terpene signals as impurities. Samples 8, 9, and 10 were supplied with identical COA's suggesting that they were from the same lot of base product but considering the difference in impurities between sample 8 and the other two this appears to not be the case. Overall, none of the samples analyzed, save for sample 4, are close to

having accurate COA purity values even when only investigating a single peak and ignoring the rest of the spectrum. Due to the chemical shift and *J*-value similarities of this peak and that found on Δ-8 THC, the compounds could reasonably be assumed to contain an arene and thus these products would very likely be UV active and detectable on an HPLC equipped with a UV detector or DAD.

Comparing the HPLC chromatogram supplied with sample 4 **(Figure 5.6)** to an HPLC-UV performed during this study **(Figure 5.7),** it is clear that the HPLC elution method used by the certifying laboratory is inappropriate for detecting impurities in this type of product.

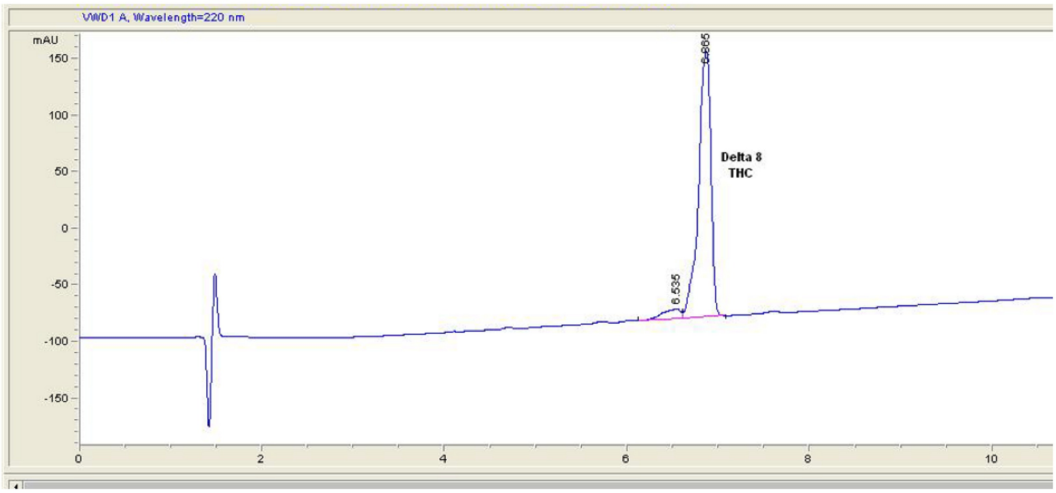

Figure 5.6. Certificate of Analysis chromatogram of sample 6.

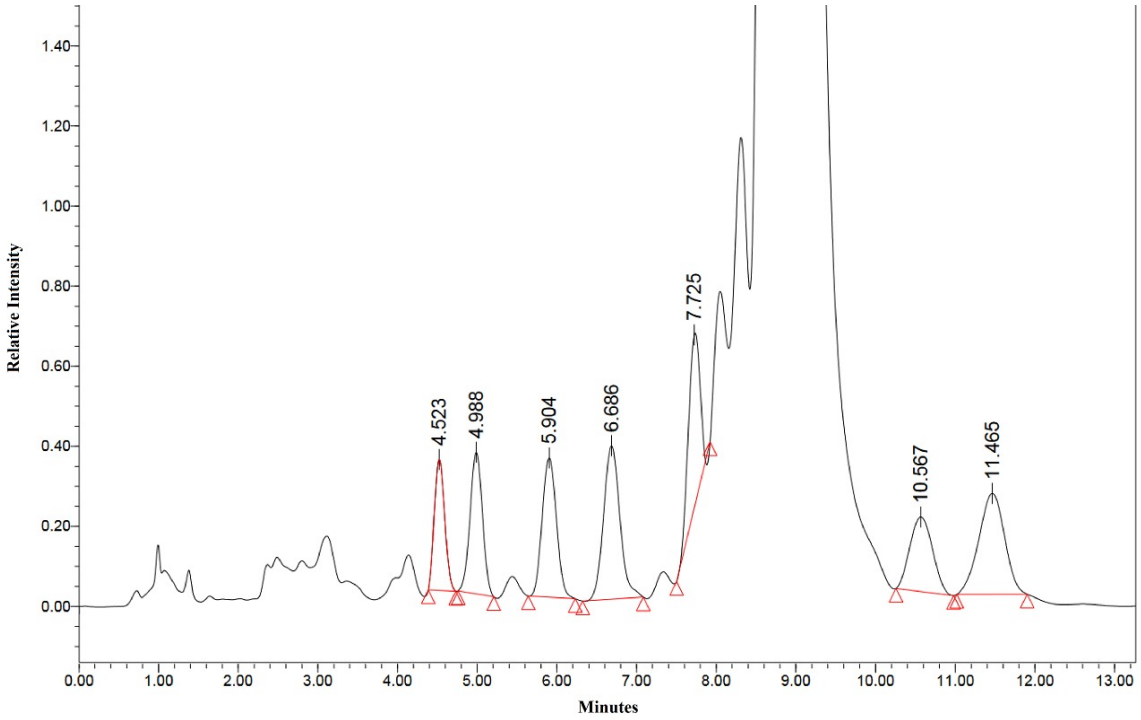

Figure 5.7. HPLC chromatogram of sample 4 performed during this study. 210nm wavelength UV detector.

Mass spectrometry and MS^2 analysis of peaks in sample 4 revealed several impurity peaks. **Figure 5.8** is the total ion chromatogram for sample 4 over the mass range of 317-750 Da.

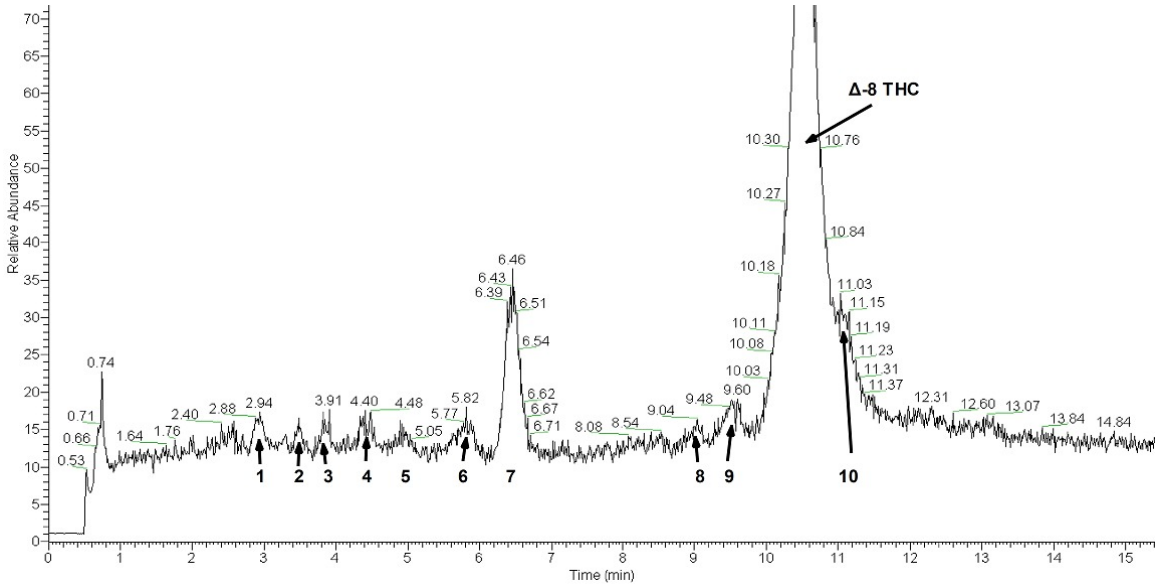

Figure 5.8. Total ion chromatogram of sample 4 in positive mode. Mass range of 317 to 750 Da.

Table 5.3 is a summary of the LC/MS experiment. The peak number in the first table column correspond to the numbers shown in Figure 5.8. The second column indicates the retention time of the peak. The "major peak" column indicates the mass of the base peak observed for each chromatographic peak. The last column shows the masses of other peaks observed in the mass spectrometry scan.

Table 5.3. List of peaks observed in positive mode total ion chromatogram.

Peak	Retention time, min	Major Peak [M + H], Da	Minor peaks (>60% intensity relative to base peak), Da
1	2.94	329.22	270.44, 254.42, 212.84, 166.84
2	3.65	329.13	315.20, 262.60, 212.79, 207.74, 166.86
3	3.91	254.04	330.23, 329.11, 254.60,

			212.79, 207.67, 166.86
4	4.40	345.11	311.18, 246.48, 166.86
5	5.05	331.28	166.87
6	5.82	287.29	None
7	6.46	331.13	None
8	9.04	315.12	None
9	9.60	315.24	None
10	11.03	329.19	315.20

Table 5.4 shows the results of several MS/MS experiments. Each of the labeled peaks in Figure 5.8 were subjected to MS^2 analysis. The parent ion column in Table 5.5 is the same as the major peak listed in Table 5.4. The parent ion was isolated and then fragmented in the MS/MS experiment. The "Base Peak" in Table 5.5 indicates the mass of the largest ion intensity in the MS/MS spectrum. The last column identifies other fragment ions in the MS/MS spectra.

Table 5.4. List of peaks observed in MS^2 spectra.

Peak	**T_R (min)**	**Parent Ion [M+H], Da**	**Base Peak, Da**	**Fragment Ions, Da**
1	2.94	329.22	287.15	311.10, 301.30, 287.15, 272.97, 271.07, 245.17
2	3.65	329.13	287.07	311.08, 301.04, 287.07, 273.01, 271.14, 269.11, 259.10, 245.14, 231.09, 217.11
3	3.91	254.04	196.95	238.89, 235.81, 218.19, 217.15, 208.88, 196.95, 196.14, 194.80, 168.53, 160.90
4	4.40	345.11	327.02	327.02, 317.09, 303.02, 298.99, 289.87
5	5.05	331.28	313.12	313.12, 289.00, 273.11, 271.04,

				259.01, 193.12, 106.92
6	5.82	287.29	231.07	269.09, 245.07, 231.07, 207.07, 205.06, 193.01, 165.07, 135.03
7	6.46	331.13	150.87	313.04, 289.09, 243.13, 233.05, 150.87, 107.04
8	9.04	315.12	259.07	297.16, 273.05, 259.07, 245.11, 233.06, 221.01, 207.05, 193.08, 181.04, 134.97
9	9.60	315.24	259.08	297.12, 273.06, 259.08, 235.08, 233.09, 231.15, 193.10, 181.04, 135.01
10	11.03	329.19	287.07	311.12, 287.07, 286.10, 273.04
Δ-8 THC	10.50	315	259	297, 235, 233, 193, 135
CBD	5.13	315	259	297, 235, 233, 193, 135

Analysis of the MS^2 spectra yielded interesting results showing a variety of what appear to be both impurities from low quality CBD feedstock and known side reaction products from the cyclization reaction used to convert CBD into Δ-8 THC.

Peak 1 exhibits a molecular mass of 328 Da, and as such, this impurity is certainly not CBD or Δ-8 THC. The MS^2 spectra compares well with published data describing cannabidihexol (CBDH) or tetrahydrocannabihexol.[5.5] **(**See appendix A2 for spectra)

Peak 2 also exhibits a molecular mass of 328 Da and possesses a similar MS^2 spectrum to peak 1. Due to the longer retention time would suggest that this impurity may be an isomer of the impurity in peak 1.

Peak 3 with an odd mass of 253 Da appears to contain an amine. The use of amine containing reagents do not appear in any published literature describing the conversion of CBD to Δ-8 THC and as such the origin of this impurity is unknown. A mass transition of

$[M-85]^+$ may indicate the presence of a piperidine. However further work would be required for definitive identification.

Peak 4 exhibits $[M-18]^+$, $[M-42]^+$, and $[M-56]^+$ mass transitions suggesting that it is also a cannabinoid analogue. However, the mass of 344 Da suggests that this compound may be an O-alkylated cannabinoid analogue, which is supported by the $[M-46]^+$ mass transition showing the loss of an ethyl ester.

MS^2 spectra for peak 5 appears to show transitions expected from 5″-hydroxy-CBD or 5″-hydroxy-THC. With the characteristic loss of water at $[M-18]^+$, an $[M-60]^+$ ion suggesting the loss of C_3H_7OH, an $[M-72]^+$ transition for loss of C_4H_8OH, and an $[M-74]^+$ transition for a loss of $C_4H_{10}OH$. Remaining $[M+H]^+$ ions of 193 Da and 107 Da are suggestive that this is likely a 5″-hydroxy CBD or THC analogue. This impurity likely arises from side reactions in the CBD to Δ-8 THC conversion reaction.[5.7]

Peak 6 appears consistent with published MS^2 spectra of cannabidivarin (CBDV).[5.6] Due to being a metabolite found in cannabis, this is likely an impurity carried over from low purity CBD feedstock.

Peak 7 is quite unusual compared to the other impurities investigated in this study. In MS^2 spectra the base peak has a mass transition of $[M-180]^+$ from the molecular ion suggesting the presence of a hexose moiety in this contaminant. The source for this impurity is unknown and further investigation would be required for full structural elucidation.

Peak 8 with an $[M+H]^+$ molecular ion of 315 Da is consistent with MS^2 spectra of THC or CBD. However, due to the longer retention time of 9 min compared to CBD's T_r

of 6.46 minutes and the slightly longer T_r for Δ-8 THC of 10.5 minutes, it would appear to be a CBD or THC isomer.

Peak 9 exhibits MS^2 spectra similar to peak 8 with a slightly longer T_r of 9.5 minutes. This is also likely another CBD or THC isomer.

Peak 10 MS^2 transitions are similar to published spectra of cannabidihexol.[5,6] However, the $[M-42]^+$ base peak, is significantly more intense in spectra collected in this study. This impurity is tentatively identified as cannabidihexol or an isomer thereof.

With several of these impurities now having tentative identifications it appears that the problem with these products is threefold: impure CBD feedstock, poor post-reaction purification, and poor analytical practices during certification of purity. With NMR, HPLC-UV, and HPLC-MS data, it is clear that the current analysis methods need to be improved. Inadequate purification and testing protocols gives rise to a situation where consumers make use of products with far higher levels of impurities than they were led to believe, a situation that could potentially give rise to catastrophic consequences. A less extreme and possibly even more concerning problem arises from considering that failures such as this could lead to a loss of public confidence in laboratory testing of consumer goods altogether.

Even a simple HPLC-UV analysis of these products shows that the certifying labs are failing their customers and consumers by using inappropriate HPLC conditions. While NMR and HPLC-MS could be an arguably more precise methods for detecting and analyzing these impurities the low cost of HPLC is undeniably appealing. HPLC is certainly still a viable method for analysis of these products but certifying laboratories

must be vigilant regarding the effectiveness of the methods used in these analyses as demonstrated by the clear failings described above.

5.6 References

5.1 **H.R.2-Agriculture Improvement Act of 2018** <https://www.congress.gov/bill/115th-congress/house-bill/2/text> (accessed Sep 14, 2021)

Golombek, P., Müller, M., Barthlott, I., Sproll, C. and Lachenmeier, D., 2020.

5.2 **Conversion of Cannabidiol (CBD) into Psychotropic Cannabinoids Including Tetrahydrocannabinol (THC): A Controversy in the Scientific Literature.** *Toxics*, 8(2), 41.

5.3 Erikson, B., 2021. **Delta-8-THC craze concerns chemists.** *Chemical & Engineering News*, [online] (99), 25-28. Available at: <https://cendigitalmagazine.acs.org/2021/08/30/delta-8-thc-craze-concerns-chemists-3/content.html> [Accessed 31 August 2021].

5.4 Choi, Y., Hazekamp, A., Peltenburg-Looman, A., Frédérich, M., Erkelens, C., Lefeber, A. and Verpoorte, R., 2004. **NMR assignments of the major cannabinoids and cannabiflavonoids isolated from flowers ofCannabis sativa.** *Phytochemical Analysis*, 15(6), 345-354.

5.5 Radwan, M., ElSohly, M., El-Alfy, A., Ahmed, S., Slade, D., Husni, A., Manly, S., Wilson, L., Seale, S., Cutler, S. and Ross, S., 2015. **Isolation and Pharmacological Evaluation of Minor Cannabinoids from High-Potency Cannabis sativa.** *Journal of Natural Products*, 78(6), 1271-1276.

5.6 Linciano, P., Citti, C., Russo, F., Tolomeo, F., Laganà, A., Capriotti, A., Luongo, L., Iannotta, M., Belardo, C., Maione, S., Forni, F., Vandelli, M., Gigli, G. and

Cannazza, G., 2020. **Identification of a new cannabidiol n-hexyl homolog in a medicinal cannabis variety with an antinociceptive activity in mice: cannabidihexol.** *Scientific Reports*, 10(1). 1-11.

5.7 Kiselak, T., Koerber, R. and Verbeck, G., 2020. **Synthetic route sourcing of illicit at home cannabidiol (CBD) isomerization to psychoactive cannabinoids using ion mobility-coupled-LC–MS/MS.** *Forensic Science International*, 308, 110173.

Chapter 6. Conclusions and Further Directions

6.1 Conclusions

NMR as an analytical tool for the purpose of detecting food adulteration is currently seeing a resurgence in popularity, and rightly so. However despite its utility, NMR remains a rather expensive method for analysis. Even with new applications, improved methods, and greater acceptance of the technique food adulteration is still a real problem faced by society. Food fraud is as always a moving target with new methods of adulteration being developed and employed every bit as quickly or even more rapidly than detection methods are. However due to the ever evolving nature of food fraud targets, development of NMR based food authenticity testing will continue to be a rewarding field for ongoing research.

Analytical NMR requires adopting strategies and techniques different than one would use in typical NMR analyses such as structure elucidation. The analyst must be constantly aware of the importance of using sufficient, or even seemingly excessive relaxation delays in all experiments used for these analyses. As the relaxation time for individual peaks does vary, many T_1 experiments on multiple samples must be performed to determine the relaxation time for each analyte peak. A final relaxation time of at least ten times the T_1 value of the slowest relaxing peak of interest must be used, lest the analysis be rendered faulty by inconsistent peak intensity. Failing to allow sufficient relaxation time between scans leads to fewer nuclei realigning themselves with the

magnetic field, and subsequent pulses will return lower intensity peaks leading to slow-relaxing peaks appearing to be of lower concentration than in reality.

Similarly the standard for the quality of magnetic field homogeneity must be extremely high compared to qualitative experiments. Verification of well shimmed spectra must be performed and any samples exhibiting signs of poor shimming must be run again, sometimes with more advanced shimming techniques. While verification techniques vary, a careful critique of the internal reference peak can be extremely useful. Whether the peak arises from TMS, DSS, TMSP-D_4, or any other proton shift reference compound, the singlet at 0 ppm is extremely helpful for determining the quality of shims for each experiment. While this peak is generally considered to be a singlet for the sake of simplicity, this is not actually the case. Instead it is three singlet peaks arising from the natural isotopic distribution of silicon in the tri/tetramethyl silane moiety in these compounds. With high quality shims the central and most intense peak will be a symmetrical singlet without signs of splitting and the ^{30}Si isotopic peaks at the base of the main ^{28}Si peak must be clearly visible and relatively symmetrical.

High-field superconducting NMR instrumentation is inherently expensive. While this is somewhat offset by its generally greater sample throughput compared to other instruments, endeavoring to develop methods for lower cost instruments in the 400-500MHz class is essential. While it is true that higher field strength NMR spectrometers exhibit higher resolution and sensitivity, the price of these instruments is likewise significantly higher. An example of this was shown in the Δ-8 THC study in chapter 5 comparing the resolution of an 800MHz instrument versus that of a 400MHz. While the

800MHz spectra resolved peaks far more cleanly, the price difference between these instruments is on the order of several million US dollars. This price disparity makes the appeal and utility of methods developed for lower field strength instruments obvious. Developing methods on an instrument such as the 400MHz unit used for the olive oil study added considerable difficulty to the project, but this was intentional for the aforementioned reasons. Robust methods allowing the use of lower cost and thus more widely available instruments was a key goal for this project allowing wider application of the method.

In chapter 1 the observation of cyclodextrin-internal reference inclusion compounds affecting the spectra's overall chemical shift due to automated spectral referencing was a serendipitous discovery. It was also an important lesson on the pitfalls of blind faith over-reliance on automation and the inherent problems that can arise from "black box" analysis systems such as the Bruker Foodscreener. In that particular case, a sample of honey with extremely low levels of incidental cyclodextrin contamination will be falsely flagged as being extremely adulterated by the Foodscreener. This result is simply a side effect of an inflexible screening method that is incapable of compensating for the effects of a harmless contaminant caused by a careless beekeeper. Great care must be exercised in order to avoid false positives, and this requires careful observation by the spectroscopist or technician performing the analysis.

NMR spectra lends itself well to several approaches to analyzing the resulting spectra. Direct quantification of specific metabolites such as demonstrated on coffee is an excellent method of detecting adulteration by identifying compounds that belong to

known adulterants, but the inverse is also an effective method of detecting dilution. If expected metabolites in a compound are found in unexpectedly low abundance this could be a sign of dilution. The absence of specific markers such as methylglyoxal which is expected in manuka honey is another route to detect fraud. Caution must of course be taken in the case of a previously unknown or unstudied varietal or cultivar being used as the food product source.

Multivariate analysis such as principal component analysis of sample spectra such as demonstrated in chapter 3 on food oils is a powerful method useful in comparing samples that are largely similar. The most obvious case is differentiating high-oleic cultivars of sunflower and safflower oil from olive oil which has a similar lipid profile. This approach lends itself well to automation and greatly reduces the workload of the analyst after building an effective model. Building an effective PCA model is something of a challenge and one must take care to avoid including portions of the spectrum that may vary naturally, such as water content or variations in the degree of deuteration of the solvent from batch to batch. Failing to account for problems of this sort leads to poor results based on the PCA model separating samples based on irrelevant differences. Blinding the model to peaks arising from these variations is absolutely critical to succeeding in endeavors such as this.

Ratiometrics such as demonstrated in chapter 4 with cheese reduces the amount of effort required to build a workable method. It is somewhat more labor intensive when assessing each individual sample, requiring manual integration of peaks or verification of the same if automated integration is used. Despite this, it does tend to automatically

eliminate issues stemming from deuteration inconsistencies in solvent, water content of the sample or solvent, or any other spurious signals that the analyst chooses to ignore. Using the sample to measure itself via ratometrics eliminates measurement errors inherent to adding internal reference compounds, improving precision. As with other methods, improper relaxation delays will lead to poor results caused by incomplete relaxation of protons responsible for peaks of interest.

While the focus of these studies was on developing NMR based methods the utility of chromatography and mass spectrometry cannot be ignored, especially when faced with unexpected metabolites or impurities of unknown origin. This is particularly true when investigating low abundance metabolites or impurities. Preparatory HPLC separation allowing for quantities of the impurity making NMR analysis viable is invaluable to identifying these compounds. Mass spectrometry can also be quite helpful to identify adulterants in low abundance, provided that the offending NMR peak can be matched to the impurity or impurities analyzed with MS.

The ability to detect adulteration is important to these studies, but this ability is nigh on useless if the analyst is unable to identify the adulterant. This changes the study from one of ordinary analytical chemistry into one combining that with detective work. In the case of edible oils, a PCA based method can give clues as to the identity of the adulterant based on where the adulterated oil falls on the PCA plot. The adulterated oil will generally fall somewhere between the genuine oil and the adulterant in PCA, but only if the adulterant is part of the PCA model. When faced with an unknown adulterant such as encountered with palm oil in cheese in chapter 4, determining the identity of the

adulterant can become rather labor intensive. Serial adulteration of genuine samples with potential adulterants is effective as demonstrated in that study but this may not be the most efficient approach. Looking for spectral clues such as unexpected peaks can be invaluable. Online databases of chemical shifts, especially combined with molecular weight taken from mass spectra makes determining the identity easier. An analyst's intuition is another invaluable tool in this case when considering likely adulterants, or at least families of adulterants, in order to reduce the labor required to make a positive identification. Of course the final step to prove the identity is to intentionally adulterate samples to not only spectrally prove the identity, but also the rough concentration of the adulterant. Without this proof, the determination is little more than educated speculation that is unlikely to hold up in court if the adulterer ever faces such actions.

6.2 Future Directions

Potential future projects focusing on continuing or expanding on the works detailed in this dissertation includes a wide range of potential target products. The olive oil and cheese projects showed how application of NMR lipid profiling can be used to detect adulteration in those products. The coffee analysis demonstrated how basic metabolomic concepts could be applied to detecting adulterated products. Both the coffee and cheese projects demonstrated how simple extractions could be used to analyze solid products with solution-state NMR as well. Investigating impurities in Δ-8 THC demonstrated the power of combining NMR and mass spectrometry, particularly when investigating low

abundance impurities or metabolites. Applying these methods to other products involves some unconventional thinking such as thinking like a food fraudster. Considering how products could potentially be adulterated is an invaluable skill, particularly when attempting to identify the nature of an adulterant. Likewise, considering potential avenues to adulterate products not normally considered at high risk for adulteration may pay off greatly with successful new research projects.

Lipid profiling could be applied to many products other than just hard cheese and oils. Butter and ghee, a clarified butter product, are products with great potential for vegetable oil adulteration. Simple ratiometric lipid profiling such as that demonstrated with the cheese project would likely work quite well for these products. Some adjustments to the previous procedures will certainly be required with butter due to the inherent water content, but this can be overcome. Suppressing the water peak with a solvent suppression experiment could reduce or eliminate problems stemming from a large water peak obscuring important regions in the spectrum. Drying the butter sample under vacuum or via lyophilization is another approach worth considering. Separating the water fraction by centrifugation at elevated temperatures may also prove effective, however care must be taken to avoid overheating the sample and inadvertently changing the nature of the sample via thermal degradation.

Extracts of solid samples and powders such as detailed in the coffee study opens up a myriad of possibilities for NMR analysis. Spices could easily be adulterated with fillers that may be identifiable via NMR. For example, differentiating spices such as genuine saffron from inexpensive substitutes like safflower. However even if spice samples are

adulterated with materials that are invisible to ^{1}H NMR, such as table salt, the question becomes one of "what is not there?" Determining normal levels of various metabolites in a wide variety of genuine samples could lead to the ability to detect dilution of this sort by finding abnormally low levels of these metabolites. Obviously this would involve determining the concentration by a method such as ERETIC or internal standards, and determining an ideal concentration envelope for each metabolite versus the mass of the sample. The pitfall here involves unknown or untested cultivars, regional differences, and other natural variations in metabolite levels possible in any natural product. A large set of samples from a wide geographic area, and over multiple years of production would greatly aid in mitigating this issue.

With the advent of relatively affordable permanent or electromagnet benchtop Fourier Transfer NMRs in the 60-100+ MHz field strength range, efforts should be made to develop screening methods using these instruments. While they do suffer from lower resolution inherent to their lower resonant frequency, clever experiment design, statistical analysis, or spectral analysis could be used to overcome this shortcoming. Spectral fingerprinting such as used in the olive oil project, or ratiometrics such as applied to cheese may work nicely to assess the purity of various samples. The greatest benefit of projects such as these would be the ability to screen food products via NMR instruments that cost an order of magnitude less than a superconducting instrument with vastly reduced recurring costs such as those from cryogens. Such reduced costs would lead to a much wider application of NMR screening due to being in the same price range as a low

cost mass spectrometer. As magnet technology improves the field strength and field homogeneity of these systems is quite likely to improve as well.

Appendix

A1 List of Coffee Samples Analyzed

Coffee Type	Mass	3.16ppm Peak?	ERETIC value (mMol)	% adulteration high	% adulteration low	% adulteration avg.	Note
Name Brand	0.1026	No					
Name Brand	0.1092	No					
Name Brand	0.1020	No					
Name Brand	0.1040	No					
Store Brand	0.1051	Yes	0.0635	14.7	N/A	N/A	Prior to weighted averaging
Store Brand	0.1081	No					
Name Brand	0.1090	No					
Name Brand	0.1032	No					
Name Brand	0.0993	No					
Store Brand	0.1086	No					
Store Brand	0.1035	Yes	0.0342	7.9	N/A	N/A	Prior to weighted averaging
Store Brand	0.0509	No					
Name Brand	0.0502	No					
Name Brand	0.0515	No					
Store Brand	0.0512	No					
Store Brand	0.0516	No					
Store Brand	0.0513	No					
Store Brand	0.0497	No					
Store Brand	0.0507	No					
Store Brand	0.0517	No					
Store Brand	0.0505	No					
Store Brand	0.0508	No					
Store Brand	0.0511	No					
Store Brand	0.0512	No					
Store Brand	0.0512	No					
Store Brand	0.0508	No					
Store Brand	0.0512	No					
Store Brand	0.0496	Yes	Below LOQ				Below LOQ
Store Brand	0.0508	No					
Store Brand	0.0509	No					
Store Brand	0.0511	No					

Name Brand	0.0497	Yes					
Store Brand	0.0504	No					
Store Brand	0.0500	No					
Store Brand	0.0506	No					
Store Brand	0.0516	No					
Store Brand	0.0499	No					
Store Brand	0.0513	No					
Store Brand	0.0500	No					
Store Brand	0.0506	Yes	0.0552	41.7	27.1	35.6	
Store Brand	0.0510	No					
Store Brand	0.0517	No					
Store Brand	0.0507	Yes	0.0173	13.1	8.5	11.1	
Store Brand	0.0509	No					
Store Brand	0.0515	No					
Store Brand	0.0510	No					
Store Brand	0.0516	No					
Name Brand	0.0508	No					
Name Brand	0.0509	No					
Wellsley Classic	0.0508	No					
Store Brand	0.0505	No					
Store Brand	0.0501	Yes	0.0173	13.2	8.6	11.3	
Store Brand	0.0500	No					
Store Brand	0.0496	No					
Store Brand	0.0497	No					
Store Brand	0.0502	No					
Store Brand	0.0494	No					
Store Brand	0.0507	No					
Store Brand	0.0517	No					
Store Brand	1mL	No					Liquid/Liquid extraction sample test with pre-brewed sample. Not a viable test method.
Store Brand	0.0511	No					
Store Brand	0.0522	No					
Store Brand	0.0521	No					
Store Brand	0.0496	Yes	0.0133	10.3	6.6	8.8	Method validation re-run
Store Brand	0.0507	Yes	0.0182	13.7	8.9	11.7	Method validation re-

							run
Store Brand	0.0502	Yes	0.0073	5.6	3.6	4.8	Below LOQ
Store Brand	0.0499	No					Blinded sample
Store Brand	0.0517	No					Blinded sample
Store Brand	0.0504	No					Blinded sample
Store Brand	0.0509	No					Blinded sample
Store Brand	0.0500	Yes	0.0192	14.6	9.5	12.4	Blinded sample
Store Brand	0.0498	No					Blinded sample
Store Brand	0.0496	No					Blinded sample
Store Brand	0.0507	No					
Store Brand	0.0505	Yes	0.0166	12.6	8.2	10.7	
Store Brand	0.4930	Yes	0.0210	16.3	10.6	13.9	
Store Brand	0.0514	Yes	0.0188	14.0	9.1	11.9	
Store Brand	0.0494	No					
Store Brand	0.0499	No					
Store Brand	0.0508	No					
Store Brand	0.0512	Yes	BELOW LOQ				Below LOQ
Store Brand	0.0500	No					
Store Brand	0.0508	No					
Store Brand	0.0499	No					
Store Brand	0.0500	Yes	0.0162	12.4	8.0	10.6	
Store Brand	0.0510	Yes	0.0185	13.9	9.0	11.8	
Store Brand	0.0513	No					

A2 Δ-8 THC Supplemental Spectra

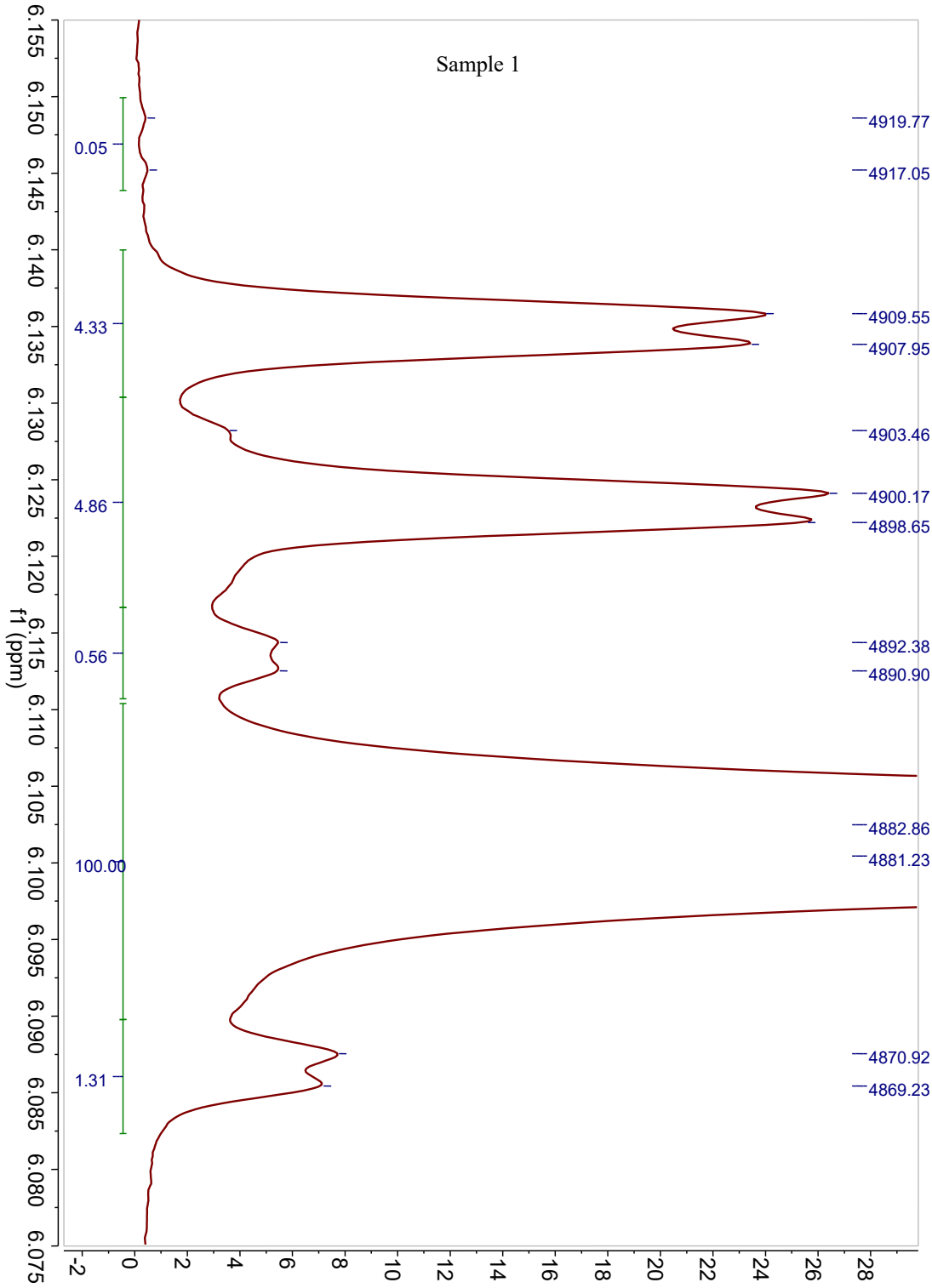

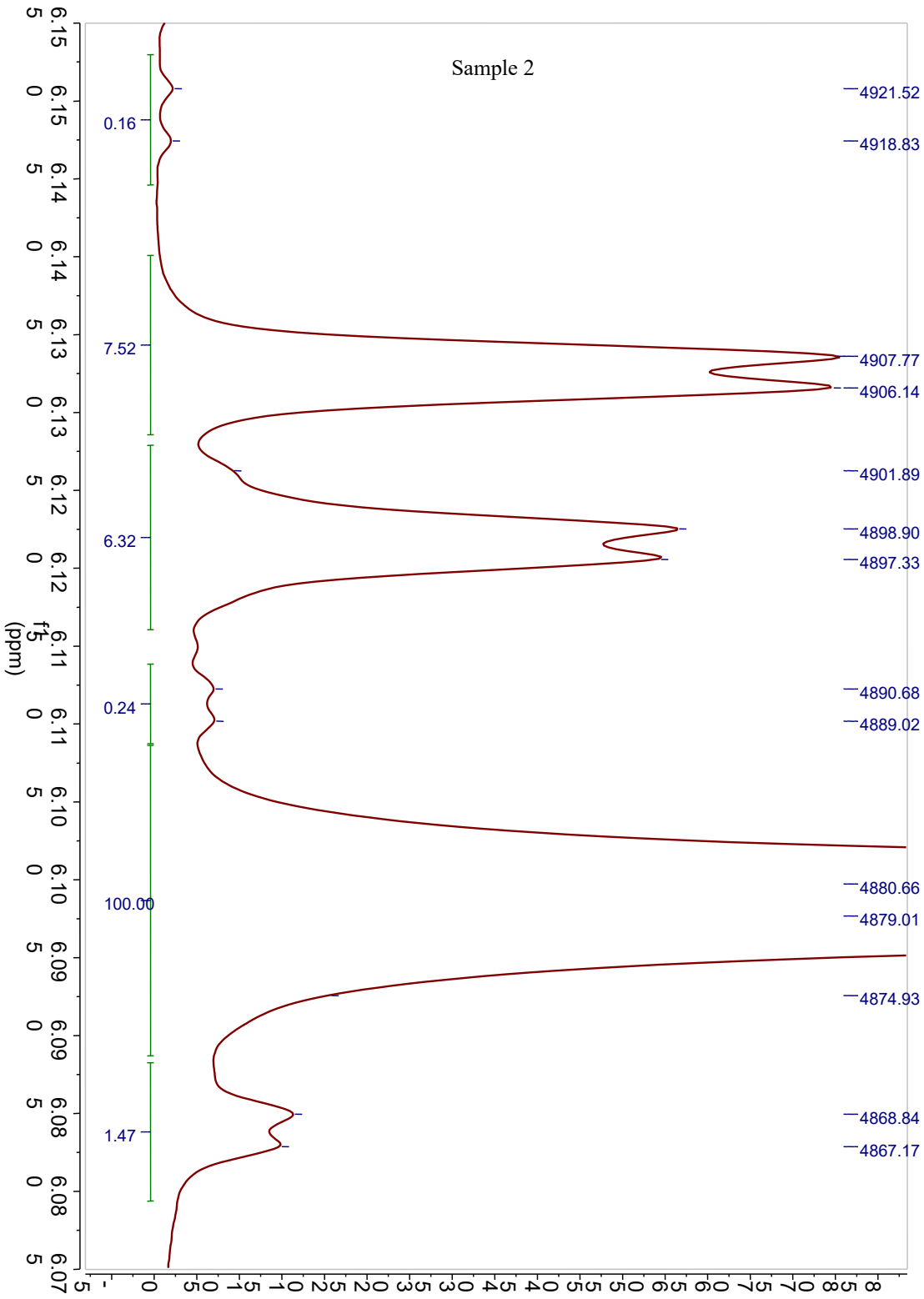
Sample 2
4921.52
4918.83
4907.77
4906.14
4901.89
4898.90
4897.33
4890.68
4889.02
4880.66
4879.01
4874.93
4868.84
4867.17
0.16
7.52
6.32
0.24
100.00
1.47
f1 (ppm)

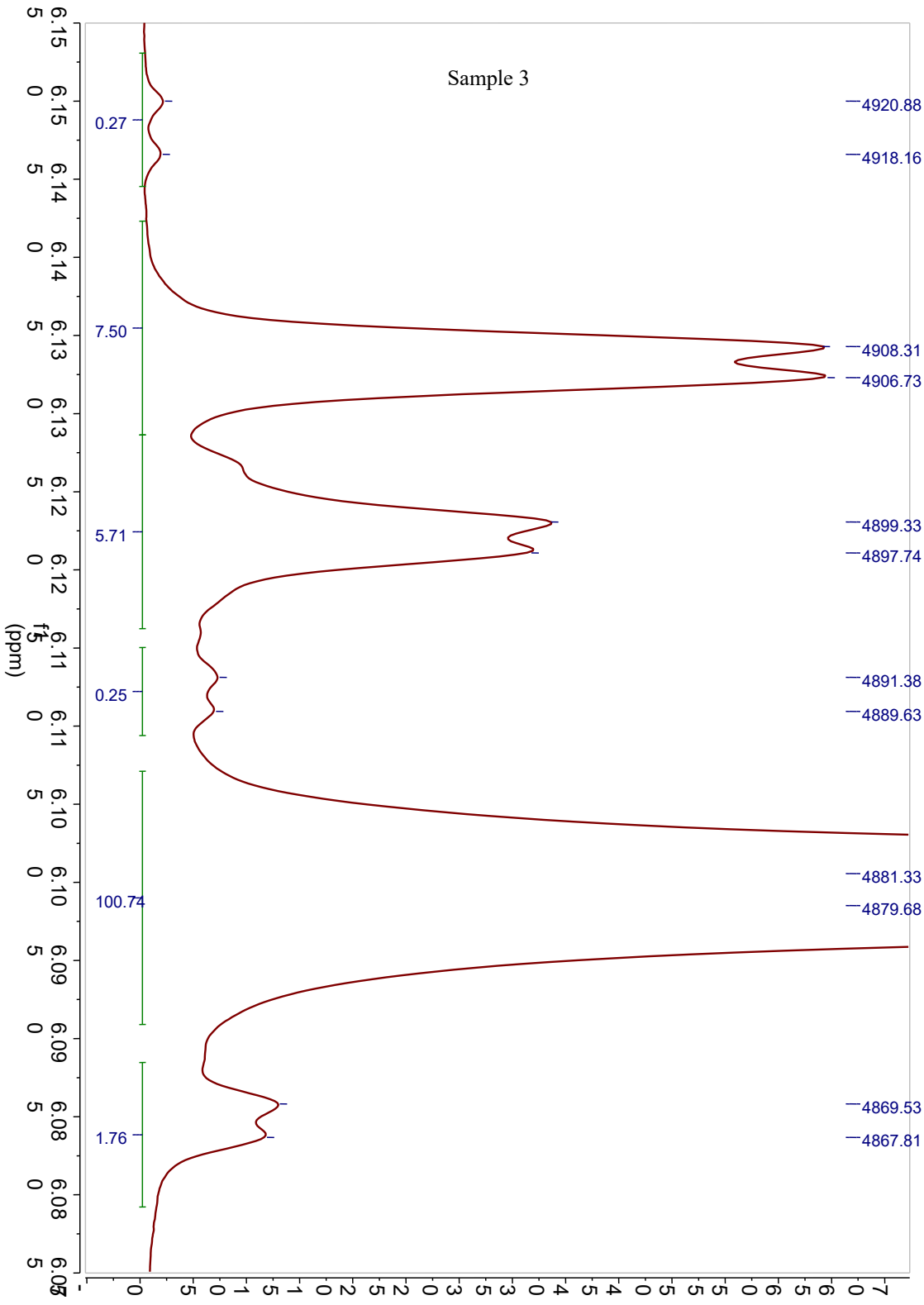
Sample 3
0.27
7.50
5.71
0.25
100.74
1.76
4920.88
4918.16
4908.31
4906.73
4899.33
4897.74
4891.38
4889.63
4881.33
4879.68
4869.53
4867.81
f1 (ppm)

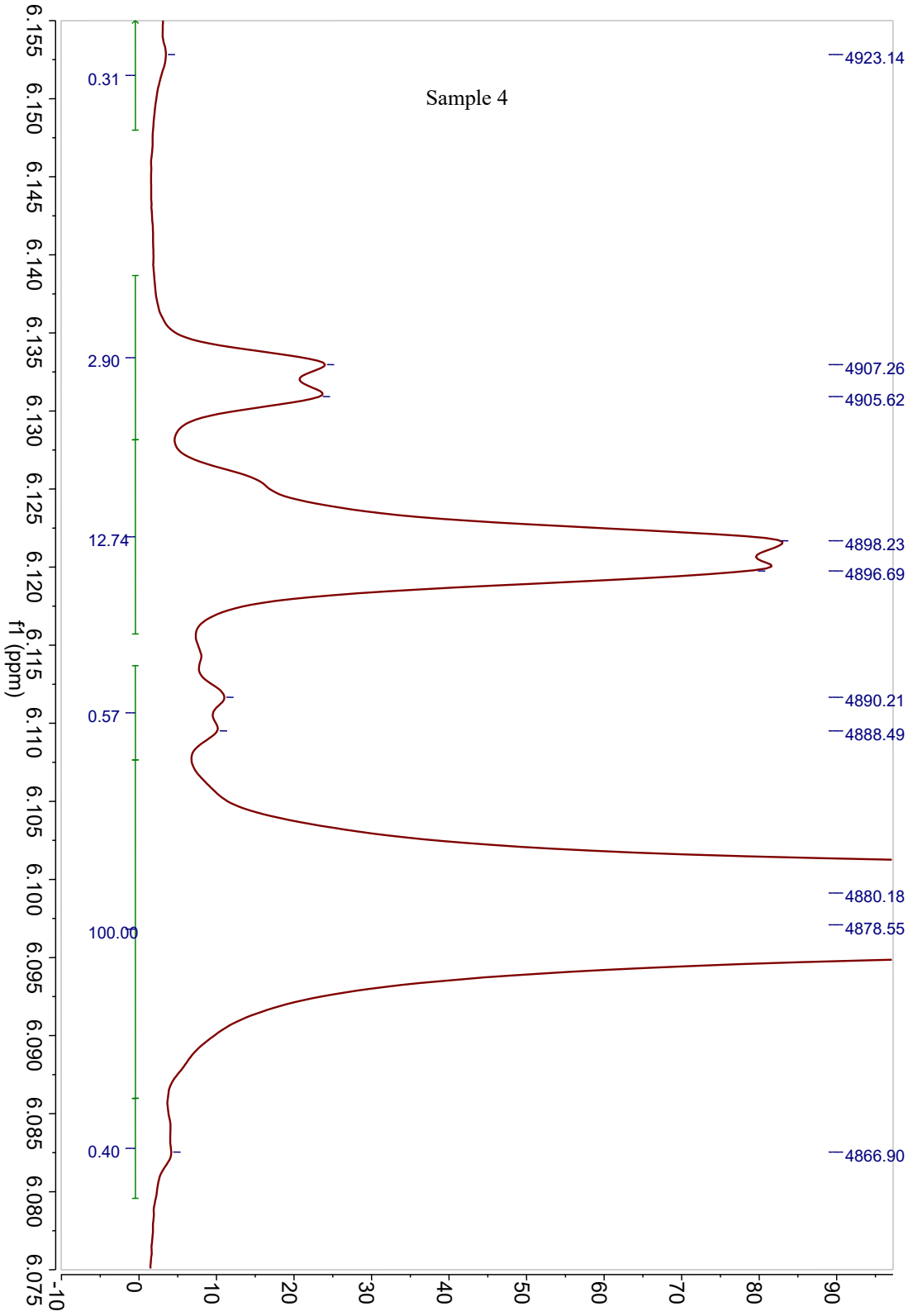
Sample 4
f1 (ppm)
6.155
6.150
6.145
6.140
6.135
6.130
6.125
6.120
6.115
6.110
6.105
6.100
6.095
6.090
6.085
6.080
6.075
-10
0
10
20
30
40
50
60
70
80
90
0.31
2.90
12.74
0.57
100.00
0.40
4923.14
4907.26
4905.62
4898.23
4896.69
4890.21
4888.49
4880.18
4878.55
4866.90

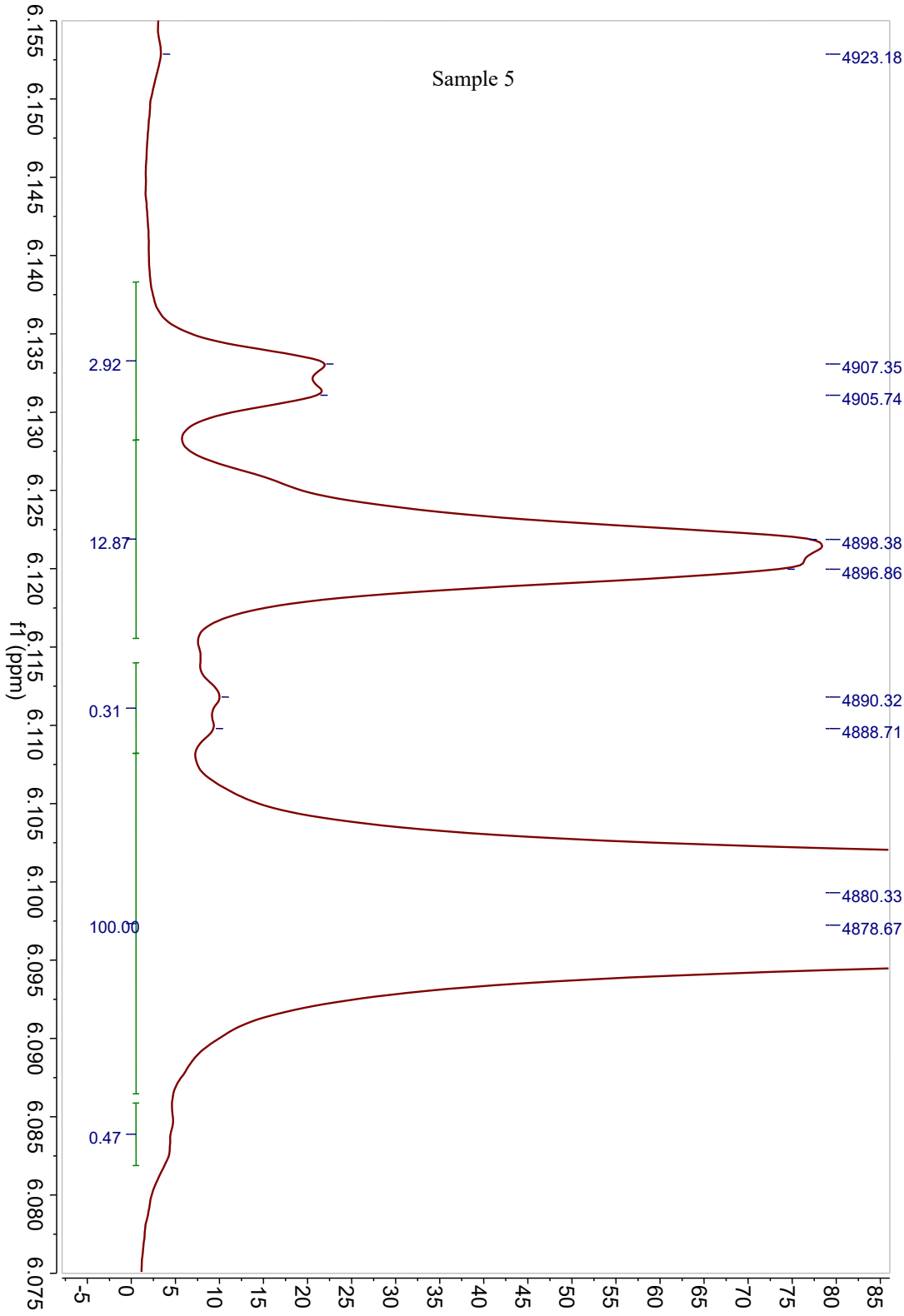
Sample 5
4923.18
4907.35
4905.74
4898.38
4896.86
4890.32
4888.71
4880.33
4878.67
2.92
12.87
0.31
100.00
0.47
f1 (ppm)
6.155
6.150
6.145
6.140
6.135
6.130
6.125
6.120
6.115
6.110
6.105
6.100
6.095
6.090
6.085
6.080
6.075
-5
0
5
10
15
20
25
30
35
40
45
50
55
60
65
70
75
80
85

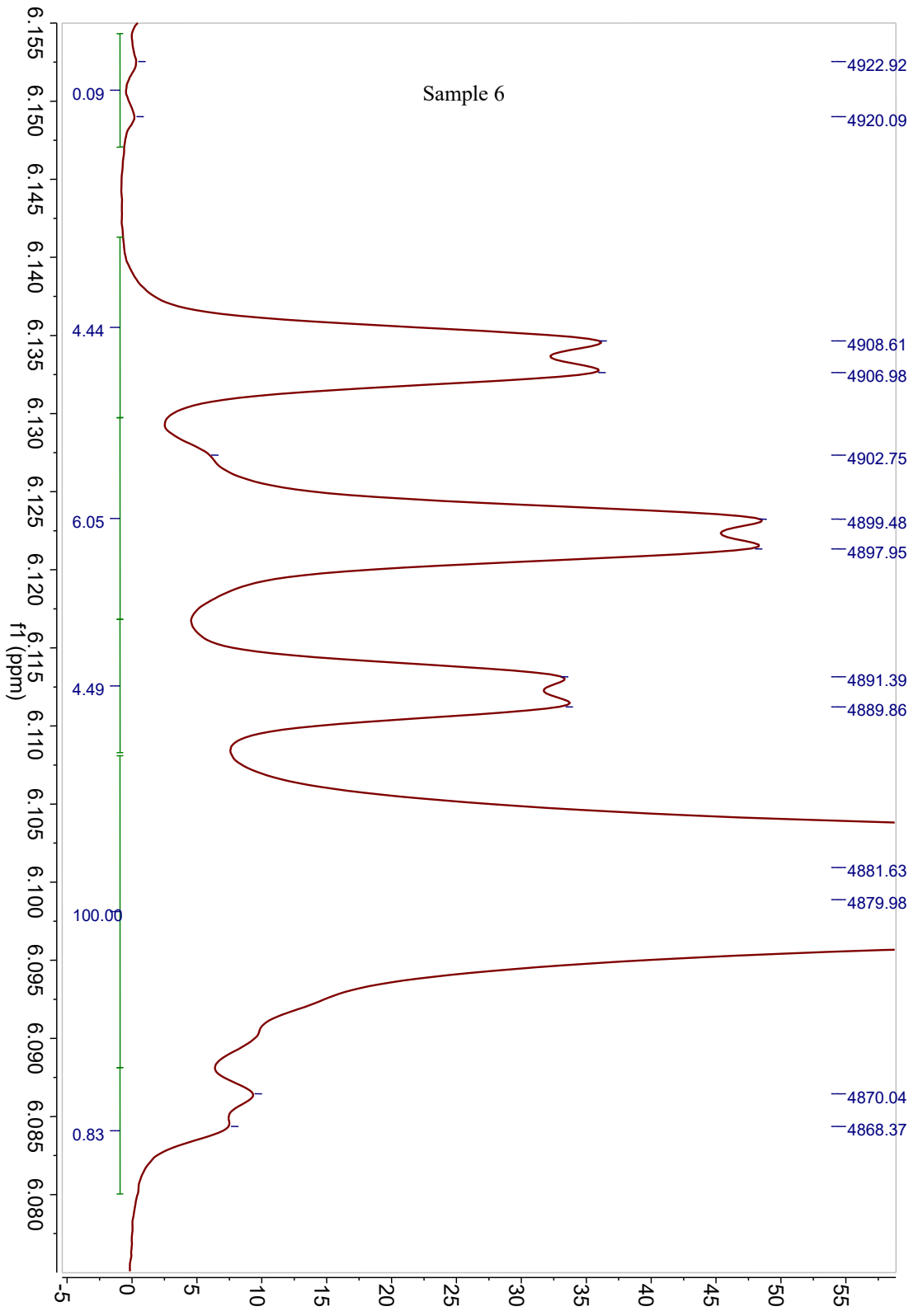
Sample 6
f1 (ppm)
6.155
6.150
6.145
6.140
6.135
6.130
6.125
6.120
6.115
6.110
6.105
6.100
6.095
6.090
6.085
6.080
0.09
4.44
6.05
4.49
100.00
0.83
4922.92
4920.09
4908.61
4906.98
4902.75
4899.48
4897.95
4891.39
4889.86
4881.63
4879.98
4870.04
4868.37
-5
0
5
10
15
20
25
30
35
40
45
50
55

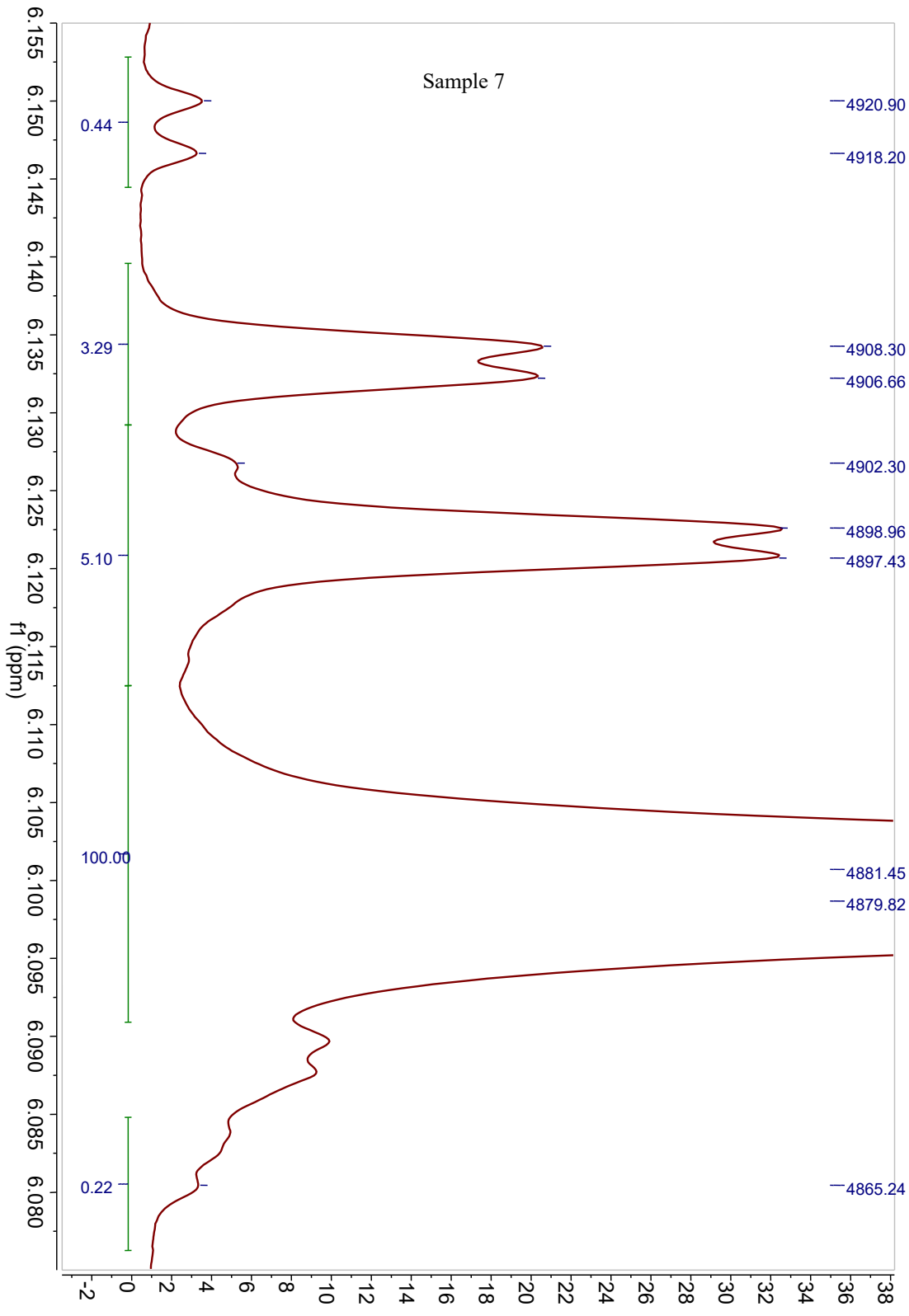
Sample 7
f1 (ppm)
6.155
6.150
6.145
6.140
6.135
6.130
6.125
6.120
6.115
6.110
6.105
6.100
6.095
6.090
6.085
6.080
0.44
3.29
5.10
100.00
0.22
4920.90
4918.20
4908.30
4906.66
4902.30
4898.96
4897.43
4881.45
4879.82
4865.24
-2
0
2
4
6
8
10
12
14
16
18
20
22
24
26
28
30
32
34
36
38

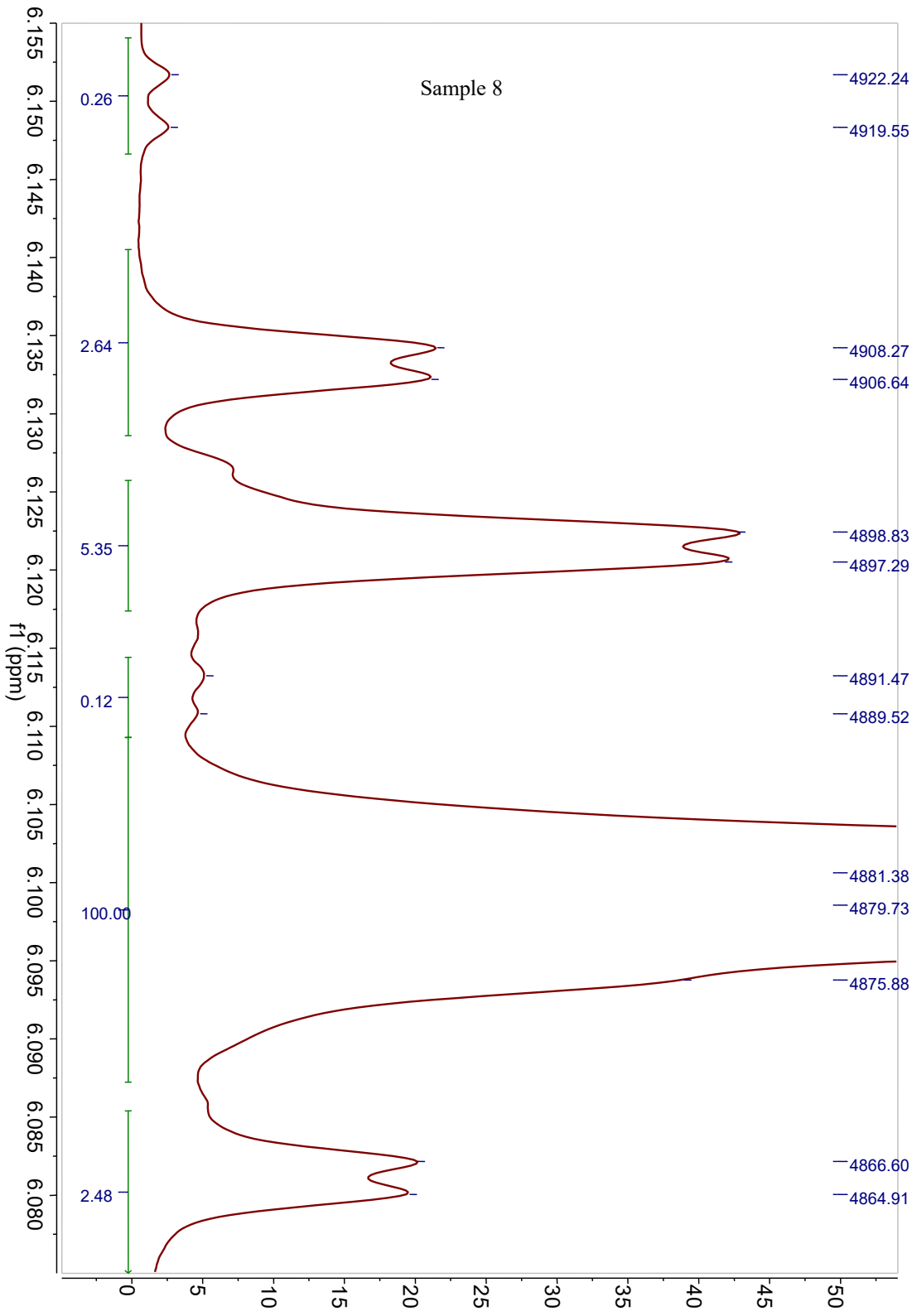
Sample 8
f1 (ppm)
6.155
6.150
6.145
6.140
6.135
6.130
6.125
6.120
6.115
6.110
6.105
6.100
6.095
6.090
6.085
6.080
0.26
2.64
5.35
0.12
100.00
2.48
4922.24
4919.55
4908.27
4906.64
4898.83
4897.29
4891.47
4889.52
4881.38
4879.73
4875.88
4866.60
4864.91
0
5
10
15
20
25
30
35
40
45
50

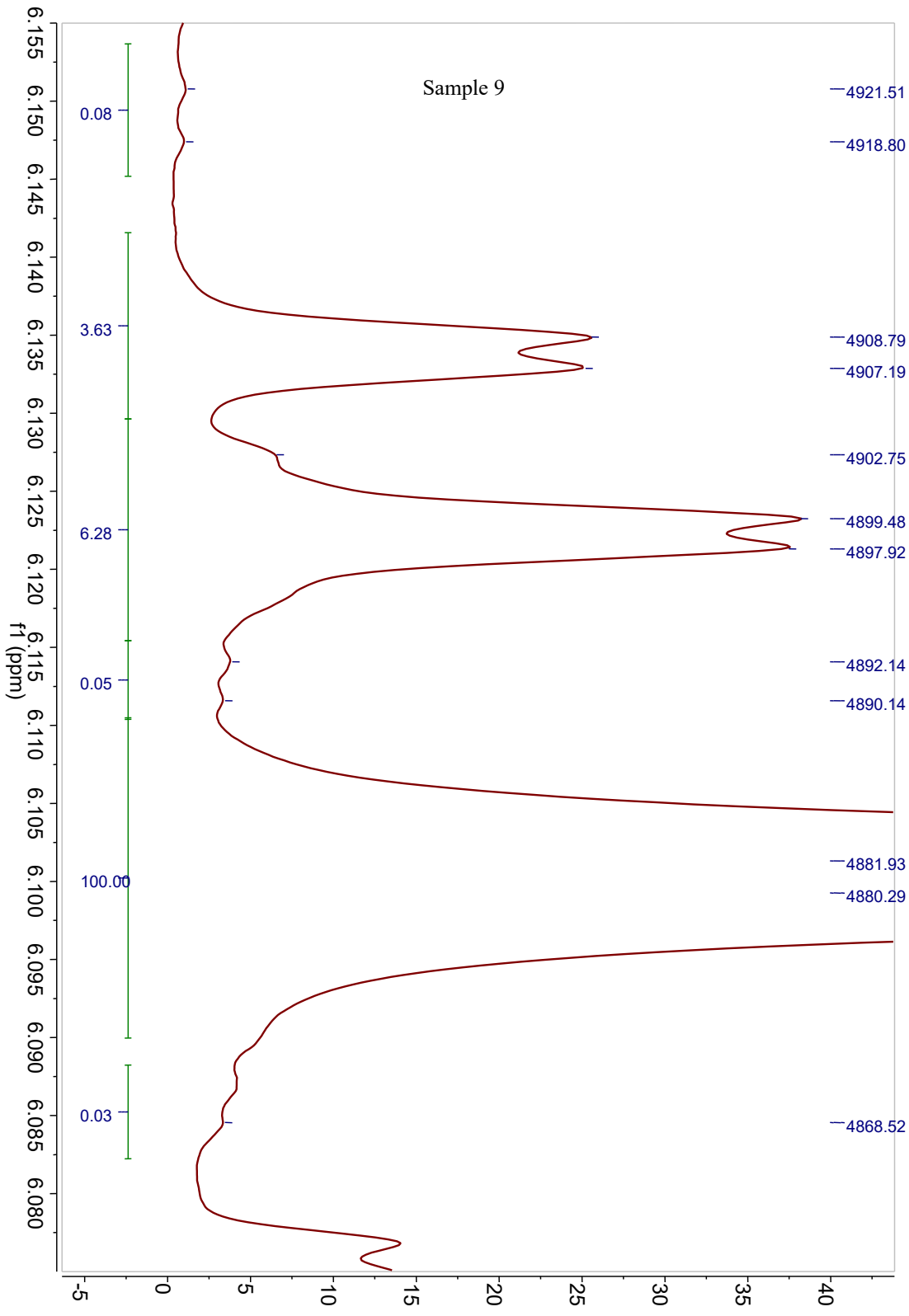
Sample 9
f1 (ppm)
6.155
6.150
6.145
6.140
6.135
6.130
6.125
6.120
6.115
6.110
6.105
6.100
6.095
6.090
6.085
6.080
0.08
3.63
6.28
0.05
100.00
0.03
4921.51
4918.80
4908.79
4907.19
4902.75
4899.48
4897.92
4892.14
4890.14
4881.93
4880.29
4868.52
-5
0
5
10
15
20
25
30
35
40

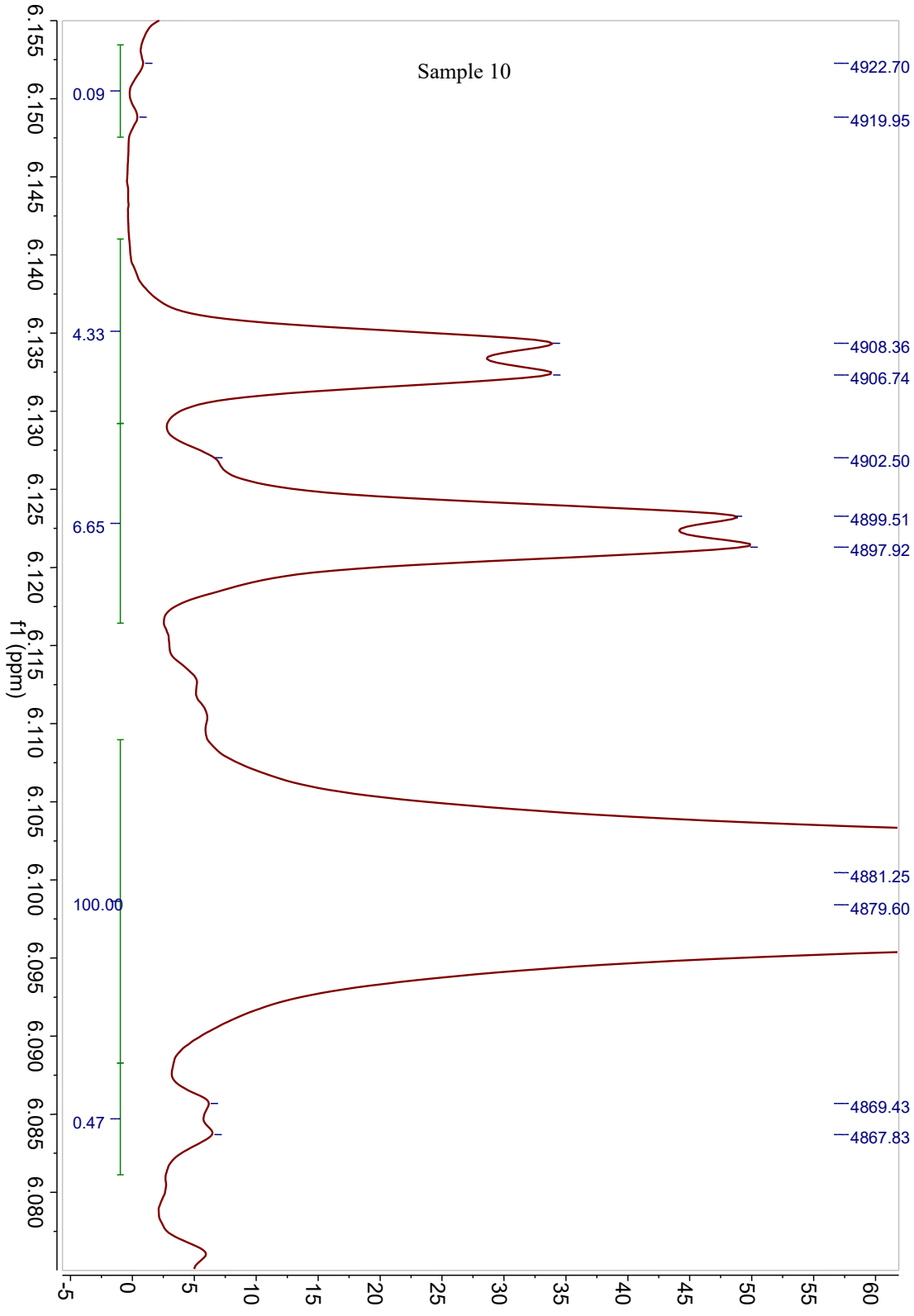
Sample 10
4922.70
4919.95
4908.36
4906.74
4902.50
4899.51
4897.92
4881.25
4879.60
4869.43
4867.83
0.09
4.33
6.65
100.00
0.47
f1 (ppm)
6.155
6.150
6.145
6.140
6.135
6.130
6.125
6.120
6.115
6.110
6.105
6.100
6.095
6.090
6.085
6.080
-5
0
5
10
15
20
25
30
35
40
45
50
55
60

Peak 1

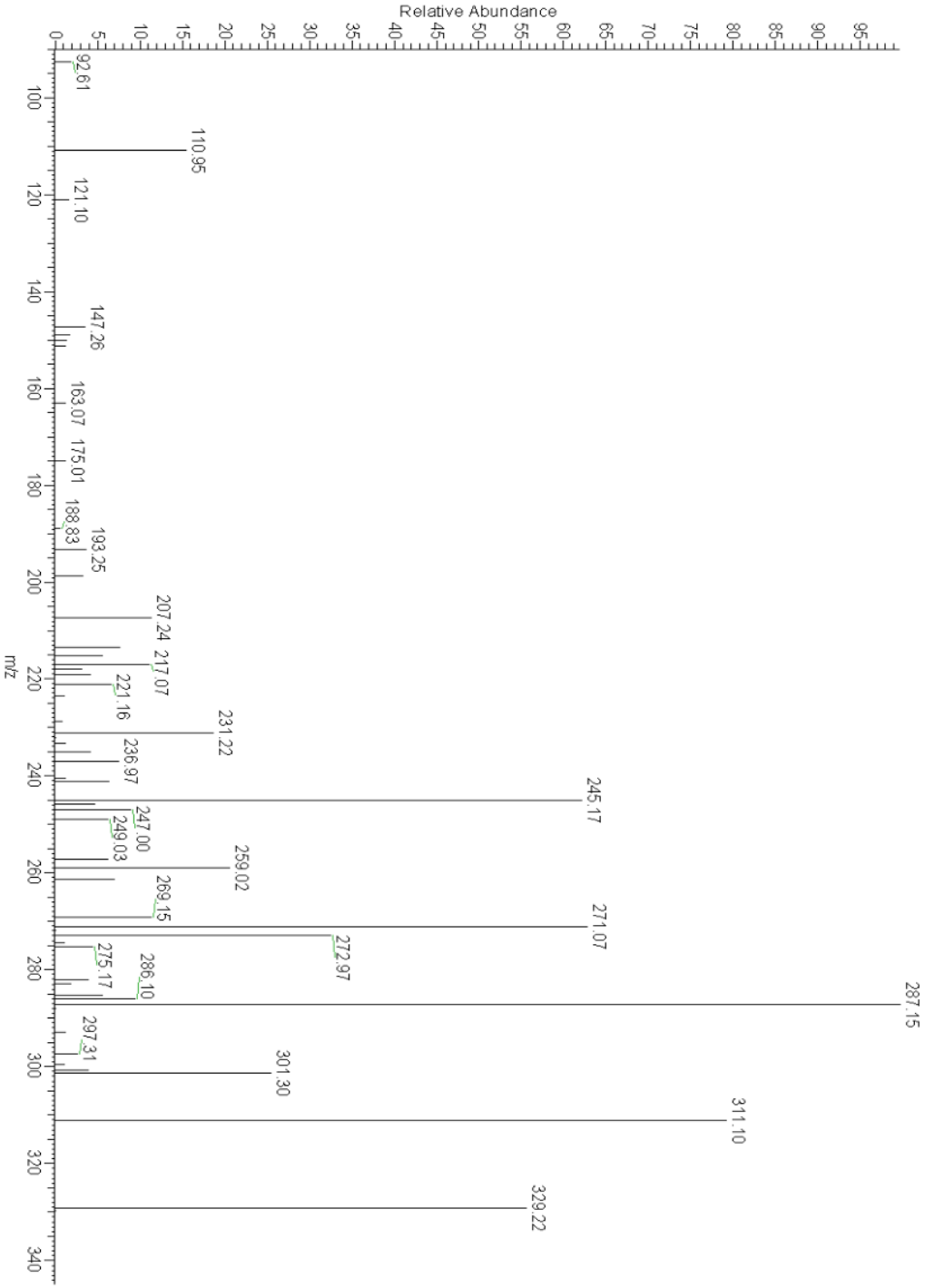
Relative Abundance
m/z
92.61
110.95
121.10
147.26
163.07
175.01
188.83
193.25
207.24
217.07
221.16
231.22
236.97
245.17
247.00
249.03
259.02
269.15
271.07
272.97
275.17
286.10
287.15
297.31
301.30
311.10
329.22

Peak 2

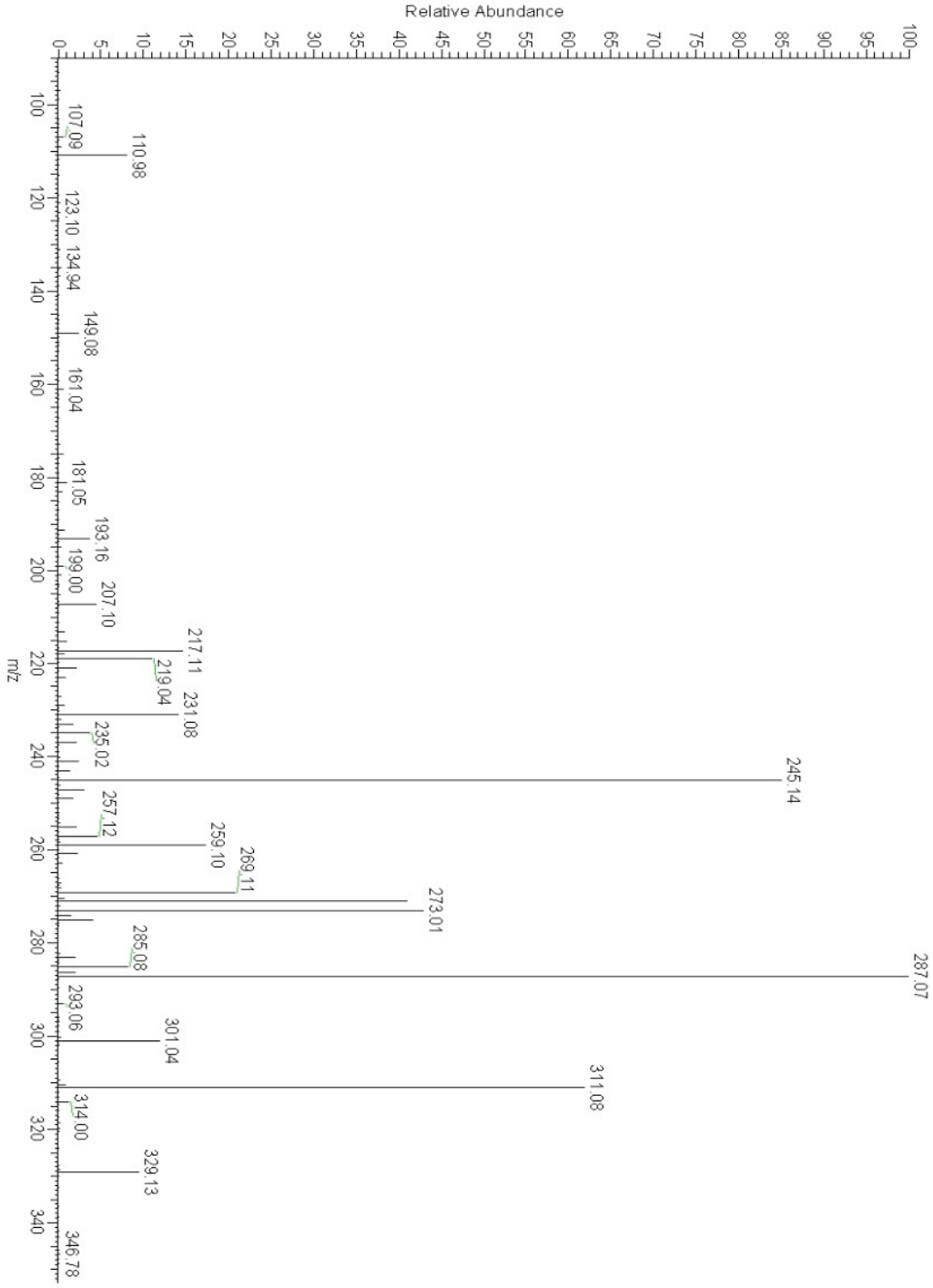
Relative Abundance
m/z
107.09
110.98
123.10
134.94
149.08
161.04
181.05
193.16
199.00
207.10
217.11
219.04
231.08
235.02
245.14
257.12
259.10
269.11
273.01
285.08
287.07
293.06
301.04
311.08
314.00
329.13
346.78

Peak 3

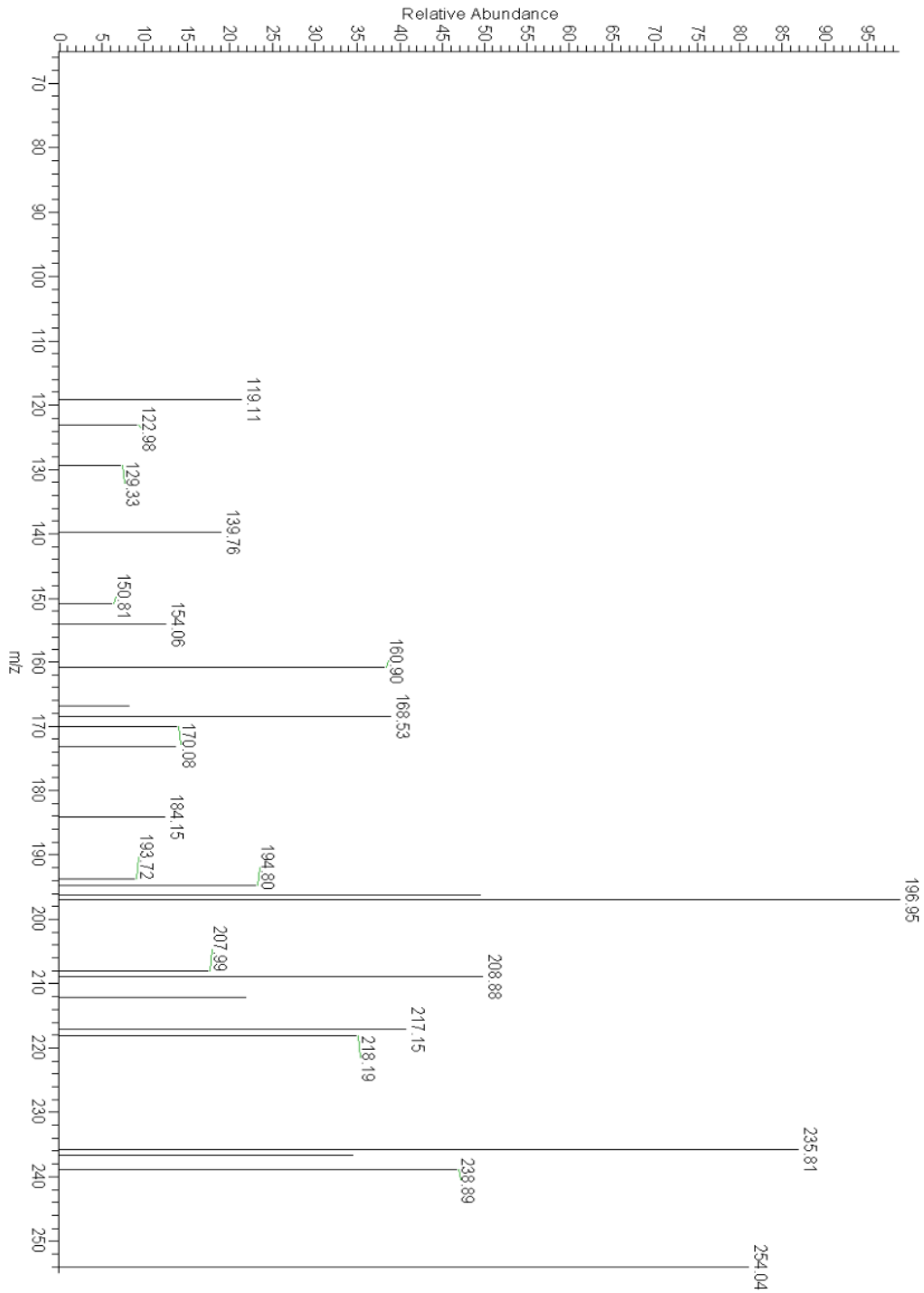
Relative Abundance
m/z
119.11
122.98
129.33
139.76
150.81
154.06
160.90
168.53
170.08
184.15
193.72
194.80
196.95
207.99
208.88
217.15
218.19
235.81
238.89
254.04

Peak 4

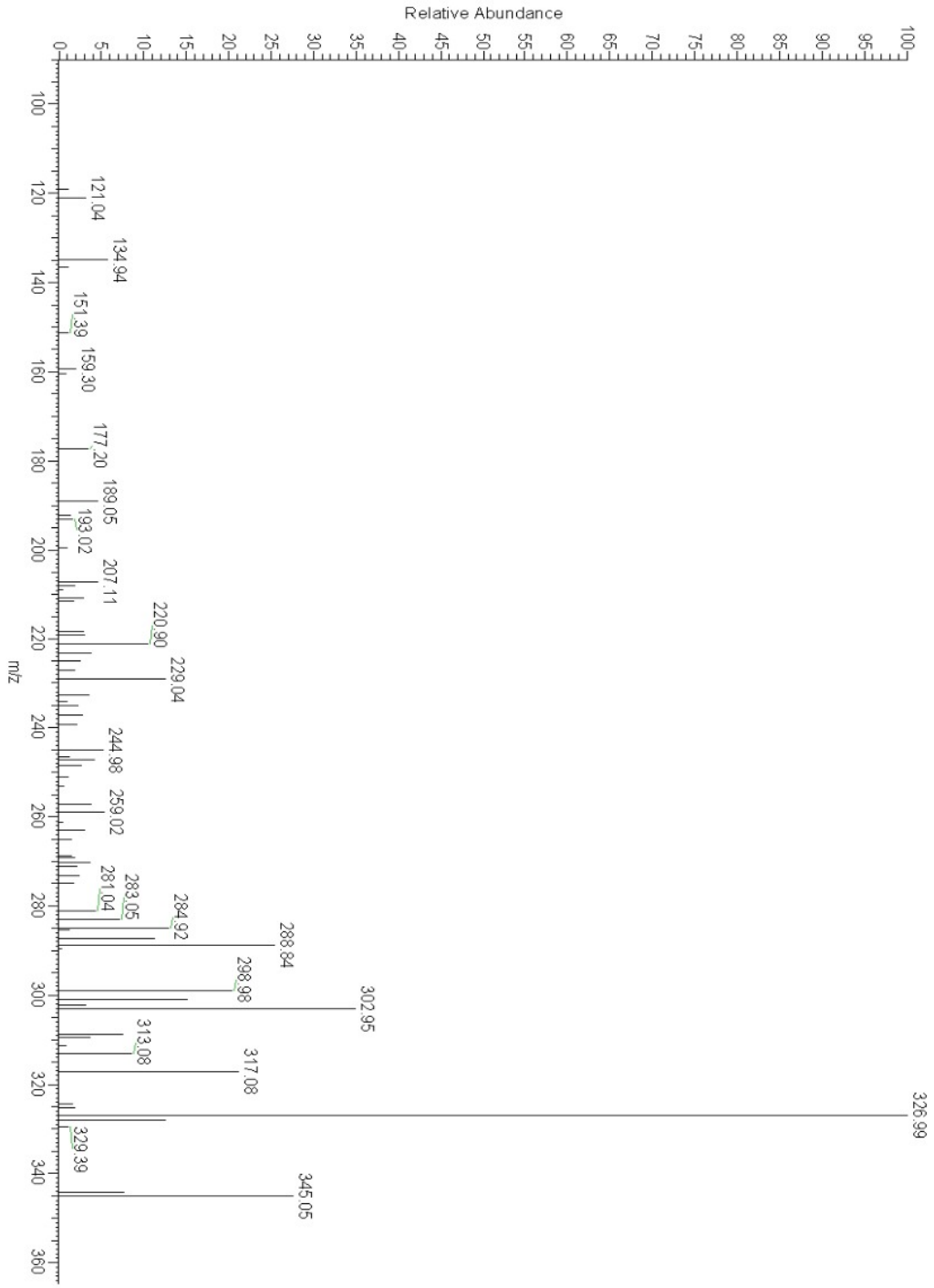
Relative Abundance
m/z
121.04
134.94
151.39
159.30
177.20
189.05
193.02
207.11
220.90
229.04
244.98
259.02
281.04
283.05
284.92
288.84
298.98
302.95
313.08
317.08
326.99
329.39
345.05

Peak 5

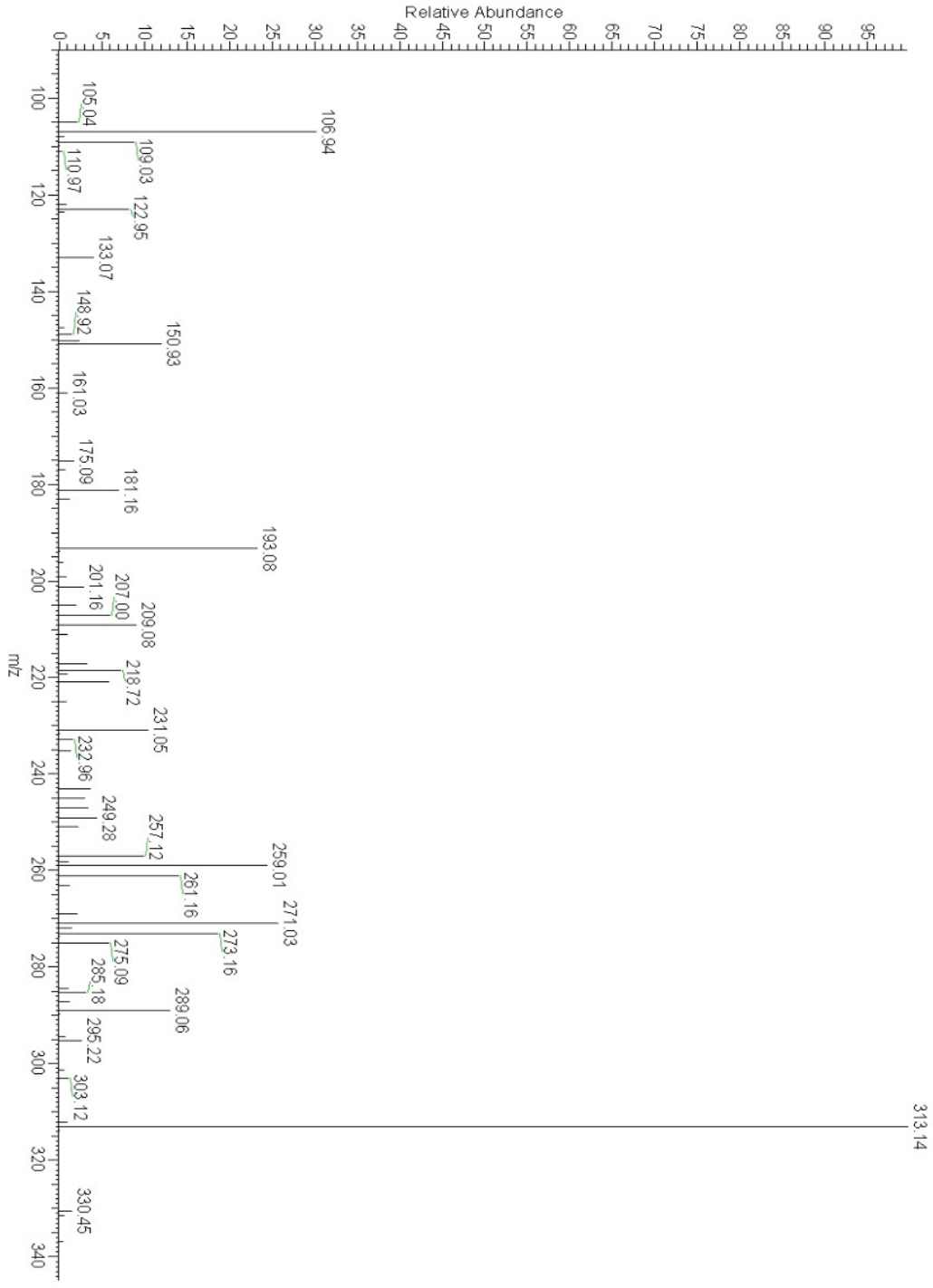
Relative Abundance
m/z
105.04
106.94
109.03
110.97
122.95
133.07
148.92
150.93
161.03
175.09
181.16
193.08
201.16
207.00
209.08
218.72
231.05
232.96
249.28
257.12
259.01
261.16
271.03
273.16
275.09
285.18
289.06
295.22
303.12
313.14
330.45

Peak 6

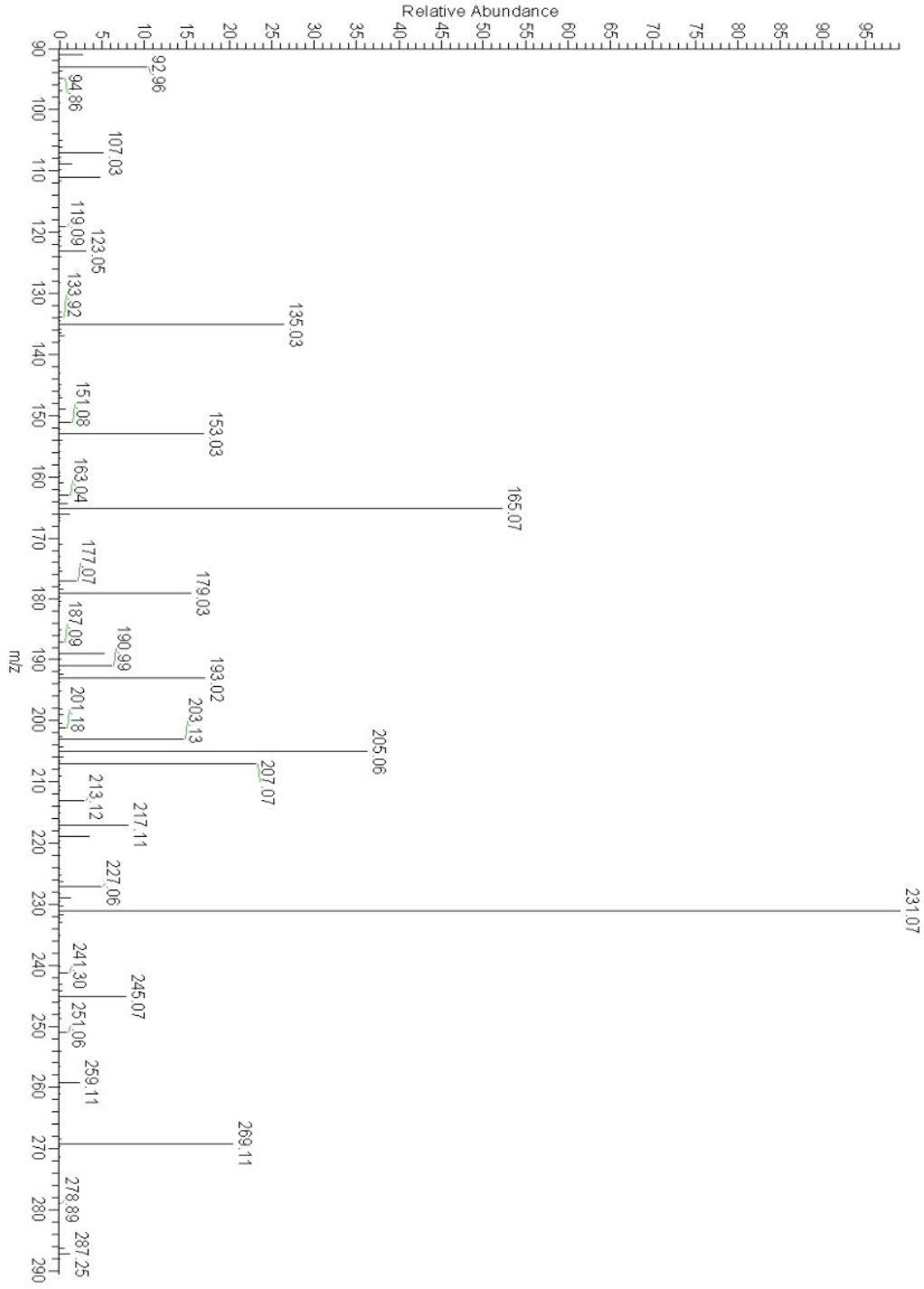
Relative Abundance
m/z
92.96
94.86
107.03
119.09
123.05
133.92
135.03
151.08
153.03
163.04
165.07
177.07
179.03
187.09
190.99
193.02
201.18
203.13
205.06
207.07
213.12
217.11
227.06
231.07
241.30
245.07
251.06
259.11
269.11
278.89
287.25

Peak 7

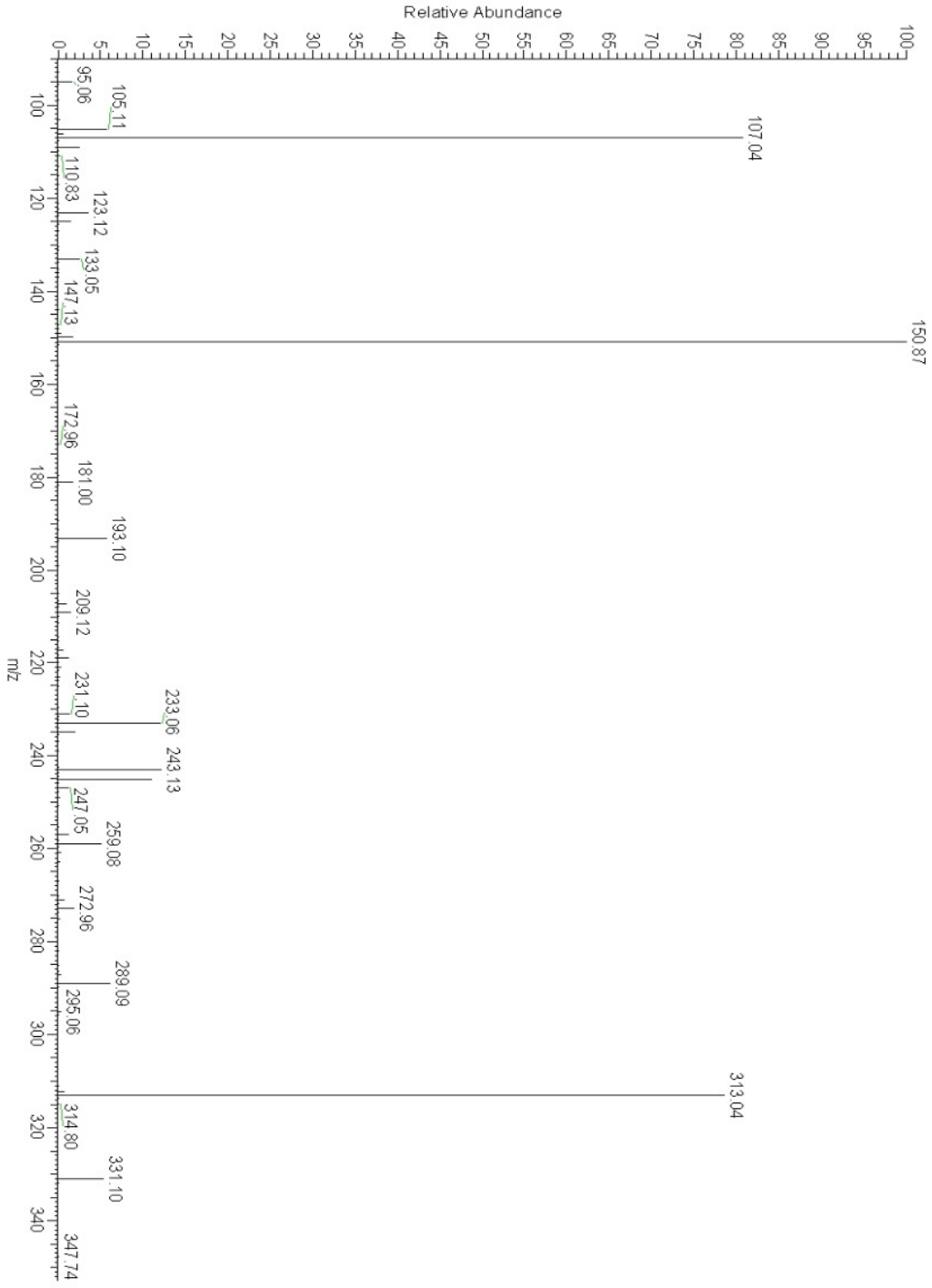
Relative Abundance
m/z
95.06
105.11
107.04
110.83
123.12
133.05
147.13
150.87
172.96
181.00
193.10
209.12
231.10
233.06
243.13
247.05
259.08
272.96
289.09
295.06
313.04
314.80
331.10
347.74

Peak 8

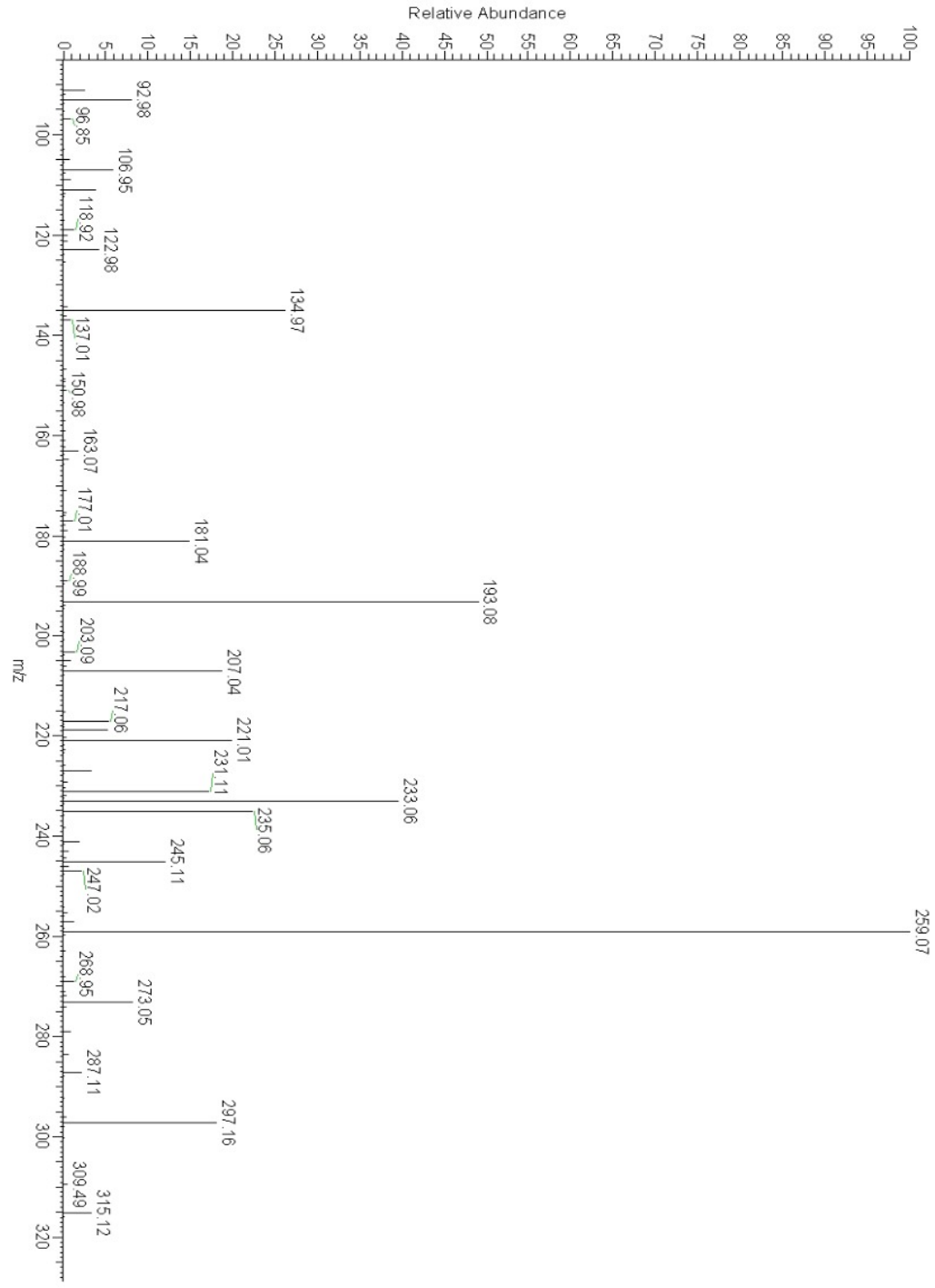
Relative Abundance
m/z
92.98
96.85
106.95
118.92
122.98
134.97
137.01
150.98
163.07
177.01
181.04
188.99
193.08
203.09
207.04
217.06
221.01
231.11
233.06
235.06
245.11
247.02
259.07
268.95
273.05
287.11
297.16
309.49
315.12

Peak 9

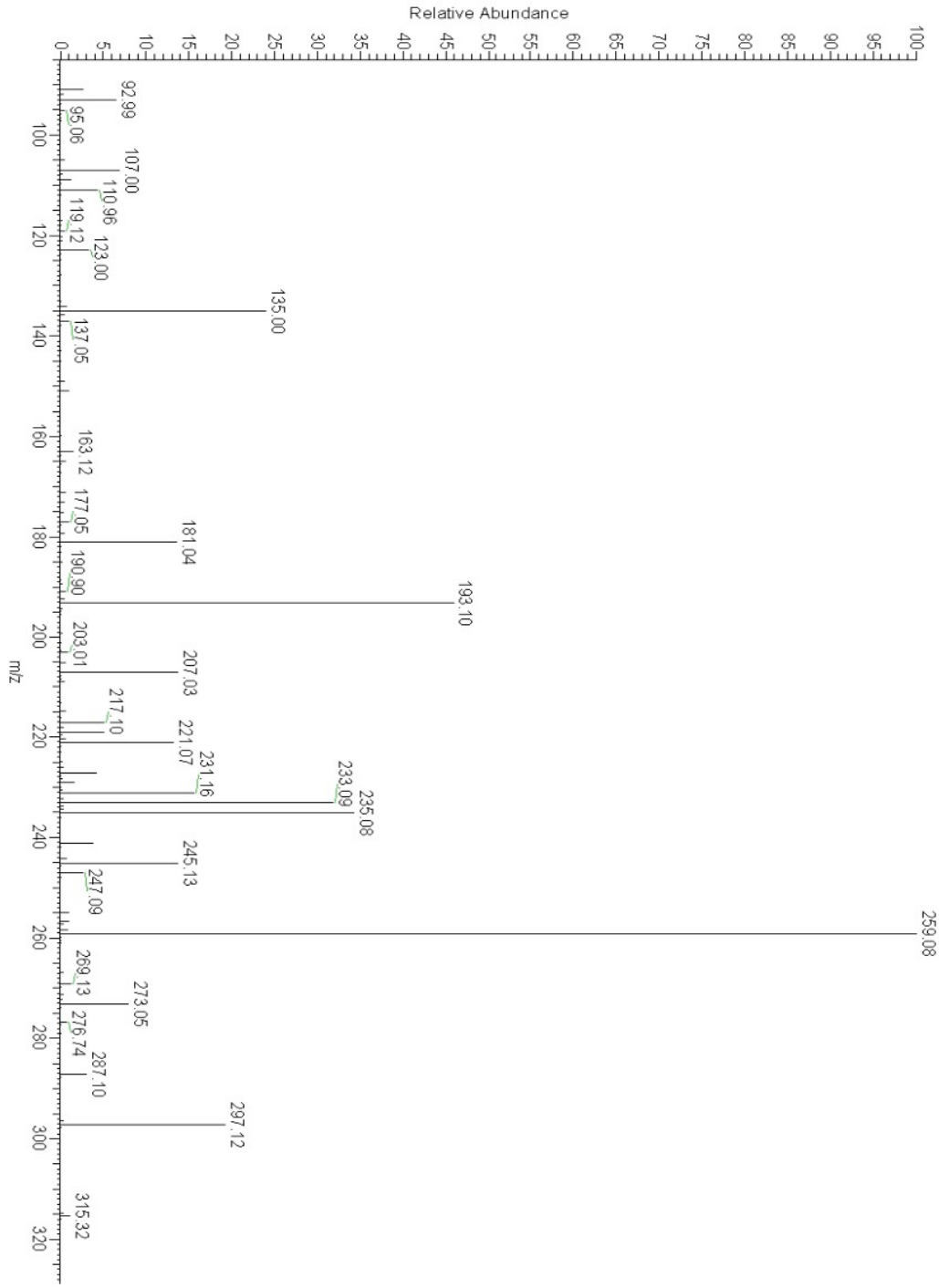
Relative Abundance
m/z
92.99
95.06
107.00
110.96
119.12
123.00
135.00
137.05
163.12
177.05
181.04
190.90
193.10
203.01
207.03
217.10
221.07
231.16
233.09
235.08
245.13
247.09
259.08
269.13
273.05
276.74
287.10
297.12
315.32

Peak 10

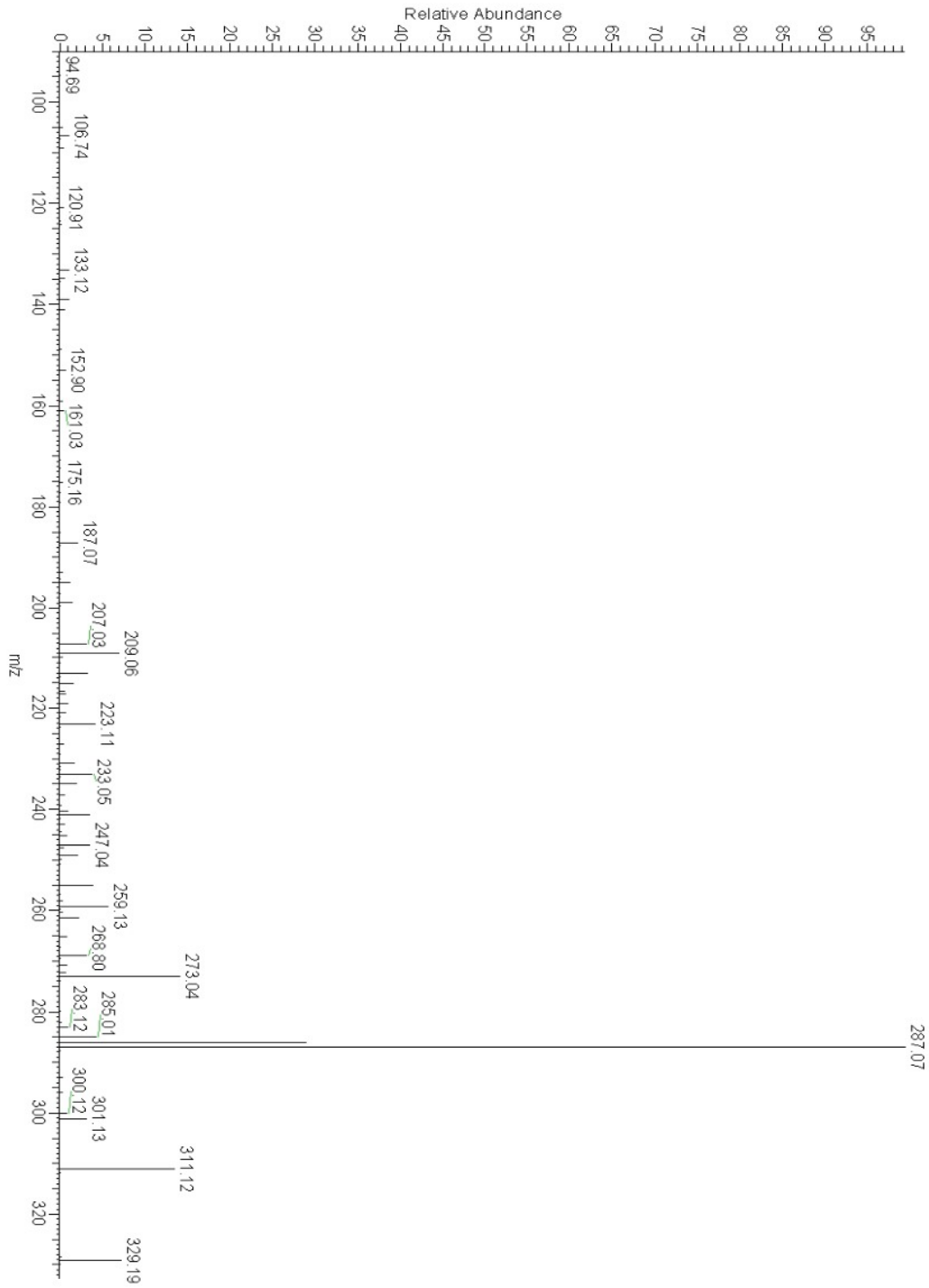
Relative Abundance
m/z
94.69
106.74
120.91
133.12
152.90
161.03
175.16
187.07
207.03
209.06
223.11
233.05
247.04
259.13
268.80
273.04
283.12
285.01
287.07
300.12
301.13
311.12
329.19

Δ-8 THC

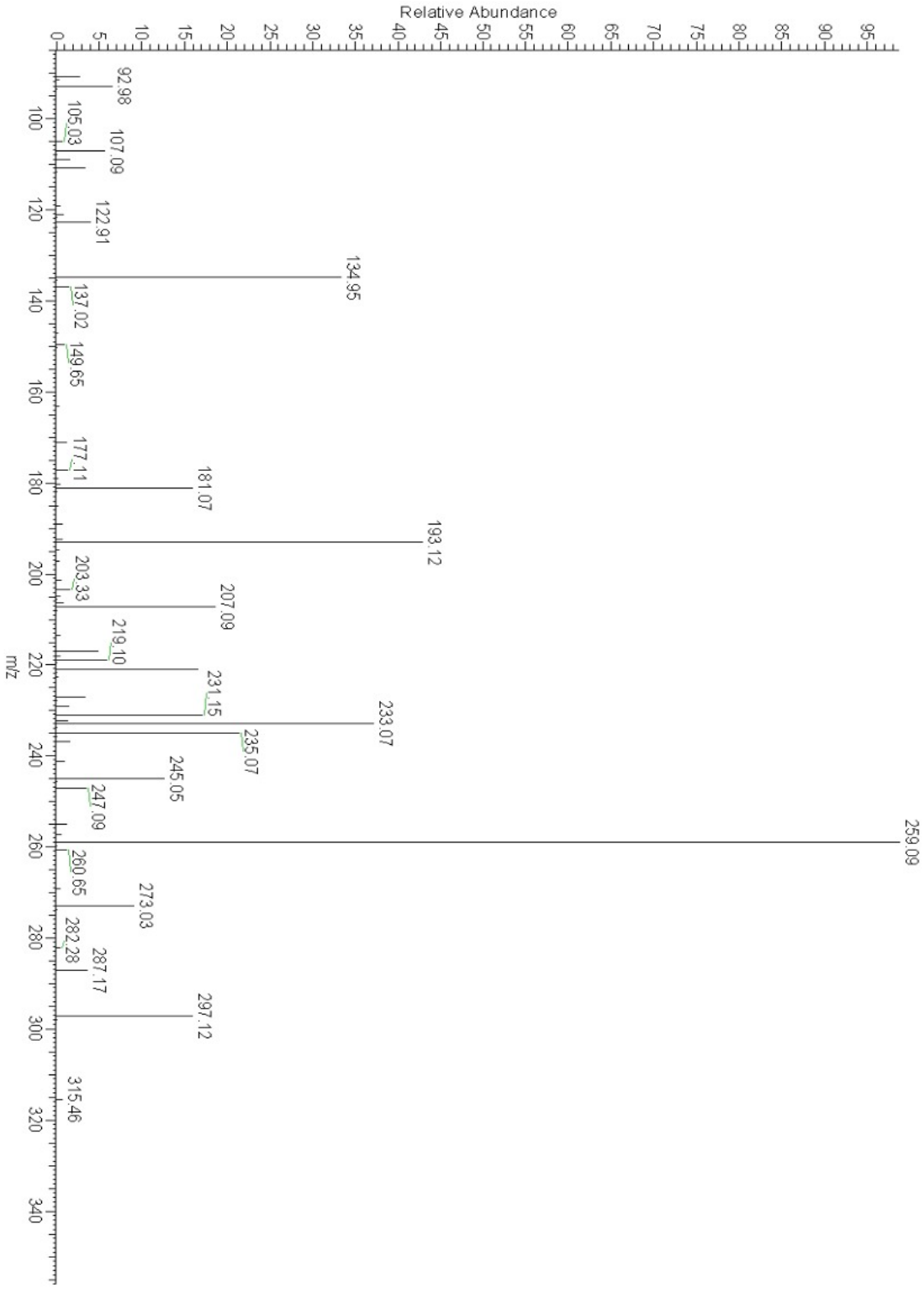
Relative Abundance
m/z
92.98
105.03
107.09
122.91
134.95
137.02
149.65
177.11
181.07
193.12
203.33
207.09
219.10
231.15
233.07
235.07
245.05
247.09
259.09
260.65
273.03
282.28
287.17
297.12
315.46

CBD

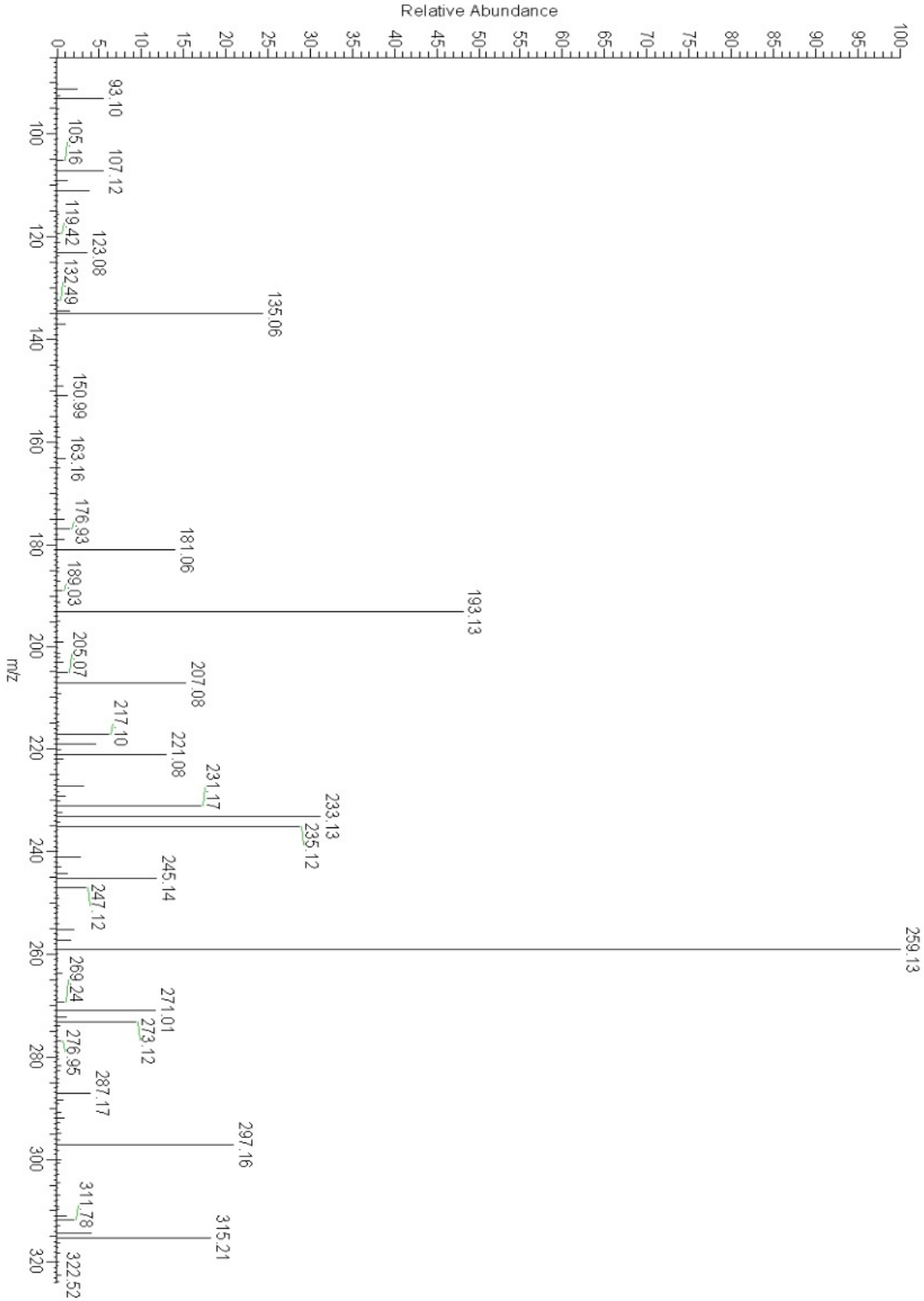
Relative Abundance
m/z
93.10
105.16
107.12
119.42
123.08
132.49
135.06
150.99
163.16
176.93
181.06
189.03
193.13
205.07
207.08
217.10
221.08
231.17
233.13
235.12
245.14
247.12
259.13
269.24
271.01
273.12
276.95
287.17
297.16
311.78
315.21
322.52

A3 Raw Integral Values of Cheese Spectra

Sample	Unsaturated Bond Raw Integral	Triglyceride C2 Raw Integral	Polyunsaturated Raw Integral	ω3 Methyl Raw Integral
B1	11215.03	6122.93	1507.62	5867.57
B2	13330.51	7326.82	1786.93	6523.03
B3	16721.61	9873.71	2058.03	9654.26
B4	19120.96	9915.66	2398.15	9495.54
B5	12633.80	7511.8	1750.22	6795.81
B6	13392.30	7256.98	1905.7	5485.73
B7	14440.66	7160.02	2057.87	4612.56
B8	16858.04	11285.08	1703.53	10900
B9	13560.41	7564.52	1763.59	7293.11
B10	9598.85	5555.48	1296.17	5260.06
1	29517.02	10284.10	4468.45	5419.31
2	30490.16	10523.53	4598.03	4720.94
3	29149.25	9828.02	4397.71	4245.48
4	28481.36	9292.80	4323.40	4499.07
5	23567.49	13155.93	2805.12	13134.30
6	22827.78	12886.91	2796.74	13459.23
7	21543.35	11747.87	3217.43	11939.72
8	24574.88	9402.02	3567.79	5221.23
9	24233.60	10812.65	3364.62	8115.01
10	15873.56	7846.85	1968.87	7599.99
11	26441.74	14705.49	3273.75	15018.02
12	25361.17	14291.36	3117.73	13290.77
13	18807.29	5548.86	2979.17	1633.16
14	15386.89	4082.96	2520.28	1046.20
15	22006.39	12258.78	2776.24	11842.54
16	29979.40	9661.08	4620.69	3492.43
17	13671.69	6961.02	1752.13	6241.94
18	16402.28	9205.36	2022.72	9377.52
19	15234.79	8064.80	2053.37	8458.72
20	15251.12	6933.54	1977.17	6825.74
21	15564.70	9201.76	1921.62	8598.86
22	16954.23	9608.00	2033.48	9109.76

23	15673.78	8661.35	2001.03	8532.18
24	17217.09	9404.12	2100.22	9616.26
25	14541.49	8166.92	1812.29	8074.21
26	13631.51	6010.32	1648.23	7004.57
27	14411.33	8542.10	1748.98	8273.64
28	10240.96	5116.26	1283.58	5018.73
29	12819.18	6649.26	1532.18	6965.63
30	14267.80	7727.85	2160.02	7600.48
31	12923.47	7242.64	1549.16	7551.71
32	12341.41	6826.59	1553.88	6724.32
33	14226.59	7920.62	1664.14	7922.23
34	24518.64	7565.97	4210.70	1785.55
35	18988.60	5791.81	2998.43	2618.79
36	14749.27	4914.61	2153.04	2365.61
37	11311.17	6455.03	1443.40	6220.89
38	12099.86	6117.10	1391.19	5693.14
39	11511.96	6481.73	1431.11	6355.87
40	12611.94	7187.84	1534.14	7002.98
41	12269.11	6993.78	1507.41	6672.01
42	10373.24	5828.77	1193.18	5789.26
43	12536.51	7127.68	1633.60	6911.82
44	18986.99	11212.00	2315.47	11496.46
45	18917.02	10793.04	2426.96	10240.92
46	23901.96	8434.01	3668.47	4011.97
47	26271.81	8174.04	4088.53	3249.94
48	23490.27	13230.16	2907.87	13495.98
49	22411.74	13121.77	2813.55	12945.46
50	29046.62	8785.84	4619.22	2952.94
51	12267.37	7569.59	1714.65	6550.53
52	13776.43	7627.66	1790.21	7244.01

A4 Cheese Integral Ratios

Sample	Unsaturated Bonds vs. Glycerol C2 Ratio	Polyunsaturated vs. Glycerol C2 Ratio	ω3 Methyl vs. Remaining Methyl Ratio	ω3 Methyl vs. Glycerol C2 Ratio
B1	1.831644	0.246225	0.117850	0.958294
B2	1.819413	0.243889	0.129701	0.890295
B3	1.693549	0.208435	0.123275	0.977774
B4	1.928360	0.241855	0.117452	0.957631
B5	1.681861	0.232996	0.107207	0.904685
B6	1.845437	0.262602	0.081174	0.755925
B7	2.016846	0.287411	0.067784	0.644210
B8	1.493834	0.150954	0.119308	0.965877
B9	1.792633	0.233140	0.121001	0.964121
B10	1.727816	0.233314	0.121384	0.946824
1	2.870161	0.434501	0.059583	0.526960
2	2.897332	0.436928	0.050980	0.448608
3	2.965933	0.447467	0.048042	0.431977
4	3.064885	0.465242	0.052595	0.484146
5	1.791397	0.213221	0.127508	0.998356
6	1.771393	0.217022	0.129916	1.044411
7	1.833809	0.273873	0.132512	1.016331
8	2.613787	0.379471	0.063308	0.555331
9	2.241227	0.311174	0.090138	0.750511
10	2.022921	0.250912	0.111818	0.968540
11	1.798086	0.222621	0.130623	1.021253
12	1.774581	0.218155	0.114691	0.929986
13	3.389397	0.536898	0.031562	0.294324
14	3.768563	0.617268	0.025438	0.256236
15	1.795153	0.226470	0.123481	0.966046
16	3.103111	0.478279	0.040141	0.361495
17	1.964035	0.251706	0.103302	0.896699
18	1.781818	0.219733	0.131397	1.018702
19	1.889047	0.254609	0.130511	1.048844
20	2.199615	0.285160	0.115302	0.984452
21	1.691492	0.208832	0.121023	0.934480

22	1.764595	0.211644	0.117282	0.948143
23	1.809623	0.231030	0.124763	0.985087
24	1.830803	0.223330	0.127658	1.022558
25	1.780535	0.221906	0.123193	0.988648
26	2.268017	0.274233	0.114241	1.165424
27	1.687095	0.204748	0.123297	0.968572
28	2.001650	0.250882	0.114530	0.980937
29	1.927911	0.230429	0.120420	1.047580
30	1.846283	0.279511	0.127309	0.983518
31	1.784359	0.213894	0.130280	1.042674
32	1.807844	0.227622	0.118449	0.985019
33	1.796146	0.210102	0.121922	1.000203
34	3.240647	0.556531	0.025259	0.235997
35	3.278526	0.517702	0.047650	0.452154
36	3.001107	0.438090	0.051898	0.481342
37	1.752303	0.223609	0.124178	0.963728
38	1.978039	0.227426	0.107985	0.930693
39	1.776063	0.220791	0.121196	0.980582
40	1.754622	0.213435	0.122717	0.974282
41	1.754289	0.215536	0.120147	0.953992
42	1.779662	0.204705	0.123947	0.993222
43	1.758849	0.229191	0.125583	0.969715
44	1.693453	0.206517	0.130724	1.025371
45	1.752705	0.224863	0.120957	0.948845
46	2.833997	0.434962	0.054101	0.475690
47	3.214054	0.500185	0.042771	0.397593
48	1.775509	0.219791	0.124449	1.020092
49	1.707981	0.214418	0.126485	0.986564
50	3.306072	0.525757	0.035746	0.336102
51	1.620612	0.226518	0.107960	0.865374
52	1.806115	0.234700	0.117029	0.949703

Vita

Colleen Ray was born in 1981 in Riverside, California. After a decidedly nomadic childhood, she graduated from Mountain View high school in Tucson, AZ and enlisted in the United States Army. She served two overseas deployments, one as a peacekeeper in the former Yugoslavia, and another during the lead up to and during the first months of Operation Iraqi Freedom with the 3rd Infantry Division. Colleen attended Northern Arizona University, studied under Dr. Cindy Browder performing organic synthesis research, and graduated with a B.S. in Chemistry in 2013. Next came a brief career in industry as an NMR field engineer until beginning her graduate studies in January of 2019.

Colleen's graduate research involved the development of NMR based methods for determining the authenticity of foods. She graduated from the University of Missouri-Columbia with a Ph.D in analytical chemistry in December 2022.